LUND UNIVERSITY

Improving Tröger's Base Chemistry

Developing the Chemistry of Tröger's base

Dawaigher, Sami

2018

[Link to publication](#)

Total number of authors:
1

Improving Tröger's Base Chemistry

Developing the Chemistry of Tröger's base

SAMI DAWAIGHER | CENTRE FOR ANALYSIS AND SYNTHESIS | LUND UNIVERSITY
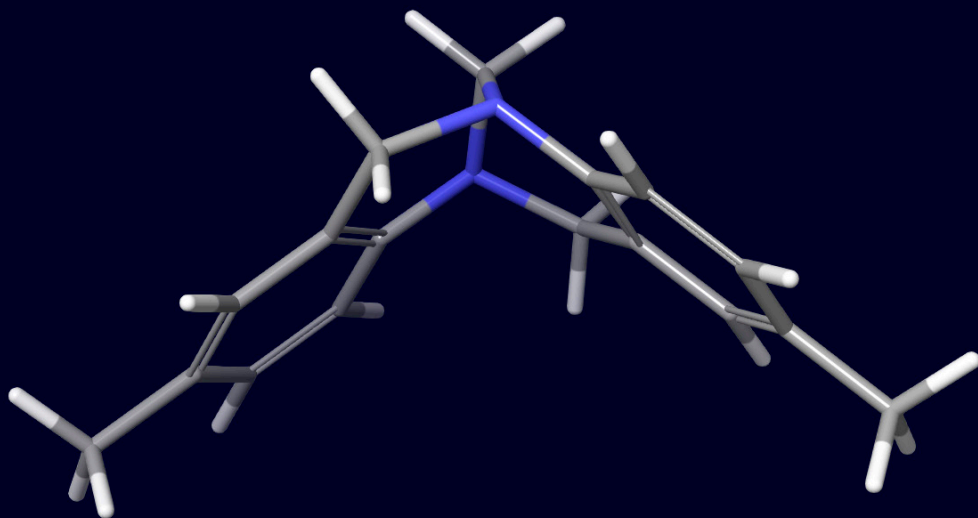
Improving Tröger's Base Chemistry

Developing the Chemistry of Tröger's base

Sami Dawaigher

DOCTORAL DISSERTATION
by due permission of the Faculty of Natural Sciences, Lund University, Sweden.
To be defended at Kemicentrum, lecture hall C. 10.15 am December 20th 2018.

Faculty opponent
Mogens Brønsted Nielsen, University of Copenhagen

Organization LUND UNIVERSITY	Document name Doctoral Dissertation
Centre For Analysis and Synthesis Departement of Chemystry Lund University, Box 124, Se-221 00 Lund, Sweden	Date of issue 2018-11-26
Author(s) Sami Dawaigher	Sponsoring organization

Title and subtitle Developing the Chmistry of Tröger's base

Abstract

The Tröger's base framework has been implemented in two different receptors. The first of these receptors, incorporating two 18-crown-6 moities, was used as a host in a binding study together with a sieries of bisammonium salts that yielded different binding constants that were then used as a benchmark to compare different computational methods (Molecular Mechanics (MM) and Density Functional Theory (DFT)) in predicting the correct results where the MM methods proved more effective. The second of the receptors incorporated two Tröger's base moieties linked together with two crown ether straps. This receptor was tested for it's affinity towards different metal cations, the receptor proved too hindered to accomodate any cations except Fe^{3+}. Furthermore, the reactivity of Tröger's base with lithium amide bases has been investigated extensively. A new protocol for preparing mono- and bissubstistuted Tröger's base derivatives has been developed where Tröger's base is treated with sBuLi/TMEDA followed by an electrophilic quench resulting in a Tröger's base derivative substituted in the *exo*-6 and *exo*-12 positions. In addition to this method, a method for converting *exo*-6- and *exo*-12 substituted Tröger's base amides into *endo*-6 and *endo*-12 substituted Tröger's base amide has been developed. A study of the reduction of Tröger's base amides is described herein.

Key words Tröger's base, Host Guest Chemistry, Metalation, Computational Chemistry, Supramolecular Chemistry.

Classification system and/or index terms (if any)

Supplementary bibliographical information	Language English
ISSN and key title	ISBN 978-91-7422-614-0 (print) 978-91-7422-615-7 (pdf)

Recipient's notes	Number of pages 118	Price
	Security classification	

Improving Tröger's Base Chemistry

Developing the Chemistry of Tröger's Base

Sami Dawaigher

LUND
UNIVERSITY

Cover by Sami Dawaigher and Paula Leckius

Table of Contents

Acknowledgement

List of Papers

This thesis is based on the following papers that will be referred to by the roman numerals I-IV.

I. **Tröger's Base Twisted Amides: *Endo* Functionaliztion and Synthesis of an inverted Crown Ether.**

   Josep Artacho, Erhad Ascic, Toni Rantanen, Carl-Johan Wallentin, Sami Dawaigher, Karl-Erik Bergquist, Michael Harmata, Victor Snieckus, and Kenneth Wärnmark. *Org. Lett.* **2012**, *14*, pp 4706-4709.

   Contribution: Colorimetric study.

II. **A Protocol for the *exo*-Mono and *exo,exo*-Bis functionalization of the Diazocine Ring of Tröger's Base.**

   Sami Dawaigher, Kristoffer Månsson, Erhad Ascic, Josep Artacho, Roger Mårtensson, Nagarajan Loganathan, Ola F. Wendt, Michael Harmata, Victor Snieckus, and Kenneth Wärnmark. *J. Org. Chem.* **2015,** *80*, 12006-12014.

   Contribution: Conception of reverse addition methodology, Majority of experimental work and writing of manuscript.

III. **The Synthesis of Mono *endo*-6- and Bis *endo,endo*-12 *N,N*-Diethyl Carbamoyl Derivatives of Tröger's Base – The Isomerization Approach.**

   Sami Dawaigher, Emil Lindbäck, Daniel Strand, Michael Harmata, Victor Snieckus and Kenneth Wärnmark. *In manuscript*.

   Contribution: Conception of mechanistic study, majority of experimental work and writing of manuscript.

IV. **The Discrimination of 4-Substituted Heptane-1,7-diyl Ammonium Salts by a Bis(Crown-Ether) Tröger's Base Analogue: A Biological model and evaluation of computational methods.**

   Sami Dawaigher, Carlos Solano Arribas, Anna Ryberg, Jacob Jensen, Karl Erik Bergqvist, Anders Sundin, Per-Ola Norrby, Kenneth Wärnmark. *In manuscript*.

Contribution: Parts of the optimization of the synthesis of the bisammonium ligands, The Configurational analysis of free ligands using NMR. The Molecular modeling and DFT calculations, writing of the manuscript.

List of Papers not included in this thesis:

I. **Synthesis of Cr(III) Salen Complexes as Supramolecular Catalytic Systems for Ring-Opening Reactions of Epoxides.**
    Emil Lindbäck, Hassan Norouzi-Arasi, Esamel Sheibani, Dayou Ma, Sami Dawaigher, Kenneth Wärnmark. *Chemistry Select,* **2016,** *1*, 1789-1794.

II. **Substrate-Selective Catalysis**
    Emil Lindbäck, Sami Dawaigher, Kenneth Wärnmark. *Chemistry – A European Journal,* **2014**, *20*, 13432-13481.

III. **A Double Conformationally Restricted Dynamic Supramolecular System for the Substrate-Selective Epoxidation of Olefins-A Comparitive Study on the Influence preorganization.**
    Emil Lindbäck, Sawsen Cherraben, Jean-Patric Francoia, Esmaeil Sheibani, Bartoz Lukowski, Agnieszka Pron, Hassan Norouzi-Arasi, Kristoffer Månsson, Pawel Bujalowski, Anna Cederbalk, Thanh Huong Pham, Torbjörn Wixe, Sami Dawaigher, Kenneth Wärnmark. *ChemCatChem,* **2015,** *7*, 333-348.

Popular Summary

In this Work, Tröger's base, a molecule first discovered in 1887 that has found wide utility in recent years, is described, studied and utilized. This molecule, being chiral (meaning it has two forms that are each others mirror images called enantiomers), has found a wide range of uses over in recent years. Its been used in the evaluation of chiral HPLC columns (since it is easily split to its to enantiomers on a chiral HPLC column), derivatives and analogues of Tröger's base have found use as dopants that induce chirality in liquid crystals used in display screens, and some of its derivatives have been found to be cytotoxic and could provide new treatments for cancer.

The chemistry of Tröger's base is explored in the literature and a summary of its reactions and utility are provided in the introduction. In the chapters that follow the efforts made to develop the chemistry of this fascinating molecule are further described. Among other things we manage to install substituents on sites previously not accessible.

Following the development of the chemistry we describe how Tröger's base framework is used in a model of a pocket in a protein to better understand the interactions between proteins and peptides. In the process we develop a benchmark test for different computational methods used in modeling molecules in computer simulations.

List of Abbreviations

BINAP	(±)-2,2'-Bis(diphenylphosphino)-1,1'-binaphthalene
BTEAC	Benzyltriethylammonium Chloride
DBA	Dibenzylamine
DCM	Dichloromethane
DFT	Density Functional Theory
DIPA	Diisopropylamine
DMAP	4-Dimethylaminopyridine
DMDO	Dimethyldioxirane
DMSO	Dimenthylsulfoxide
HMTA	Hexamethyl tetramine
HRMS	High resolution mass spectroscopy
LAH	Lithium Aluminum Hydride
LiHMDS	Lithium bis(trimethylsilyl)amide
MD	Moleuclar Dynamics
MM	Molecular Modeling
NBS	*N*-Bromosuccinimide
NMR	Nuclear Magnetic Resonance
NOE	Nuclear Overhauser effect
NOESY	Nuclear Overhauser effect spectroscopy
ROESY	Rotating frame nuclear Overhauser effect spectroscopy
rt	room temperature
THF	Tetrahydrofuran
TMDS	1,1,3,3-Tetramethyldisilyloxane
TMEDA	*N,N,N',N'*-Tetramethylethylenediamine
Tf	Triflate (CF_3SO_2)
TMS	Trimethylsilyl
TFA	Trifluoroacetic(yl)

Abstract

The Tröger's base framework has been implemented in two different receptors. The first of these receptors, incorporating two 18-crown-6 moities, was used as a host in a binding study together with a sieries of bisammonium salts that yielded different binding constants that were then used as a benchmark to compare different computational methods (Molecular Mechanics (MM) and Density Functional Theory (DFT)) in predicting the correct results where the MM methods proved more effective. The second of the receptors incorporated two Tröger's base moieties linked together with two crown ether straps. This receptor was tested for it's affinity towards different metal cations, the receptor proved too hindered to accomodate any cations except Fe^{3+}. Furthermore, the reactivity of Tröger's base with lithium amide bases has been investigated extensively. A new protocol for preparing mono- and bissubstistuted Tröger's base derivatives has been developed where Tröger's base is treated with sBuLi/TMEDA followed by an electrophilic quench resulting in a Tröger's base derivative substituted in the *exo*-6 and *exo*-12 positions. In addition to this method, a method for converting *exo*-6- and *exo*-12 substituted Tröger's base amides into *endo*-6 and *endo*-12 substituted Tröger's base amide has been developed. A study of the reduction of Tröger's base amides is described herein.Bodytext where every paragraph is separated by a little space vertically.

Chapter 1: Introduction to Tröger's base and its properties.

1.1 Historical Overview

Tröger's base (**1**), depicted in figure 1.1.1, was first discovered and prepared in 1887 by Julius Tröger during the study of the condensation of anilines with formaldehyde.[1] However, the structure of **1** was not elucidated until 1935 by Spielman, who was able to deduce the structure of **1** to be racemic 2,8-dimetyl-*6H,12H*-5,11-methanodibenzo[*b,f*][1,5]diazocine by carefully monitoring its reactivity.[2] In the same year, a mechanism for the condensation reaction was suggested by Wagner.[3]
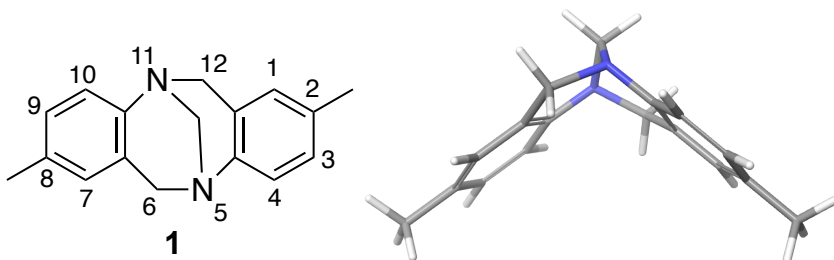
Figure 1.1.1
(±)-Tröger's base (**1**) with the accepted numbering system and a 3D model depicting its structure.

Compound **1** is a V-shaped chiral molecule, it is C_2 symmetric with two stereogenic centers located on its nitrogen atoms as can be deduced from looking at the structure. In 1944, **1** became one of the first racemates to be resolved to its two enantiomers by the means of chromatography.[4] The structure of **1** proposed by Spielman was confirmed in 1986 by single-crystal X-ray diffraction (XRD).[5] The (+)-**1** was found out to be the (*S,S*) enantiomer in 1991 using XRD.[6]

Up until the 1980s, the main area of interest for **1** was in the field of chromatography where it was used as a model substance for the evaluation of

chiral chromatography techniques. In 1985, this changed; Wilcox reported the synthesis of a host of Tröger's base analogs and suggested using them as host molecules in biomimetic systems.[7] This development encouraged several different research groups to pursue the development of new methods of making Tröger's base derivatives and analogues.

1.2 Chemical Properties of Tröger's base

1.2.1 Configuration and Structural Properties

When examining **1**, one can notice that it is comprised of a bicylclic aliphatic unit that is connected to two aromatic rings making a V-shape. The cavity formed inside the V-shape is hydrophobic due to the aromatic rings being present. As mentioned earlier, **1** is a C_2-symmetric chiral molecule. The nitrogen atoms constitute stereogenic centers and are locked in configuration by the methylene bridge preventing the nitrogen atoms from pyramidal inversion. Due to this lock, only *R,R* or *S,S* configurations are geometrically feasible and hence the diastereomeric *R,S* configuration is not encountered.

1.2.2 The Basicity of Tröger's Base

In 50% aqueous alcohol, the monoprotonated salt of **1** has a pK_a value of 3.2. This is approximately a unit lower than the pK_a value of the anilinium ion (4.6) in aqueous media.[8] This is rather surprising since the free electrons on the nitrogen atoms of the bridgehead are forced to be oriented 45° with respect to the aromatic plane due to the rigid structure and this hampers conjugation with the aromatic system, a conjugation with the aromatic system would likely increase the electron density around the nitrogen atoms and would thereby increase the pKa value. One would expect that the monoprotonated salt of **1** would have a higher pK_a value than aniline and closer to that of methyl ammonium that has pK_a=10.6 due to the aforementioned decrease in electron density. It has been suggested that the rather low pK_a of **1** is due to an overlap between the lone electron pair and the antibonding orbital of the bond the methylene carbon and second nitrogen (see Figure 1.2.2.1).[9]
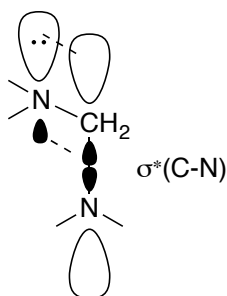
Figure 1.2.2.1
Overlap of nitrogen lone pair and the antibonding orbital of the methylene carbon and the second nitrogen atom.

1.2.3 Racemization of Tröger's Base

Tröger's base is known to racemize in weakly acidic solutions.[10] In an attempt to rationalize the racemization, Prelog suggested that this occurred through the reversible formation of methyleneiminium ion (**2**) as a key intermediate (Scheme 1.2.3.1).[4] To date, there is no spectroscopic evidence for the existence of **2**. It was suggested that this is due to **2** being a transient species it is present in too low concentrations to be detected. Further support for this mechanism can be found in the observation that the ethano-bridged TB's (not able to form a methyleneiminium ion) does not racemize in acidic conditions.[11-13] The methyliminium mechanism can also explain why **1** does not racemize in concentrated acidic conditions, due to that the double protonation makes it impossible to form the methyleneiminium ion (Scheme 1.2.3.2).[10] In 2006, Lenev reported that a substantial increase in racemizaton energy could be measured if the methyl groups on the aromatic ring were in a position *ortho* to the nitrogens. It was argued that this increase in racemization energy was due to that the *ortho* substituted Tröger's base analog has a less stable methyleniminum transition state and that this would account for the difference.[14] Work in our group has also shown that *ortho* substituted tris Tröger's base analogs did not readily isomerize in both weak and strong acidic media.
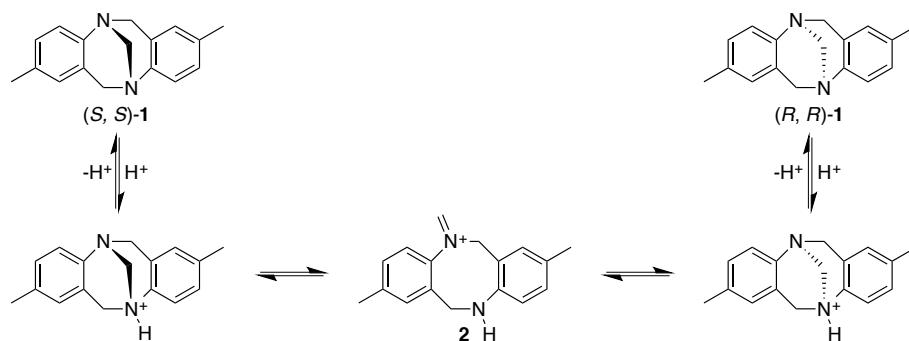
Scheme 1.2.3.1
The racemization mechanism of **1** in weakly acidic media
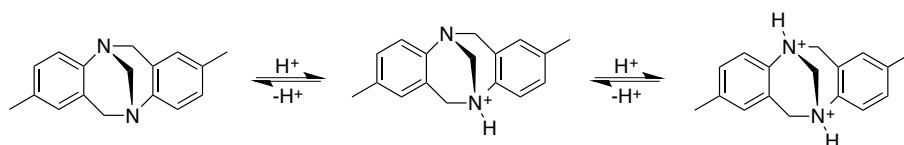
Scheme 1.2.3.2
A mechanistic overview of why **1** does not racemize in strongly acidic media

Trapp suggested another racemization mechanism of Tröger's base involving a Diels-Alder mechanism in gas phase at ambient temperature. In this mechanism depicted in Scheme 1.2.3.3, **1** would ring open with a retro-hetero-Diels-Alder to give intermediate **3**, which would undergo a hetero-Diels-Alder reaction to provide a 1:1-mixture of (*S,S*)-**1** and (*R,R*)-**1**.[15] It was however later observed by Schröder that the presence H⁺ was necessary for racemization to occur, suggesting that the mechanism suggested by Prelog is more likely.[16]
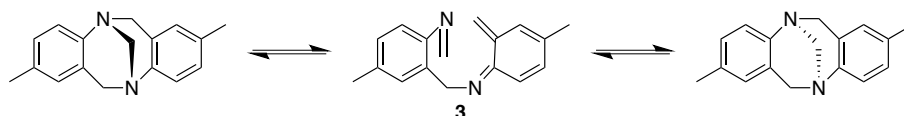
Scheme 1.2.3.3
Retro-Diels-Alder mechanism of Tröger's base racemization

18

1.3 Synthesis of Compounds with the Tröger's Base Framework.

1.3.1 Tröger's Base Condensation

The first time Tröger's base was synthesized, a condensation reaction of *p*-toluidine and methylal in aqueous HCl was used (Scheme 1.3.1.1).[1]
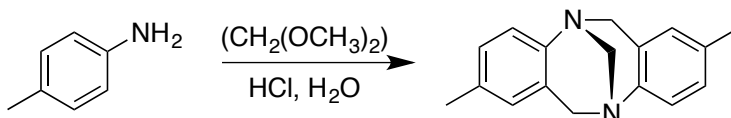
Scheme 1.3.1.1
The first Tröger's base condensation reaction

    Condensation reaction variations have remained the most popular method to synthesize Tröger's base analogs over time. Hence, a suitably substituted aniline is allowed to react with formaldehyde or another methylene synthon precursor under acidic conditions.[7,17-21] There has been an ongoing quest for new and improved synthetic protocols such as using DMSO as a methylene source,[22] using Lewis acids as catalysts,[23-24] as well as conducting the condensation in ionic liquids[25] or diglycolic acid/polyphosphoric acid.[26] Variations of the conditions in this general approach have revealed that the electronic properties of substituents and the substitution pattern of the aniline both have a substantial effect on the outcome of the reaction. A major drawback with the condensation reaction is that electron deficient anilines reacted in a sluggish manner with low yields,[27-28] also, in order to avoid polymerization, the aniline should be *para*-substituted.

    In 2001, a major breakthrough in the protocols for Tröger's base condensations was developed by the Wärnmark group that allowed the synthesis of halogenated Tröger's base analogues. It was found that using paraformaldehyde (as methylene synthon) and triflouroacetic acid (TFA) in the condensation overcame the requirement of having electron-donating groups on the aniline.[29] With this protocol available, a wide array of functional groups have been introduced on the aromatic rings of the Tröger's base framework including halogens, alkyl chains, MeO, MeS, COOR, CF$_3$, and NO$_2$.[30-39] Our protocol has even made it possible to use aniline in a TB condensation resulting in an unsubstituted TB analogue.[40]

1.3.2 Mechanism of the Condensation

As mentioned in section 1.1, Wagner was the first to propose a mechanism for the formation of Tröger's base[3, 17, 41] this was further researched by Farrar.[42] In this mechanism, a series of electrophilic aromatic substitutions are suggested to be the key steps in the reaction as seen in Scheme 1.3.2.1.
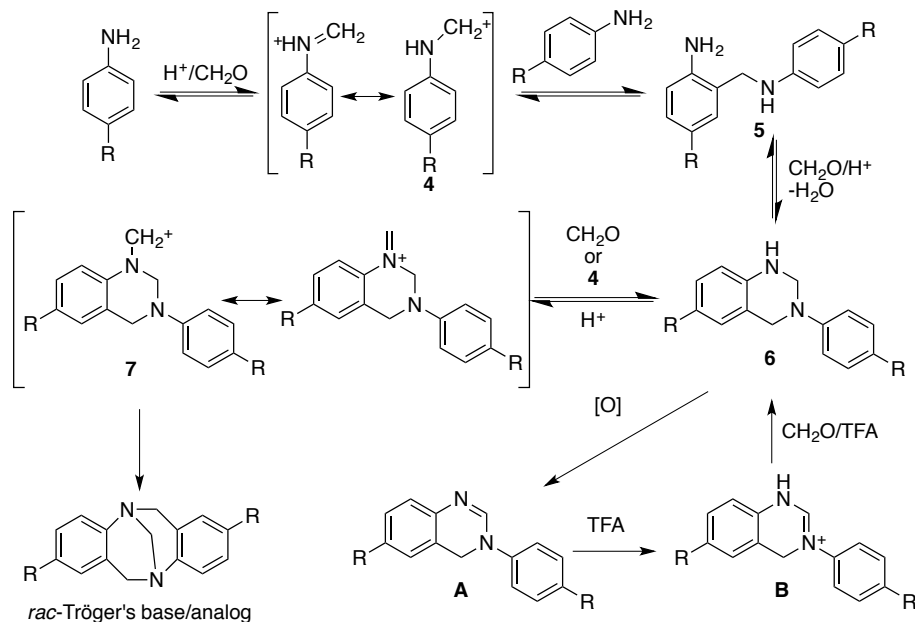
Scheme 1.3.2.1
The mechanism of the Tröger's base condensation as proposed by Wagner with probable side reaction.

To begin, iminium ion **4** is formed by the acid catalyzed reaction of the *p*-aniline with the formaldehyde. The iminium ion then undergoes an electrophilic aromatic substitution with a second molecule of *p*-aniline to give intermediate **5**. This intermediate then undergoes an acid catalyzed iminium ion formation that is followed by an electrophilic aromatic substitution cyclization that forms tetrahydroquinazoline derivative **6**. In a similar manner, intermediate **7** is formed from **6**. The Tröger's base or analog of it is formed from **7** by a final electrophilic aromatic substitution. It seems that the rate-limiting step of the reaction is the transformation of **6** to **7**. If electron withdrawing groups are present on the aromatic ring, the nucleophlicity of the secondary amine of **6** is reduced that will in turn reduce the rate of the intramolecular electrophilic aromatic substitution, this gives **6** time to undergo an undesired side reaction since it is readily oxidized to dihydroquinazoline **A**. Our group attempted to use paraformaldehyde in TFA in order to improve the reaction compared to using formalin/HCl.[29] We propose that

this works in two ways. First, it increases the amount of protonated formaldehyde and increases the rate of formation of **7**. Second, the TFA allows the reduction of **A** back to **6**. This occurs via the protonation of **A** resulting in the protonated intermediate **B**. This intermediate is then involved in a hydride transfer with the formaldehyde resulting in **6**.

Other authors have had different views on the mechanism. Sergeyev argued that the rate of formation of **7** is influenced by the imminium ion **4**. Rationalizing that **4** is abundant to begin with resulting in the rapid formation of **7**. As the reaction proceeds, **4** becomes less abundant and this gives rise to side products and slow formation of **7**. However, no explanation was provided as to why the reaction proceeds smoothly in TFA and not in formalin/HCl.[31] Farrar proposed another intermediate in the mechanism instead of **7**,[42] namely intermediate **8** (Figure 1.3.2.1). In the same study, byproduct **9** (Figure 1.3.2.1) was isolated and this was shown to not transform to **1** when exposed to the reaction conditions and was this later confirmed by Aiken and coworkers.[43] Further support for the Wagner mechanism was provided by Eberlin and Coelho when they monitored the Tröger's base condensation using mass spectrometry. In this study, *p*-toluidine together with either formaldeyde or hexamethylenetetramine (HMTA) in TFA was allowed to condence *in situ* while monitoring the reaction electrospray ionization mass and tandem mass spectroscopy [ESI-MS(/MS)].[44] With this technique, iminium ion **4** could be detected as well as the cationic forms of **6** and **7**. The presence of cationic species is expected in ESI, where the ESI source is expected to oxidize **6** and **7**. Wu and coworkers provided even more proof for the Wagner mechanism when **10** and **11** where isolated from their Tröger's base condensation in ionic liquid. Upon subjecting **10** and **11** to the reaction conditions again, more **1** was formed from proving them both to be intermediates in the formation of **1**.[45]
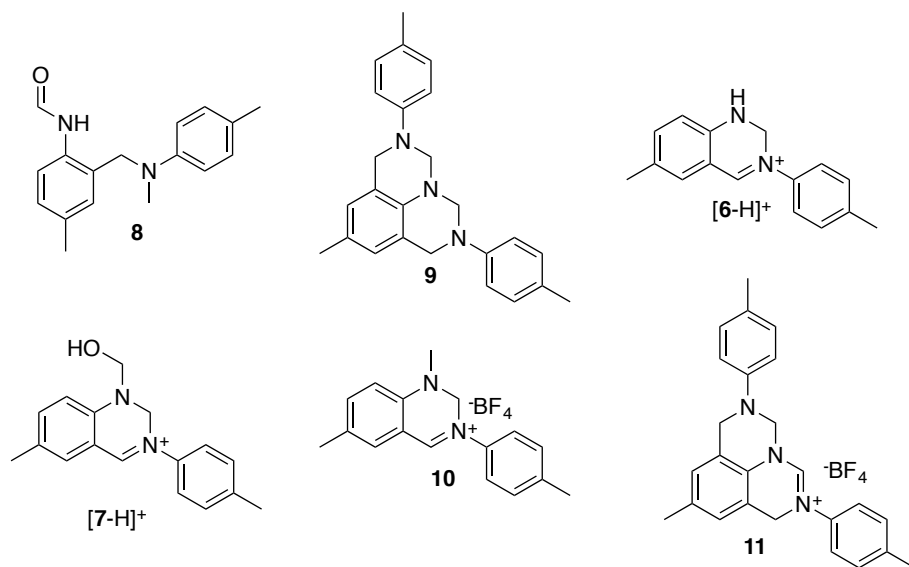
Figure 1.3.2.1
Intermediates and byproducts detected or isolated from the Tröger's base condensation.

1.3.3 Other Methods of Synthesis of Tröger's base analogs

The Tröger's base condensation mentioned above is not without its limitations. It requires the aniline to be of a certain substitution pattern and the relatively harsh conditions involved somewhat limits the Tröger's base analogs that can be made with the condensation. Also, one has to keep in mind that the condensation only gives access to symmetric Tröger's base analogs. For these reason alternative methods have been investigated to synthesize Tröger's base analogs.

Webb and Wilcox attempted the synthesis of unsymmetrical analogues of Tröger's base by using a tethering strategy. Hence two differently substituted anilines were linked together using a methylene unit and were then allowed to cyclize in the presence of formaldehyde (Scheme 1.3.3.1). This method provided the first method of preparing analogues carrying electron-withdrawing groups.[46]
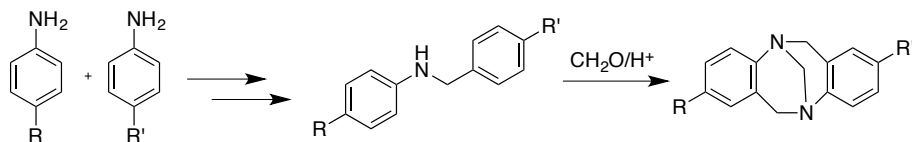
Scheme 1.3.3.1
Preperation of Tröger's base analogues using a stepwise tethering strategy

Another methodology to reach unsymmetrical Tröger's base derivatives and analogues is to start with Tröger's base or one of its symmetrical analogues and by means of a lithium amide base deprotonate the benzylic proton in the 6-position followed by an electrophilic quench. This methodology has been intensely studied by our group and will receive a more thorough introduction in chapter 2 (Scheme 1.3.3.2).
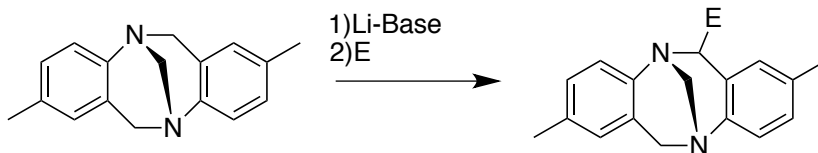
Scheme 1.3.3.2
Preparation of unsymmetrical Tröger's base derivatives using a lithium amide base to deprotonate the 6-position followed by an electrophilic quench

Becker using another stepwise approach reacted a highly substituted aniline with ethyl oxalyl chloride and then heated the resulting amide in DMSO resulting in a highly functionalized TB analog (Scheme 1.3.3.3).[47]
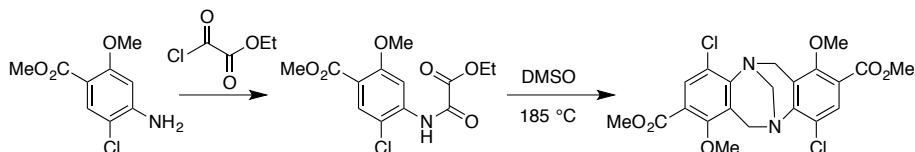
Scheme 1.3.3.3
Preperation of a highly substituted TB analog using a stepwise strategy utilizing DMSO as the methylene equivalent

Another strategy to make TB analogs is to start with the tetrahydro dibenzo[*b,f*][1,5]diazocine precursor and allow it to react with an aldehyde or ketone. This will place a 5,11-methylene bridge with substituents that originate from the aldehyde or ketone used (Scheme 1.3.3.4).[48-49]
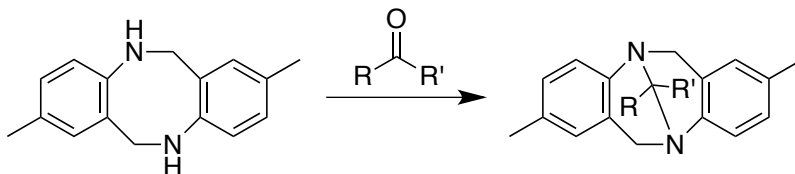
Scheme 1.3.3.4
Synthesizing Tröger's base analogs by inserting a methylene bridge in the tetrahydro dibenzo[*b,f*][1,5]diazocine precursor using an aldehyde or ketone

Maitra and coworkers linked two aniline moieties to a template of 7-deoxycholic acid, and then subjecting the anilines to condensation conditions. This resulted in a TB analog that was 40% ee due to the chiral induction provided by the template (Scheme 1.3.3.5).[50-51]
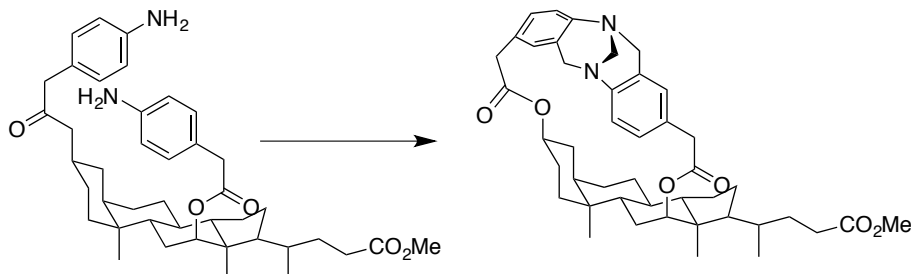
Scheme 1.3.3.5
Asymmetric Tröger's base condensation using a chiral template

1.4 Applications of Tröger's Base Analogues

Up until the 1980s, the only utilization of Tröger's base was as a standard for the evaluation of chiral chromatography columns. In 1985, Wilcox proposed the use of Tröger's base analogues as chiral host molecules and as metal ligands,[7] with this report, Tröger's base gained popularity as a building block in the field of supramolecular chemistry and molecular recognition.

1.4.1 in Supramolecular Chemistry

Wilcox and Adrian utilized the framework of Tröger's base in a hydrogen bonding receptor. In their study, they appended two carboxylic acid moieties to Tröger's base (**12**, Figure 1.4.1.1) that would H-bond to cyclic urea derivatives or adenine moieties. UV/fluorescence and NMR spectroscopy were used to investigate the binding process.[52] This receptor was also used in another study to determine the effects of residual water in solvents on the binding abilities of different receptors.[20]

Goswami and Ghosh synthesized the amidopyridine analogues of Tröger's base **13** and **14**. These two receptors were used as receptors for di-carboxylic acids. In their studies, incorporating NMR titrations, it was concluded that **13** showed selectivity for suberic acid and that **14**, being more flexible, exhibited a weaker tendency to bind the same acid and any substrate selectivity was lost.[53-54]

Our group has used the 18-crown-6 Tröger's base analog **15a** (Figure 1.4.1.2) as a receptor for bisammonium salts (see chapter 3 and paper III for a detailed account).[55] Another receptor incorporating crown ether and the Tröger's base skeleton made by our group is receptor **15b**, this receptor exhibited some affinity towards Li^+, Na^+, and Cs^+ in gas phase.[*113]
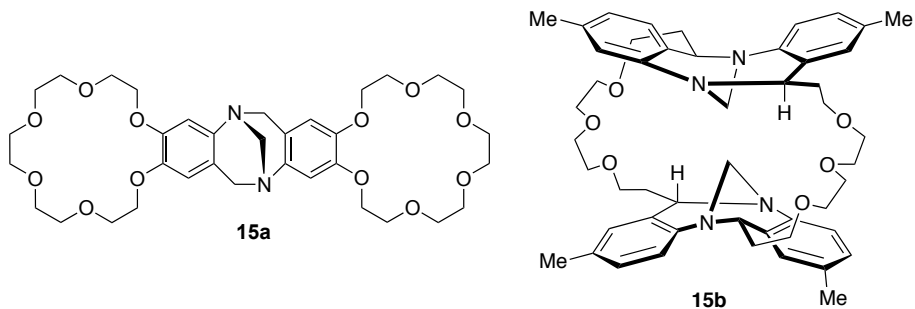
The Tröger's base framework has been incorporated into several macrocycles (Figure 1.4.1.3). Macrocycles have several properties that make them suitable as hosts/receptors for relatively unfunctionalized guests with the cavity of the macrocycle providing a steric constraint (Van der Waals) and a solvophobic environment as the primary recognition elements. Inazu and Fukae were the first to attempt to incorporate the TB framework in the cyclophane **16**.[56] The size of the

cavity in this macrocycle proved to be too small and hampered any host-guest complex formation. The same group incorporated the TB framework in a crown ether (17), here the selectivity of the polyether was impeded regardless of the chain length due to the high degree of flexibility that the TB framework introduced to the chain hence it exhibited similar binding affinities to all cations investigated.[57]
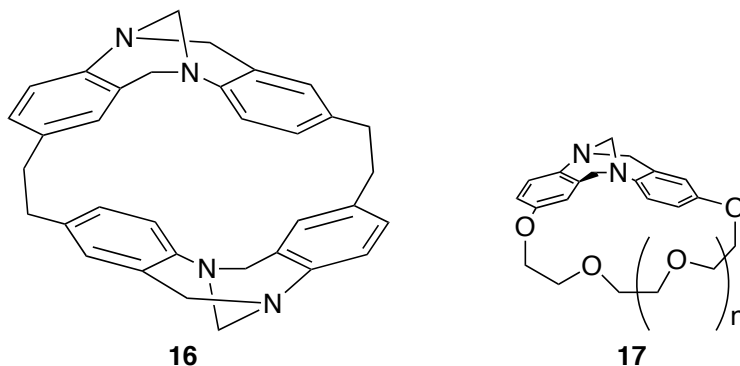
Figure 1.4.1.3
Examples of cyclophanes containing the Tröger's base framework.

Water-soluble cyclophanes incorporating the TB framework were designed and synthesized by Wilcox (Figure 1.4.1.4).[58-62] These molecules were used as chiral receptors for small organic molecules. The first of these receptors (18) linked the Tröger's base framework to a 2,2-di-4-ethyloxyphenyl-isopropyl moiety using secondary ammonium groups as linkages. This receptor exhibited a preference to encapsulate aromatic rings with electron-withdrawing substituents in aqueous acidic media.[58-59]
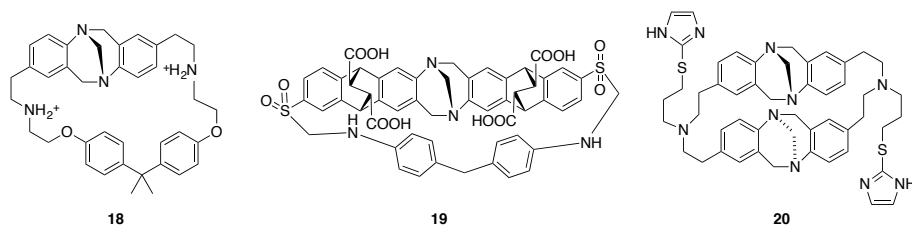
Figure 1.4.1.4
Water-soluble Tröger's base macrocylic receptors

Optically pure receptor 19, depicted in Figure 1.4.1.3, was found to selectively discriminate (+) menthol, (-) menthol and isomenthol.[60-61] In a later study, with the

aim to design a receptor for biologically relevant molecules, a cyclophane containing two Tröger's base moieties linked with two mercaptoimidazole groups (**20**) was made and was found to preferentially bind 4-nitro-phenyl phosphate over analogues without phosphate present.[62]

   Porphyrins are a class of compounds known to coordinate metal ions.[63] Crossly combined two porphyrin units with the Tröger's base framework forming a chiral cleft molecule (**21**, Figure 1.4.1.5).[64-66] When Zn^{2+} was inserted into the porphyrin moieties of **21**, the receptor exhibited strong affinities with varying selectivities towards ditopic diaminoligands[64] as well as histidine and lysine esters.[65] In addition to binding diaminoalkanes, receptor **21** was shown to form a spherical cage by encapsulating dendrimeric tetramine.[66] In another study using receptor **21** coordinating tin instead of zink, Crossley showed that the receptor could also ditopically bind dicarboxylic acids.[67]

21
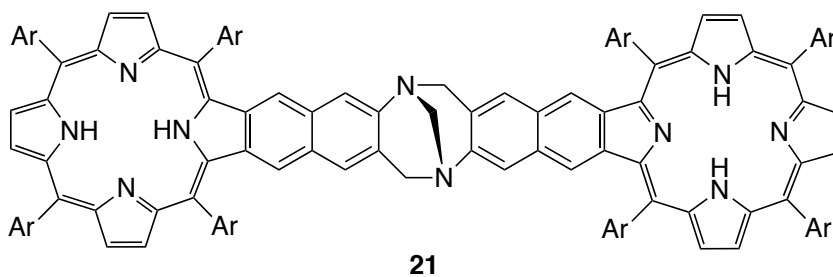
Figure 1.4.1.5
Porphyrin appended Tröger's base receptor

1.4.2 Tröger's base scaffold in a molecular torsion balance

Wilcox utilized the TB framework in a molecular torsion balance (**22**, Scheme 1.4.2.1). This balance was used to determine aromatic edge-to-face[68] and CH_3-π interactions.[69] Understanding these types of interactions are important when understanding the folding of proteins, since these interactions are present. In later studies, the TB-torsion balance was made water-soluble, this made it possible to make the measurements without corrections for dipole moments between folded and unfolded conformers.[70] Diedrich used TB torsion balances to better understand the interactions between the fluorine atoms of the triflouromethyl and the amideo group.[71] This study was followed by the development of a new molecular torsion device containing an indole moiety (**23**, Figure 1.4.2.1) that proved the existence of a favorable interaction between a fluorine atom and the carbonyl carbon of an amideo group.[72] In a later extensive study, Diedrich and coworkers were able to

conclude, using the Tröger's base Torsion balance, that the edge to face interaction was sensitive to increases in polarization of the interacting C-H bond.[73]
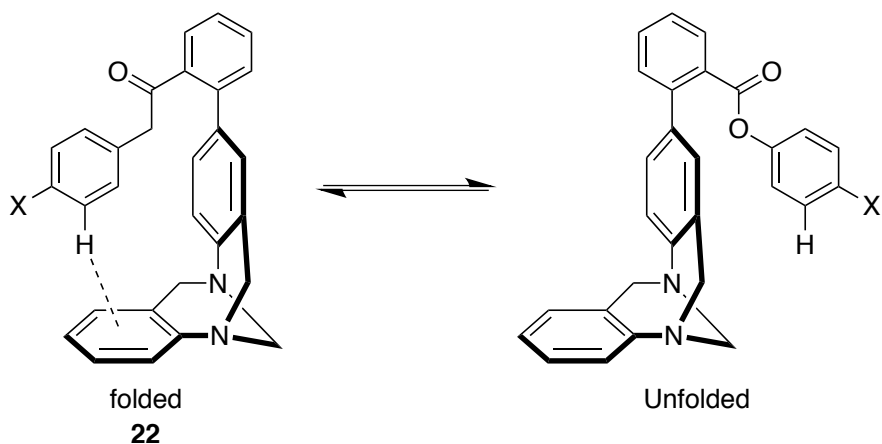
Scheme 1.4.2.1
The Tröger's base torsion balance developed by Wilcox for the determination of aromatic edge-to-face (CH$_3$-π) interaction
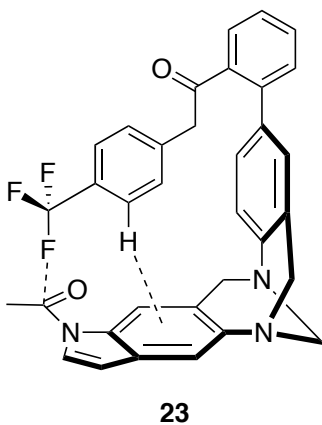
Figure 1.4.2.1
A later example of the Tröger's base torsion balance incorporating flouromethyl

1.4.3 The Interaction of Tröger's base with DNA.

If Tröger's base analogues contain heterocylic moieties, then they have the potential to bind to DNA. The first to introduce heterocylic moieties to Tröger's base and test them for interaction with DNA was Yashima and coworkers (Figure 1.4.3.1).[74] A phenantroline analogue of Tröger's base (**24**) was made that exhibited a higher affinity to bind with DNA than the parent 1, 10-phenatroline. Others, like Demeunynck and Lhomme, have made extensive studies in the field.[21, 75-79] Among the TB analogues developed[21, 75-76] was the proflavine analogue (**25**) that was found to bind a sequence-selectively to calf thymus B-DNA. [77-78] In another example, the non symmetric TB analogue (**26**) containing proflavine and phenatroline fragments showed that both fragments bound specifically to the DNA, with the acridine ring inserting between DNA pairs and the phenatroline fragment residing in one of the DNA grooves.[79]
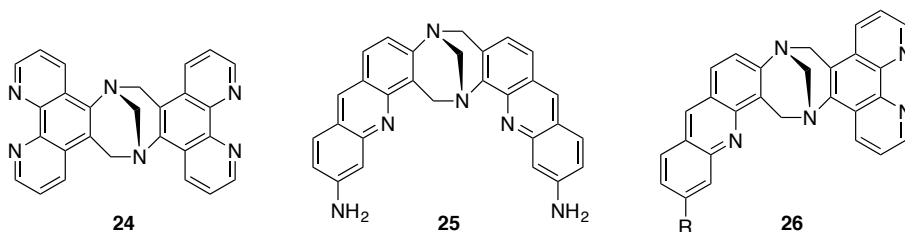
Figure 1.4.3.1
Tröger's base analogues used in studies to bind DNA

The design and making of a small array of fluorescing 1,8-naphthalamide Tröger's base was reported by Veale and Gunnlaugsson (**27**, Figure 1.4.3.2).[80-81] The aim was to have the cationic amino terminus bind to the phosphate found in the DNA backbone at physiological pH. All the variations of **27** exhibited a high affinity towards the phosphate. It could be shown by the aid of fluorescence that cancer cells readily consumed analogue **27** and the TB analogue would find its way to the nucleus.

27
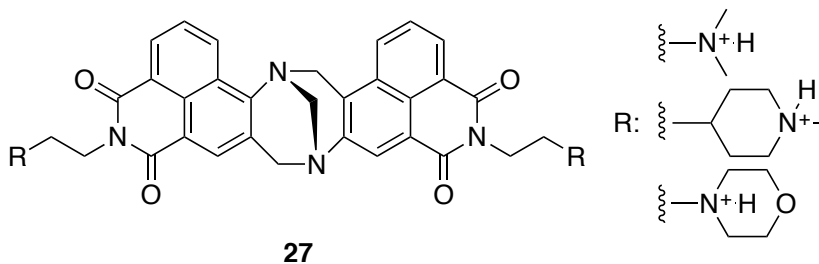
Figure 1.4.3.2
Fluorescing analgues of Tröger's designed to bind to the phosphate backbone of DNA

1.4.4 Tröger's Base as a Ligand in Asymmetric Catalysis

Tröger's base with its rigid structure and chirality makes it a good candidate as a ligand in Asymmetric catalysis. However the applications have not been as many as might be foreseen.

Tröger's base was first used as a ligand by Goldberg and Alper in the hydrosilylation of terminal alkynes. Tröger's base was found to form a stable rhodium (III) complex that catalyzed the above reaction with selectivities of up to 95% for the Z-alkene product.[82] In a later study by Baiker and coworkers, enantiopure (+)-**1** was found to give moderate enantiomeric induction (65% ee) in the Pt/Al$_2$O$_3$ hydrogenation of ethyl pyruvate.[83] Shi and coworkers found that (+)-**1** could induce results of up to 67% ee in the amine-promoted aziridation of chalcones.[84] Reider and coworkers found (-)-**1** to give up to 57% ee when used as a ligand in the 1,4-addition of alkyl lithiums to α,β-unsaturated *t*-butyl esters.[85]

Tröger's base analogues have also been tested as ligands. Harmata studied the ability of different Tröger's base derivatives to induce chirality in the addition of Et$_2$Zn to aromatic aldehydes. It was found that derivative **28** resulted in an 86% ee (Figure 1.4.4.1).[86] Wu and coworkers used the pyrazole Tröger's base analogue **29** in the organocatalytic one-pot Mannich reaction of benzaldehyde, aneline and aromatic ketone in aqueous media resulting in good yields with good *anti/syn* selectivity.[87] Tröger's base analogue **30** was used in a dimeric dipalladium complex that catalyzed the Mizoroki-Heck reaction, showing a high catalytic activity and a measurable selectivity towards *trans*-stilbenes.[88] The catalytic activity of thiourea derivatives of Tröger's base were examined in Michael additions to nitroolefins by Didier and Sergeyev. It was shown that the basicity of Tröger's base made the reaction pH sensitive and no enantioselecivity was observed.[89]

30
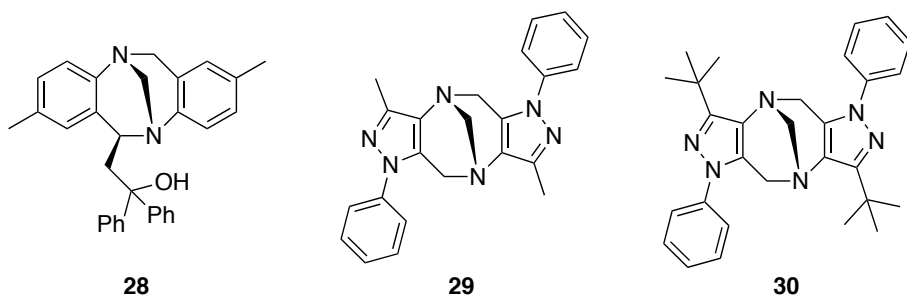
Figure 1.4.4.1
Tröger's base derivatives and analogues used in asymmetric catalysis

Tröger's base embedded materials have seen use in various heterogenous catalytic processes in recent years. Wang and coworkers reported the use of a nanoporous polymer containing covalently bonded Tröger's base frameworks in the catalysis of the addition of Et$_2$Zn to 4-chlorobenzaldehyde.[90] Corma and coworkers have incorporated Tröger's base in mesoporous organosilicates that have been used to catalyze reactions such as the Knoenvenagel, *S*-arylation of aryl iodided and azide-alkyne cycloaddition.[91]

1.5 Reactivity of Tröger's base

Tröger's Base is itself a fairly stable compound. It has 4 benzylic positions, namely on C-6 and C-12 as well as the two methyl groups attached to the aromatic ring. There are 6 aromatic hydrogen atoms that exhibit typical aromatic reactivity. There are also the two nitrogen atoms and the methylene bridge between the nitrogens that can react in some manner. One can assume that if Tröger's base is to react, one has to target one of these positions. Following is an account on what reactions Tröger's base has been involved in to this date. (One can argue that racemization is a special case of reactivity that targets the nitrogens of Tröger's base it was covered in section 1.2.3)

1.5.1 Reactions Involving the Methylene Bridge and the Nitrogens

Tröger's base can readily be alkylated by adding an alkyl iodide or bromide to a solution of Tröger's base (Scheme 1.5.1.1).[18, 92-93] In 2006, Lenev discovered that bisalkylation was possible if the reaction was conducted in dimethylsulfide that is known to be highly polar and alkylating solvent.[12] Another example of this reaction type is allowing **1** to reflux in benzene in the presence of α-bromo

acetophenone reported by Lacour and coworkers in their NMR enantiodifferation study.[94] The product of the above transformation was then treated with excess basic alumina in dichloromethane to expand the methylene bridge to a substituted ethylene bridge by a means of a Stevens rearrangement.[13]
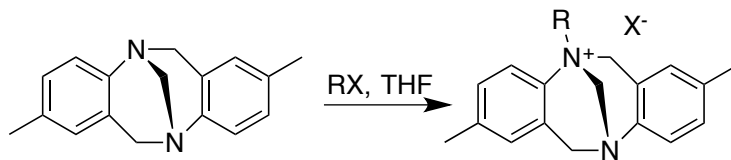
Scheme 1.5.1.1
Alkylation of Tröger's base with an alkyl halide (I or Br)

Lee and coworkers reported that **1** would react with methyl propiolate in the presence of Zink(II) Bromide in acetonitrile to yield enamineone ester **31** in excellent yield (Scheme 1.5.1.2).[95] It later turned out in a study by Lenev, that **31a** was in fact not an enamineone ester but rather the αβ-unsaturated ester **31b**.[96]
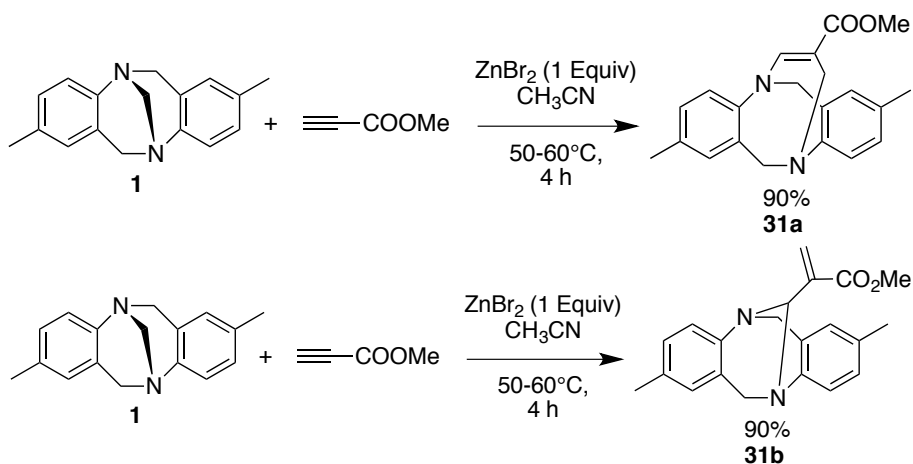
Scheme 1.5.1.2
Reaction of Tröger's base with methyl propiolate.

The apical methylene unit of Tröger's can be removed and replaced. The first example of this was the Nitrosation of **1**, followed by treatment with copper (I) chloride in acetic acid that removed the methylene bridge resulting in the cyclic secondary diamine **32** as reported by Cooper (Scheme 1.5.1.3) and further explored by Mahon.[49, 97] Treating **1** with TFA in DCM followed by treatment with NaOH in ethanol achieves similar results.[98] **32** has been reported to react with

aldehydes and ketones to yield derivatives of **1** substituted on the methylene bridge.[10, 43, 99]
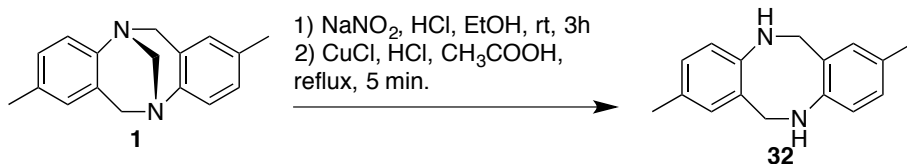
Scheme 1.5.1.3
Removal of the methylene bridge of Tröger's base.

The methylene bridge of TB can be replaced with an ethylene or propylene bridge by allowing **1** to react with the corresponding dibromo alkyl in the presence of lithium carbonate in DMF at 110°C (Scheme 1.5.4).[11, 99]

R= (CH$_2$)$_{2,}$ (CH$_2$)$_3$
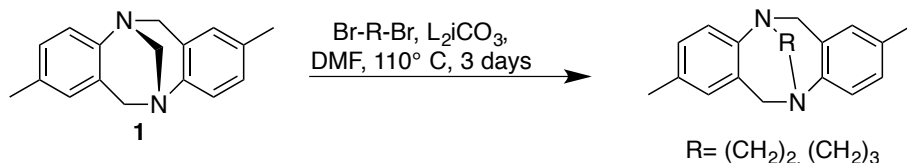
Scheme 1.5.1.4
The reaction of **1** with the dibromoalkyls

Mahon and coworkers reported replacing the methylene bridge of **1** with a [4.5] lactone by allowing **1** to react with pthaloyl chloride in the presence of Et$_3$N in dichloromethane (Scheme 1.5.1.5).[100]
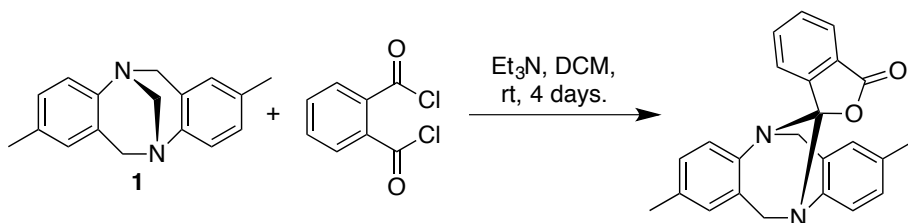
Scheme 1.5.1.5
Reaction of **1** with pthaloyl chloride

Lacaur and coworkers reported in 2011 that the bridging methylene could be expanded to a substituted ethylene in 1 step by treating **1** with diazo compounds in the presence of a [Rh$_2$(OAc)$_4$] catalyst at 100°C in toluene for 6 hours (Scheme 1.5.1.6).[101]The reaction was in a later study modified to use Copper(I) thioophene-

carboxylate as a catalyst instead of the [Rh$_2$(OAc)$_4$].[102] A direct nitrene insertion into the bridging CN bond of **1** is also possible using similar catalysts.[103]
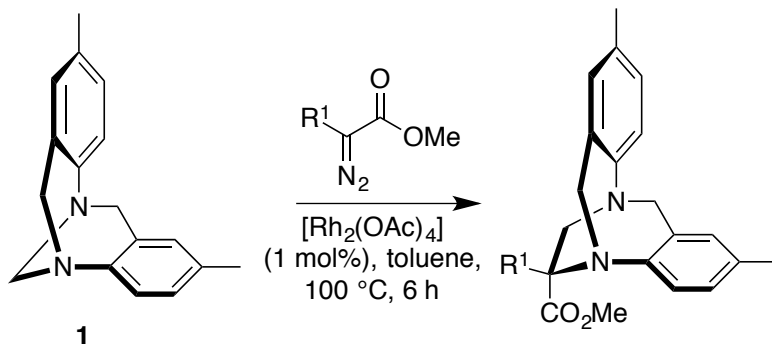
Scheme 1.5.1.6
Rhodium catalyzed expansion of the diazocine ring.

Interestingly when Tröger's base is exposed to Vilsmeier-Haack conditions, the methylene bridge is the moiety that will react and not the aromatic parts. This results in the amination of the methylene bridge (Scheme 1.5.7).[104-106]
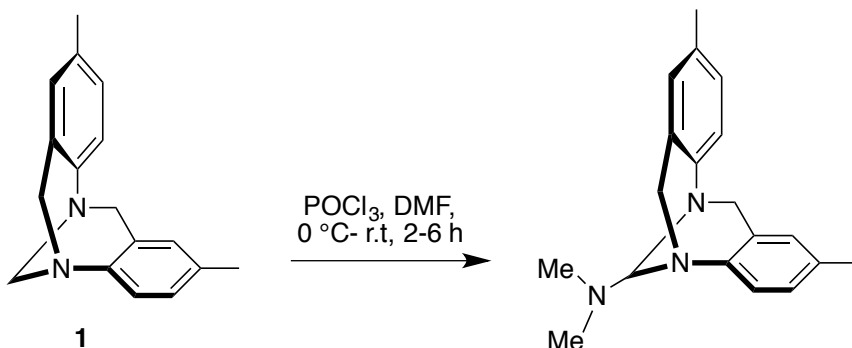
Scheme 1.5.1.7
Exposing **1** to Vilsemeier-Haack conditions

Treating **1** with TiCl$_4$ in the presence of an aldehyde or ketone in an aprotic solvent will replace the methylene fragment with a methano fragment with the substituent pattern of aldehyde or ketone used (Scheme 1.5.1.8).[107]
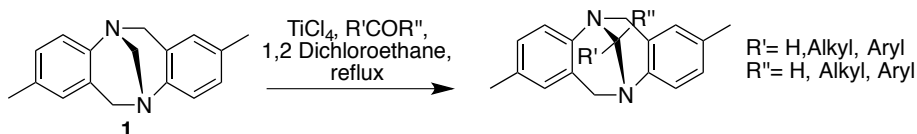
Scheme 1.5.1.8
1-pot exchange of methylene bridge using TiCl$_4$

The methylene bridge of Tröger's base can be removed by treating **1** with dimethyldioxirane (DMDO) followed by treatment with acetic acid anhydride resulting in a bicyclic hydrazine in 64%. It can be worth noting that for some Tröger's base analogues, the yields were better (Scheme 1.5.1.9).[108]
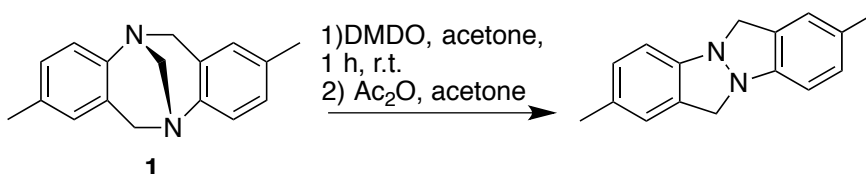
Scheme 1.5.1.9
Demthylenation of Tröger's base

1.5.2 Reaction involving the aromatic parts of Tröger's base

There have been very few reports regarding the direct reactivity of the aromatic moiety of Tröger's base, these have been limited to the reaction of N-Halosucinimide[40,109], hydroxylation in superacidic media[110] and nitration.[111] It is worth noting that is true only for **1** itself, for many Tröger's base analogues with halosubstituted aromatic moieties this is not the case, since the Jensen protocol[29] that allowed for halogenated Tröger's bases there have been a multitude of reports concerning the reactivity of the aromatic moiety of Tröger's base analogues that will not be mentioned further in this chapter.

1.5.3 Reactions involving the 6 and 12 positions

Tröger's base can be oxidized in the 6 and 12 positions using KMnO$_4$ and benzyltriethylammonium chloride (BTEAC) in anhydrous dichloromethane giving rise to the Twisted amide form of Tröger's base (**33**) in 28% yield first reported by our group (Scheme 1.5.3.1).[112] This resulting amide is unusual in the fact that it can react in a Wittig reaction.[113] This will be discussed in more detail in section 2.2.1 in this thesis.
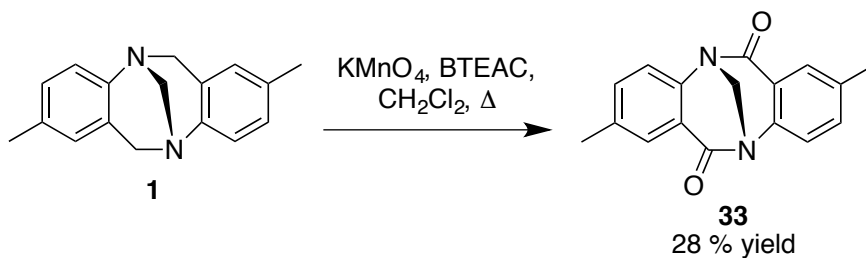
Scheme 1.5.3.1
Oxidation of Tröger's base in the 6 and 12 positions

The group of Cvengroš reported the possibility of α-acetoxylation of **1**. This was promoted by the action of NBS (2 equiv) in the presence of a catalytic amount (20 mol%) [Pd(OAc)$_2$] and a stoichiometric (2 equiv.) amount of KOAc in acetonitrile at 50°C (Scheme 1.5.3.2).[114]
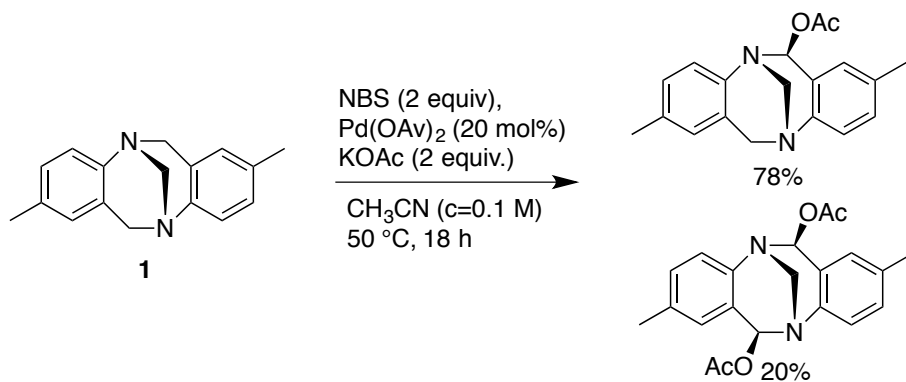
Scheme 1.5.3.2
α-acetoxylation of Tröger's base

Recently the group of Lacour reported the stereoselective and enantiospecific azidation of the 6 and 12 positions of **1**. In their study, TMSN$_3$ and PhIO were used to introduce an azide to the *exo*-6 and *exo*-12 positions of **1**. The resulting *exo*-6-azide TB would then react with different indoles in the presence of Me$_3$Al in dcm resulting in *exo*-6-indole-substituted TB Tröger's base derivatives (Scheme 1.5.3.3).[115]

36
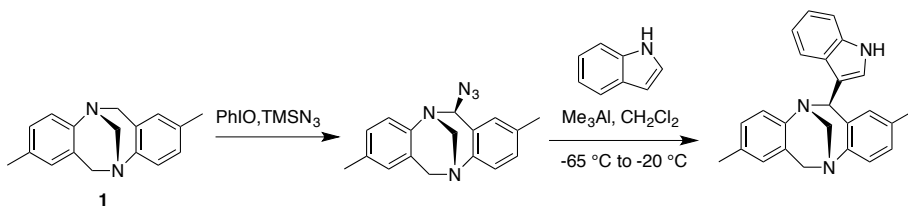
Scheme 1.5.3.3
Azidation of Tröger's base followed by introduction of an indole

The 6 and 12 positions of Tröger's base can be deprotonated with a sufficiently strong base and then quenched with an appropriate electrophile to yield 6-*exo*-substituted and 6-12- *exo, exo*-disubstituted derivatives. Since this is the topic of chapter 2 in this thesis, this will be discussed further and in much more detail there.

Chapter 2: Modification of Tröger's Base (papers I, II, III)

2.1 Background

As mentioned in the introduction, there are a plethora of reagents and methodologies that can be used to modify Tröger's base and its analogues and derivatives. In our group's research, we have attempted and succeeded in modifying **1** in a range of ways. The protocol (mentioned earlier in section 1.3.1) using TFA in the Tröger's base condensation allowed the easy access to halogen substituted Tröger's base analogues, this in turn has paved the way for cross coupling reactions between the aryl halide moiety of the Tröger's base analogue and various reactions, including palladium cross-couplings there are examples of Sonogoshira (Scheme 2.1.1, a),[116-117] Suzuki-Miyaura (Scheme 2.1.1, b),[118-121] Pd-catalyzed amination (Scheme 2.1.1, c),[122-123] Stille/ Suzuki/ or Negishi (Scheme 2.1.1, d), [121] palladium catalyzed cyanations have also proved to be effective in forming C-C bond (Scheme 2.1.1, f),[120, 122] In addition, Ulmann conditions have been employed to introduce C-O bonds (Scheme 2.1.1, g).[118, 119, 124]
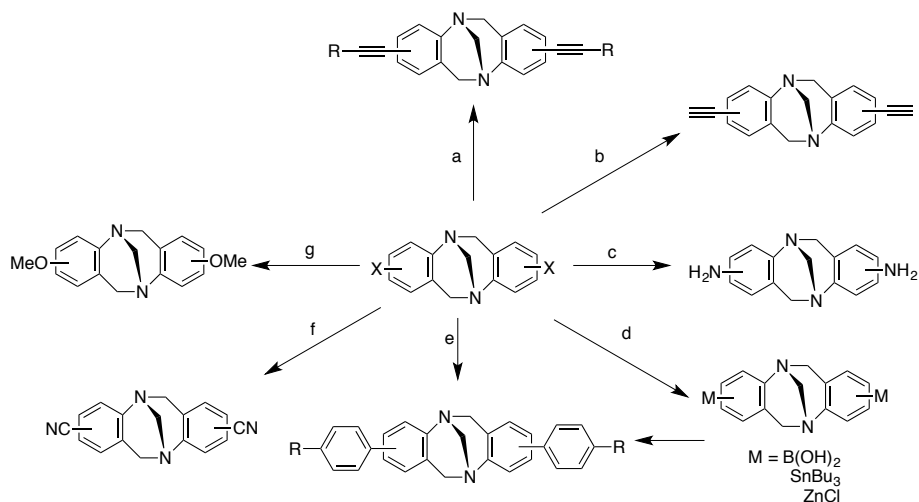
Scheme 2.1.1
Tröger's base analogues that have become accessible since our development of a protocol for the synthesis of halogen substituted Tröger's base analogues. a) Pd(PhCN)$_2$Cl$_2$, P(tBu)$_3$, CuI, alkyne-R substrate; b) ethynylmagnesium bromide, Pd(PPh$_3$)$_4$; c) 1) Pd$_2$(dba)$_3$, BINAP, NaOtBu, benzophenone imine, toluene. 2) HCl (aq), THF; d) for example, nBuLi, THF, −78 °C, B(OCH$_3$)$_3$, then Pd[P(tBu)$_3$]$_2$, CsF, substituted halobenzene; e) Pd[P(tBu)$_3$]$_2$, CsF, substituted phenylboronic acid; f) Zn(CN)$_2$, Zn, Pd(Ph$_3$)$_4$, dppf; g) NaOCH$_3$, CuCl, MeOH/DMF.

Other examples of our work in modifying **1** and its analogues and derivatives involve the metalation of the C-6 benzylic protons and then quenching with an electrophile. This has proved an effective way to obtain asymmetric Tröger's base derivatives (Scheme 2.1.2). Harmata was the first to report using such a strategy on Tröger's base itself. This involved treating **1** with BF$_3$·OEt$_2$ in THF at -78 °C followed by nBuLi and then quenching with an electrophile. This allowed the synthesis of *exo*-monosubstituted Tröger's base derivatives.[125] Dissymmetric *exo,exo*-Disubstituted derivatives could be achieved using this strategy by repeating the process on the *exo*-monosubstituted Tröger's base derivative (Scheme 2.1.2).[126] It was later reported by Harmata that the presence of the Lewis acid was not necessary if tBuLi was used instead of nBuLi.[86] Our group later developed a strategy that in addition to allowing for the direct synthesis of *exo,exo*-disubstituted TB derivative also improved the yields substantially by using sBuLi/TMEDA as a base, since this is the topic of Paper II in this thesis, it will be discussed in detail in section 2.2.
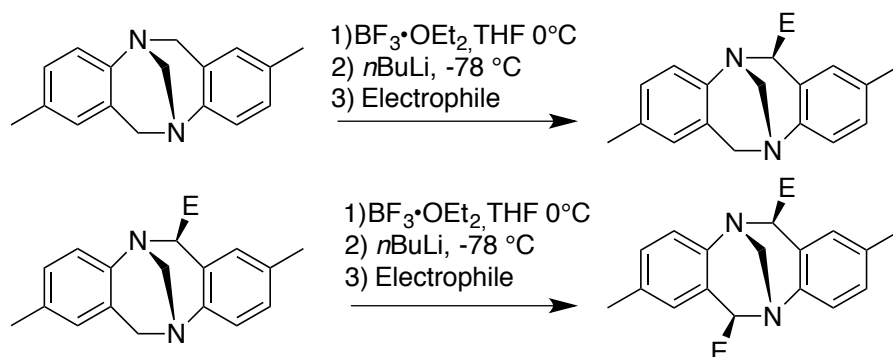
Scheme 2.1.2
Metalation and electrophilic quench of Tröger's base prior the use of TMEDA/*s*BuLi.

2.2 Modification of the 6 and 12 positions of Tröger's base

2.2.1 Benzylic oxidation and Wittig reaction (Paper I)

In our work involving the modification of **1** we developed a procedure to oxidize both the 6 and 12 benzylic positions of **1**, resulting in the amide **33** (see Scheme 1.5.3.1). This amide was interesting in that it had its nitrogen lone pair twisted out of conjugation with carbonyl double bond making it a twisted amide.[127-128] Due to this, twisted amides exhibit a much higher reactivity than regular amides, they will for example react in a Wittig olefination,[128-129] something that amides in general do not. Knowing this, a protocol for the olefination of pthalamides using commercially available (ethoxycabonylmethylene)-triphenylphospine was tested[130] and proved effective in the olefination of both the mono- (**34**) and di **33** (Scheme 2.2.1.1) This resulted in an 83:17 *E/Z* mixture of mono-olefin (**35**) in 80% (mixture) yield and a 51:39:10 *E,E:E,Z:Z,Z* mixture of di-olefin (**36**) in 77% yield (mixture). The configuration of the olefins was of no consequence in the next step and were readily hydrogenated using Pd/C resulting in the first ever synthesized *endo*-substituted Tröger's base derivatives (**37**) and (**38**).
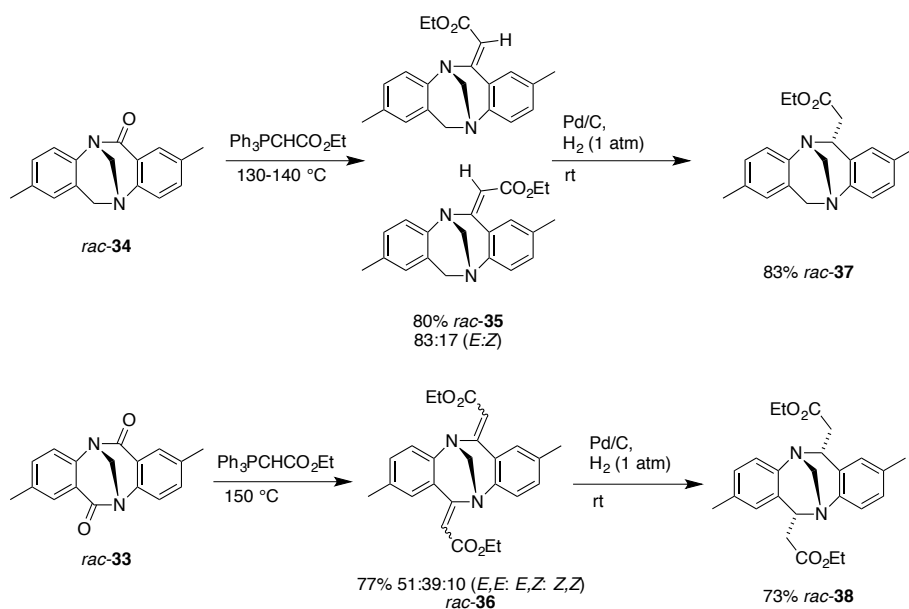
Scheme 2.2.1.1
The first reported synthesis of *endo*-substituted Tröger's base dervatives **monoendoester** and **diendoster**

Having synthesized **38**, it was decided to see if we could synthesize TB derivatives with functional groups directed towards the inside of the TB cavity. One possible approach to this was to introduce an oligoethylene glycol strap. To facilitate this the ester groups were reduced using LAH in THF at rt resulting in the alcohol **(39)** in 78% yield. An oligoethylene strap, was then introduced using by heating **39** together with diethylene glycol ditosylate in THF in the presence of NaH. This resulted in a 1:1 mixture of *meso*-**15b** and *rac*-**15b** in 30% yield (Scheme 2.2.1.2). The *meso*-**15b** was tested as a receptor for different ions and this is discussed in more detail in chapter 3.

Scheme 2.2.1.2
Synthesis of receptors *meso*-**15b** and *rac*-**15b**

2.2.2 Metalation and electrophilic quench (Paper II)

We set out to modify the benzylic 6,12 positions of **1** to improve the toolset available to modify Tröger's base and its analogues. Amide bases such as *s*BuLi/TMEDA are known to remove heterosubstituted benzylic protons, resulting in a metalated benzylic species.[131] We decided to test if this could be done on the 6 and 12 positions of Tröger's base. As it turned out (Paper I), treating **1** with 1.1 equivalents of *s*BuLi and TMEDA and then quenching with an electrophile resulted in the *exo*-6-monosubstituted TB derivative in very good to acceptable yields (see Table 2.1), traces of *exo,exo*-disubstituted were isolated from the reaction mixtures. This observation led us to try if disubstitution could be achieved by increasing the number of equivalents of base. Treating **1** with 2.2 equivalents of *s*BuLi/TMEDA followed by quenching with a desired electrophile resulted in the *exo,exo*-6,12-disubstituted TB derivative in very good to acceptable yields, (see Scheme 2.2.2.1 and Table 2.2.2.1).

Scheme 2.2.2.1
Metallation of Tröger's base and direct addition electrophilic quench

Tabel 2.2.2.1

Metalation of **1** and quenching with electrophile yielded the following results

Entry	TMEDA/ sBuLi (equiv)	Electrophile (equiv)	Product (all *rac*)	Yield
1	1.1	TMSCl (1.2)	*exo*-6-TMS-TB	76%
2	1.1	BnBr (1.2)	*exo*-6-Bn-TB	51%
3	1.1	MOMCl (1.2)	*exo*-6-MOM-TB	85%
4	0.8	Et₂NCOl (1.2)	*exo*-6-Et₂NCO-TB	42%
5	1.0	*i*PrNCOCl (1.2)	*exo*-6-*i*PrNCO-TB	32%
6	2.2	TMSCl (2.5)	*exo,exo*-6-12-diTMS-TB	62%
7	2.2	BnBr (2.5)	*exo,exo*-6-12-diBnTB	74%
8	2.2	MOMCl (2.5)	*exo,exo*-6-12-diMOM-TB	81%
9	2.2	Et₂NCOl (2.5)	*exo,exo*-6-12-diEt₂NCO-TB	42%
10	2.2	*i*PrNCOCl (2.5)	*exo,exo*-6-12-di*i*PrNCO-TB	44%

Interestingly, when electrophiles that would result in tertiary amides were used (table 2.1, entries 4, 5, 9, 10), the yields were poor and a mixture of compounds and mostly starting material was obtained. It was speculated that the α-proton of the formed amide was being deprotonated by the excess **1**-Li species /excess *s*BuLi-TMEDA present. This in turn would result in the **1**-Li reverting to **1** explaining the large presence of starting material. To counter this setback, the **1**-Li species was added dropwise to an excess of electrophile. This improved the yield of the reaction substantially, for all electrophiles tested except the monoaddition of the benzylbromide (entry 2) as seen in Scheme 2.2.2.2 and Table 2.2.2.2.
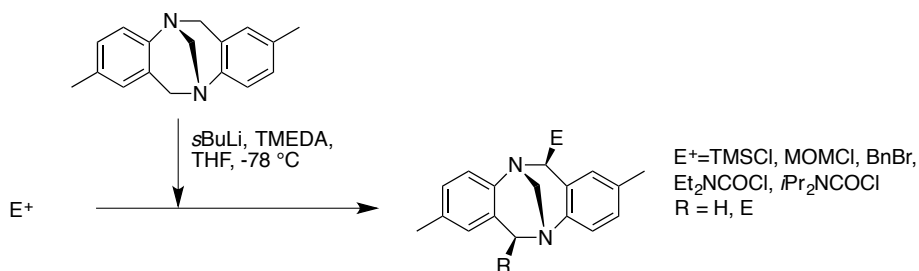
Scheme 2.2.2.2
Inverse addition method

Table 2.2.2.2
Inverse addition method

Entry	TMEDA/ sBuLi (equiv)	Electrophile (equiv)	Product (all *rac*)	Yield
1	0.95	TMSCl (>10)	*exo*-6-TMS-TB	72%
2	0.95	BnBr(>10)	non	0%
3	0.95	Et$_2$NCOCl (>10)	*exo*-6-Et$_2$NCO-TB	70%
4	0.95	*i*Pr$_2$NCOCl (7.5)	*exo*-6-*i*PrNCO-TB	73%
5	3.0	TMSCl (>10)	*exo,exo*-6-12-diTMS-TB	89%
6	3.0	BnBr(>10)	*exo,exo*-6-12-diBnTB	96%
7	3.0	Et$_2$NCOCl (>10)	*exo,exo*-6-12-diEt$_2$NCO-TB	97%
8	3.0	*i*Pr$_2$NCOCl (7.5)	*exo,exo*-6-12-di*i*PrNCO-TB	98%

In the course of the studies we attempted to see if the direct addition method could be used to modify 1 with different substituents in the *exo*-6 and *exo*-12 in one pot procedure. This was possible! Using TMSCl and BnBr as electrophiles produced the *exo*-6-TMS-*exo*-12-Bn-Tröger's base (**40**) derivative in 24% yield (Scheme 2.2.2.3).
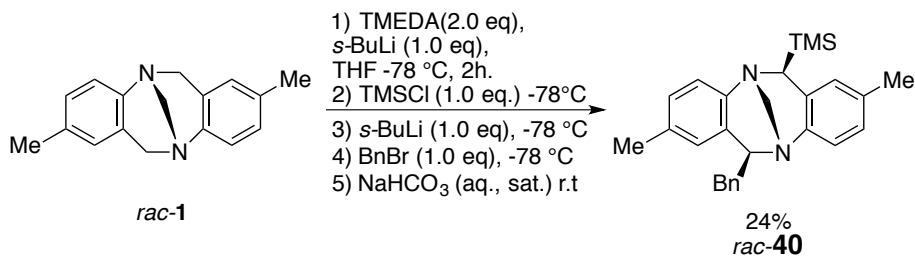
Scheme 2.2.2.3
Synthesis of Tröger's base derivative *rac*-**40** demonstrating the versatility of our methodology.

2.2.3 Isomerization of *exo*-6 monosubstituted and *exo, exo,*-6,12 disubstituted Tröger's amides into their *endo*-substituted isomers (Paper III)

Further analysis of the product mixture when adding an amide forming electrophile to the **1**-Li species it was found that roughly 20 % was *endo*-6-monosubstituted Tröger's base (Paper II). This was an interesting result, since there is only one other known pathway to *endo* substituted TB derivatives/analogues. This method involves the oxidation of the benzylic positions of Tröger's base followed by a Wittig reaction on the resulting twisted

amide. The resulting olefin is then catalytically reduced.[113] This method normally results in yields of 10-20% over 3 steps and improving this yield would make *endo*-substituted TB derivatives more accessible. Since we were able to isolate an *endo* monosubstituted derivative we decided to pursue this route further and see if we could find a new method to make *endo*-substituted TB derivatives (Paper III).

In our previous paper, we had speculated that the reason for the presence of the *endo*-substituted Tröger's base derivative was the action of a base on the α-hydrogen of the amide group. To better understand the mechanism it was necessary to determine which of the *endo* and *exo* isomers was the thermodynamic product. As experiments mentioned in paper III proved, the *exo*-isomer was the thermodynamic product. Knowing this, the stage was set to optimize the conditions to yield the *endo*-isomer.

An initial investigation showed that adding *n*BuLi (1.1 equiv) to (**41**) in THF in the presence of diisopropylamine (1.1 equiv, DIPA) at -78 °C, and allowing the reaction to slowly reach room temperature overnight resulted in a majority of (**42**) being isolated after quenching. The presence of DIPA proved essential, without it **1** was retained. It was decided to systematically to investigate 5 different parameters, namely quenching temperature, the amount and type of base used, reaction time, and the type of quencher used in order to optimize the reaction to yield (**42**).

These optimizations (paper II) helped us achieve an isolated yield of 86% of (**42**). This was done by changing the amine from DIPA to dibenzylamine (DBA) and allowing the reaction to react at -20°C for 3 hrs and then quenching with a saturated solution of sodium bicarbonate (Scheme 2.2.3.1).
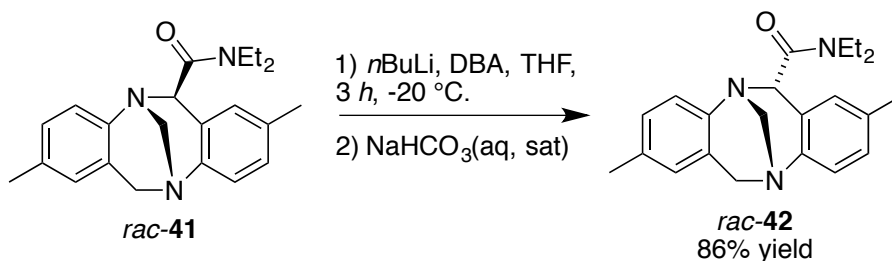
Scheme 2.2.3.1
Optimized TB-monoamide isomerization reaction

Having optimized the isomerization of **41** to **42**, attention was turned to the isomerization of the **43** to the **44**, fortunately the optimized conditions for the monoisomerization only required a slight modification of equivalents and reaction time to achieve an acceptable yield of **44** (Scheme 2.2.3.2).
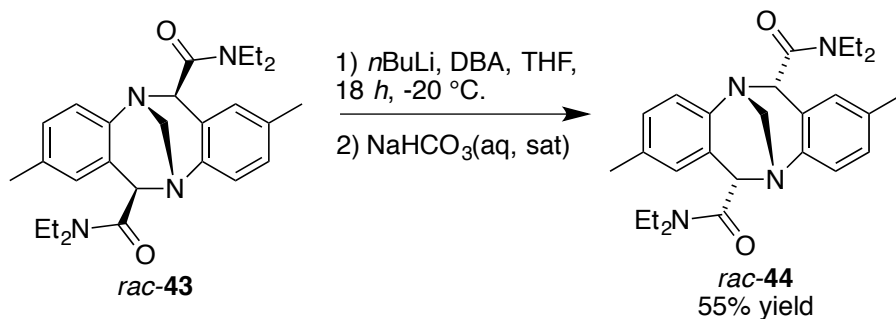
Scheme 2.2.3.1
Optimized TB-diendoamide isomerization reaction

2.2.4 Attempts to transform a tertiary amide

Tertiary amides are known to be bench stable and not very reactive; we hence set out to transform the tertiary amide into a more reactive group without changing the endo positioning of the group. A number of reagents were tested; an account of each follows bellow.

2.2.4.1 Hydride reducing agents

Hydride reducing agents were the first reagents used in our attempts to alter the amide into something more useful. The first hydride tested was LiAlH$_4$, this reagent is known to reduce tertiary amides to a mixture of amines and alcohols.[132] This proved unsuccessful in reducing our amide with no reaction taking part except the gradual base catalyzed transformation of *endo* amide **42** to *exo* amide **41**. This however did not stop us from testing other hydrides, H.C Brown reported the reduction of tertiary amides using Li(C$_2$H$_5$)$_3$BH.[133] This reagent did not react at rt after 1 hour. Leaving the reaction mixture for 12 hours offered traces of the *exo* amide indicating that the reagent was catalyzing the slow endo/exo isomerization. NaBH$_4$ did not react with the amide.[134]

2.2.4.2 Samarium iodide-Amine-Water

Since the hydrides did not manage to reduce the amide group, a method reported by Procter was tested.[135] In the report, SmI$_2$ was used together with an amine and water to reduce all types of amides (primary, secondary and tertiary) to alcohols via a single electron mechanism (Scheme 2.2.4.2.1).

47
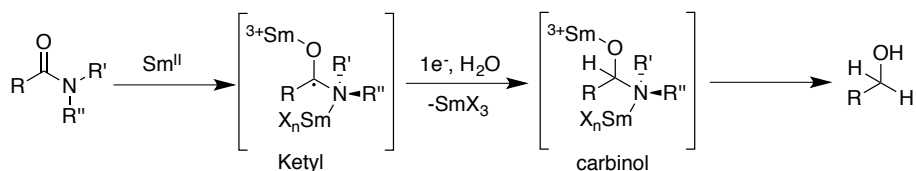
Scheme 2.2.4.2.1
Proposed mechanism for the reduction of amides using SmI$_2$

This procedure worked very well with a model compound diethyl benzyl amide (**33**), where we were able to isolate benzyl alcohol with a yield of 82%. When we attempted it with amide **42** we managed to isolate product **45** (Scheme 2.2.4.2.2). Evidently the nitrogen atoms present in the diazocene ring where coordinating with Samarium and was breaking the C-N bond between the methylene and one of the diazocene nitrogens instead of the C-N bond of the amide, also the methylene bridge was opened and hence the *endo* configuration was lost, this was the reason that this method was not further pursued.
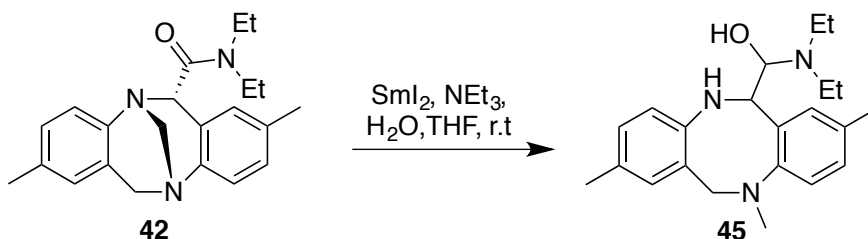
Scheme 2.2.4.2.2

Attempted reduction of diendoamide with SmI$_2$, NEt$_3$, H$_2$O in THF.

2.2.4.3 Tebbe's Reagent

Tebbe's reagent (**46**) is known to react with carbonyl carbon resulting in an alkene. It is known to work well with ketones and has also been reported to work on tertiary amides.[136] It did however not react with amides **31** and **32** using 1.1 and 2.2 equivalents of Tebbe's reagent in THF at 0° (Scheme 2.2.4.3.1).
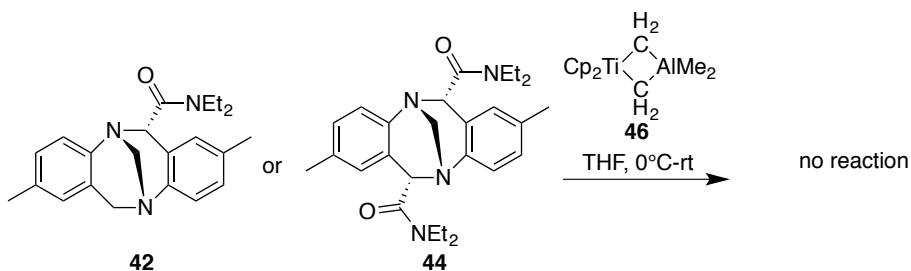
Scheme 2.2.4.3.1
Tebbe's reagent with amides **42** and **44**

2.2.4 Schwartz Reagent

Schwartz reagent (Cp$_2$ZrHCl) has been reported to reduce amides to aldehydes. However it did not reduce amide **42** (Scheme 2.2.4.4.1) with no reaction taking place. In the mechanism suggested by Spletstoser *et al*,[137] it was suggested that coordination of the amide nitrogen to the Zr atom in a 4 ring intermediate with the oxygen to be a part of the mechanism (Scheme 2.2.4.4.2). In **31** the nitrogens of the diazocene ring can also coordinate in a 5 membered ring instead (Scheme 2.2.4.4.3), and this would hinder the transformation to aldehyde taking place another reason that could also explain no reaction is the unfavorable sterics involved.
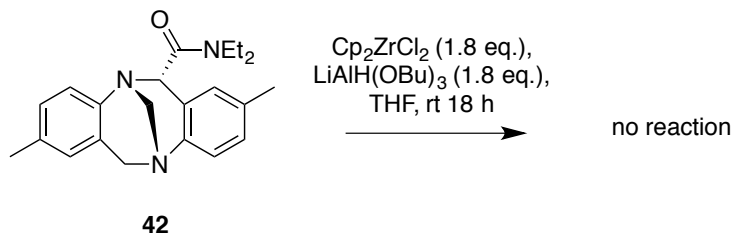
Scheme 2.2.4.4.1
The attempted reaction between **42** and Schwartz reagent
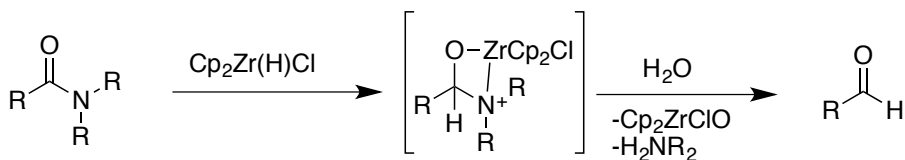
Scheme 2.2.4.4.2
Suggested mechanism for Schwartz reagent
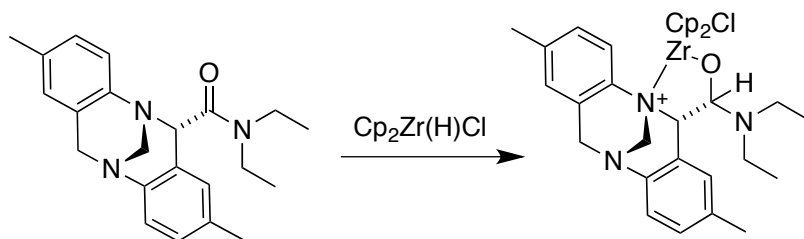
Scheme 2.2.4.4.3
suggested reason for Schwartz reagent not reacting with amide **42**.

2.2.4.5 Alkynyl boranes

Alkynyl ketones can be synthesized from tertiary amides by the action of alkynyl boranes as reported by Yamaguchi (Scheme 2.2.4.5).[138] Unfortunately, while this method did work with the model compound diethyl benzyl amide this method did not work with our Tröger's base amides, most likely due to the bridging nitrogens of **31** and **32** interacting with the BF_3 due to their Lewis bacisity.
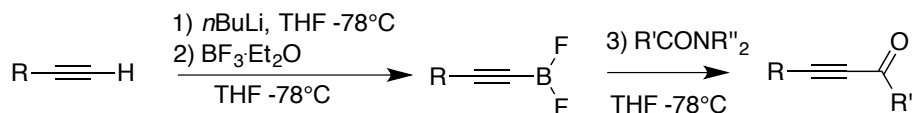
Scheme 2.2.4.5
Attempted alkynylation of **42** resulted in no reaction taking place.

2.2.4.6 Mo(CO)$_6$ TMDS THF

Tinnis *et al* reported a method that could reduce a tertiary amide into its corresponding aldehyde using a $Mo[CO_6]$ catalyst and 1,1,3,3 tetramethyldisiloxane (TMDS) as a hydride source.[139] When this method was attempted on amide **32** using 5 mol% $Mo(CO)_6$ and 8 equivalents of TMDS in THF at room temperature for 12 h no reaction took place (Scheme 2.2.4.6.1).
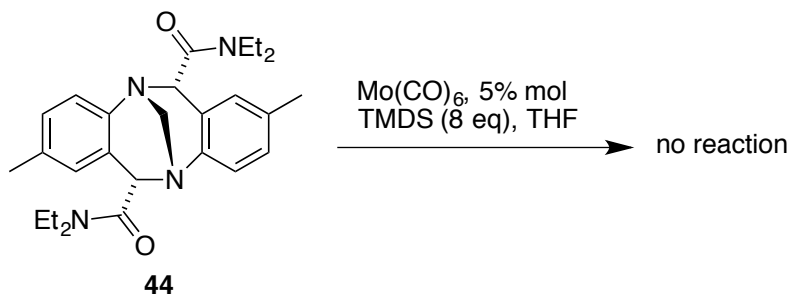
Scheme 2.2.4.6.1
Attempted reduction **44** using Mo(CO)$_6$ catalyst

2.2.4.7 Tf$_2$O, DCM, diethylmalonate/LiHMDS

Wang and coworkers reported the use of triflic anhydride (Tf$_2$O) to activate tertiary amides towards Knovenagel-type reactions.[140] While working with the model compound diethyl benzyl amide, this method did not work on our amides with no reaction occurring (apart from some isomerization to the *exo* isomer). A possible reason for this is that the triflic anhydride would coordinate to the nitrogen of the diazocene ring and hence would not activate the amide towards further reaction.

2.2.4.8 Alcoholysis

Alcoholysis of amides has been reported.[141] An attempt was made using butanol. Amide **42** was refluxed in butanol in a Dean-Stark trap for 72 h with no reaction occurring (Scheme 2.2.4.8.1).
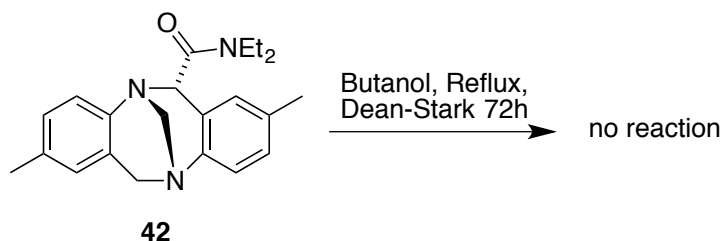
Scheme 2.2.4.8.1
Attempted alcholysis of amide **42**.

2.2.4.9 TMDS/Ti(iPrO)₄

Laval *et al* reported the use of a mild titanium-based system for the reduction of tertiary amides. In this method 1,1,3,3-tetrmethyldisiloxane was activated by Titanium(IV) Isopropoxide for the reduction of the amide.[142] In the report the method was reducing tertiary amides to aldehydes in yields of 75-90% at room temperature. This method seemed promising so the method was attempted on amide **42** (Scheme 2.2.4.9.1). When attempted at room temperature the reaction did not work, however after refluxing for 24 h, traces of new compound could be seen when monitoring the reaction with thin layer chromatography (TLC). The mass spectrum of the reaction mixture revealed a peak corresponding to the molar mass of the aldehyde form (**47**). Knowing this it was decided to see if the reaction would proceed faster using a microwave oven. It was found that microwaving the reaction mixture at 110 °C for 8h would result in full conversion of the amide. After the work-up, the formed aldehyde changed color from colorless to red in the presence of air. This is an indication of the formation of the twisted amide forming (see paper I), hence the aldehyde had to be used immediately before it was fully converted to the twisted amide form. The first thing that came to mind to use was LiAlH₄ in THF, hence the newly formed aldehyde was dissolved in dry THF and added to a suspension of LiAlH₄ in THF at 0 °C. After 1 hour TLC revealed that all the aldehyde had been converted to a new compound. The reaction was quenched using ethyl acetate followed by a saturated Rochells salt solution. After an aqueous workup and column chromatography a diol (**48**) was isolated in 65% yield from **42**. However, there was some difficulty in determining if it was *Endo, Endo* or *Exo, Exo* substituted using NMR techniques, so it was decided to convert the diol to something that could have the structure more easily determined. The diol was allowed to react with TEMPO and 3-nitrobenzoyl chloride in DCM at room temperature over 1 hour. Resulting in diester **49** in 97% yield. **49** was readily crystalized from ethyl acetate and heptane. The obtained crystals were used in crystallographic x-ray determination that revealed (rather disappointingly) an *exo, exo* substitution pattern.
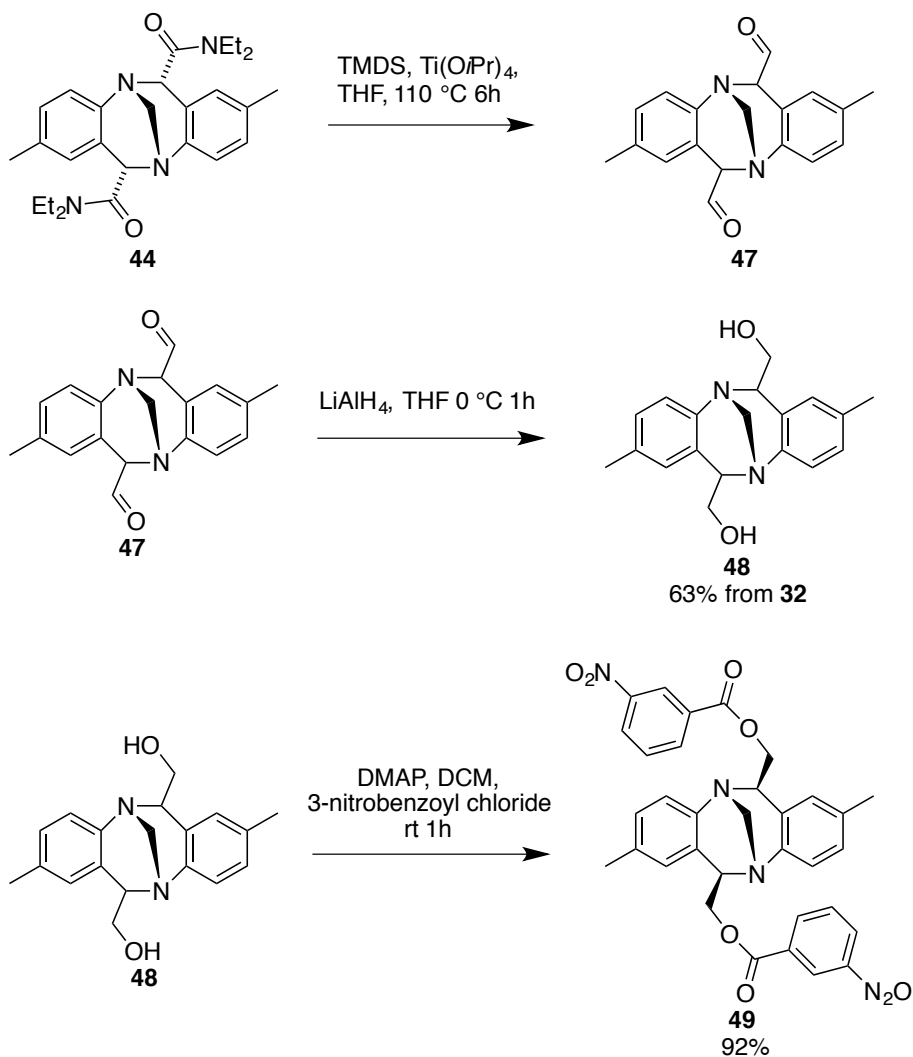
Scheme 2.2.4.9.1
Attempt to reduce amide using TMDS/Ti(O*i*Pr)$_4$

2.2.4.10 Birch Reduction variations.

Some variations of Birch reductions were attempted since there have been reports of Birch reduction variations reducing tertiary amides,[143] however these conditions proved too harsh and *p*-methylaniline was the major product (Scheme 2.2.4.10).
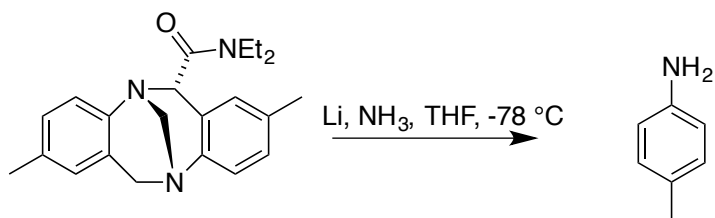
Scheme 2.2.4.10
Birch reduction of monoexoamide

2.2.5 Attempts to block the enolization of the amide

Some efforts were made to see if the enolization reaction of **41** could be manipulated by quenching the reaction with a non-protic electrophile such as TMSCl or MeI. **41** was subjected to *n*BuLi (1.1 equiv) and benzylamin (1.1 equiv) in THF at -20°C for 3h and then quenched with either TMSCl or MeI. One could see a new mass forming on HRMS that was corresponding to that of a TMS or Me group being added to the amide, however we were unable to isolate any compound using chromatography. It seems likely that what happens is that the TMS or methyl group attaches to the oxygen, trapping the enolate and this reverts to the *exo*-amide in the presence of acid (Scheme 2.2.5.1)

R= Me or TMS
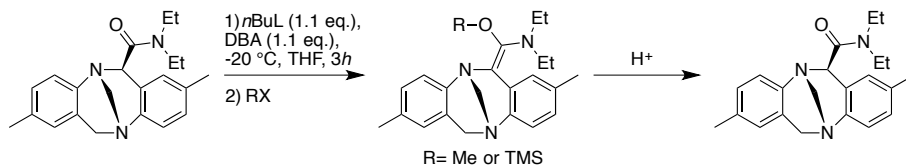
Scheme 2.2.5.1
Attempts to block enolization of amide.

Chapter 3: Tröger's base structure in receptor (Papers I and IV)

3.1 Background

Tröger's bases structure makes it an interesting building block for receptors. In chapter 1, we observed how various groups had used the Tröger's base motif in different receptors. Our group had contributed with two receptors, namely receptors **15a** and **15b** (See figure 1.4.1.2).

We developed Tröger's base analog **15a** as a receptor for bisammonium alkyl salts. The receptor was composed of a central Tröger´s base moiety with 18-crown-6 ether moieties attached to the aromatic ends. The V-shape of Tröger's base provides a hydrophobic cavity and the two crown ether moieties provide binding sites for ammonium. In an earlier study, where we tested the receptors binding affinity to terminally substituted bisammonium alkyl chains, it was found that the ideal length of the alkyl chain in the bisammonium ligand was seven carbons. Seeing as the receptor had a hydrophobic pocket and that the bisammonium ligand was stretched across it, it was concluded that if a substituent was placed attached on the C-4 of the heptane chain, the substituent would interact with the pocket and that the receptor would discriminate between different substituents on the basis of this interaction. It was also initially thought that this interaction could be used to quantify the contribution of each of the substituents to the ΔG of the reaction in the form of $\Delta\Delta G$.

Receptor **15b** was made to test the utility of the Wittig reaction of the twisted amide Tröger's base in making Tröger's base analogues with substituents oriented inside the aromatic cavity. When it was isolated it we decided to test **15b** for its affinity towards different cations. An account of the binding study of receptor **15b** is mentioned in section 3.3 below.

3.2 The 18-crown-6 Tröger's base receptor

3.1.1 Synthesis of receptor

The receptor was made simply by the acidic condensation of the commercially available aniline **50** in ethanol in the presence of formaldehyde as previously reported[55] (Scheme 3.1.1).
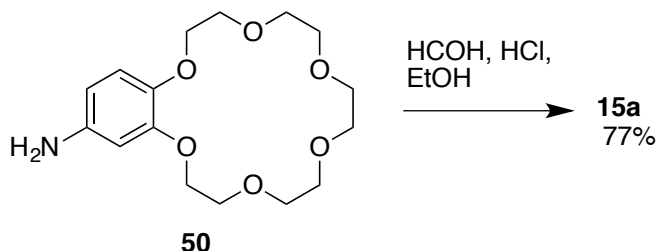
Scheme 3.1.1
Synthesis of receptor **15a**

3.1.2 Synthesis of Ligands

To test if the receptor could distinguish ligands on basis of substituents, 4 different ligands were synthesized, each with a different substituent on C-4. Methyl **(52)**, phenyl **(53)**, benzyl **(54)** and cyclohexyl **(55)** where chosen as the substituents that would be tested next to the unsubstituted ligand **(51)**. The syntheses of these ligands are described in paper IV, the ligands can be seen in figure 3.2.
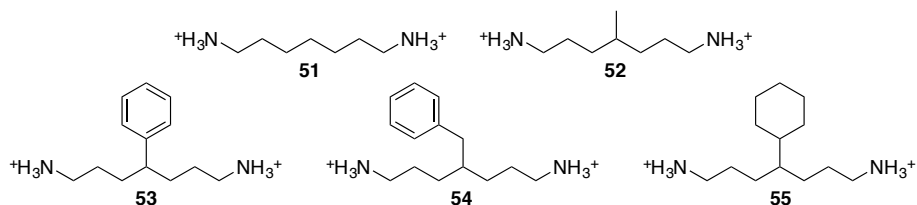
Figure 3.2
Ligands used in study

3.1.3 Experimental determination of binding constants

The binding constants were determined using NMR-titration methodology;[144-145] this basically involves recording NMR-spectra at varied concentration levels of ligand and receptor and noting differences. As mentioned in paper IV, it was observed that that the binding constant was too high to be determined directly for each ligand individually using NMR-titration methodology; performing competitive titrations between the different ligands solved this. The phenyl-substituted ligand had demonstrated the strongest binding to the receptor so this ligand was chosen to compete with the other ligands. The relative binding constants of each ligand in relation to the phenyl ligand could then be determined. However, since it is more convenient to compare to relative values to an unsubstituted ligand, the values were adjusted for this (see paper IV). We could conclude from the obtained values of ΔΔG that **53** bound most favorable to the receptor, followed by **52**, **51**, **54** and finaly **55**. Why we observe this order, is open to interpretation, a reasonable explanation for the relatively poor binding of the **54** and **55** ligands is due to the bulk of these two substituents. Both these substituents would have problems fitting into the limited space of the cavity provided by the receptor. Binding to the receptor would thus expose the largely non-polar substituents to the polar solvent that would mitigate some of the benefits of binding to the receptor. The smaller substituents would be able to orient inside the hydrophobic cavity and would lessen the amount of polar-non-polar interaction with the solvent that would essentially contribute to the more favorable binding of the **52** and **53** ligands to the receptor. An added stabilizing effect for **53** is the possibility for an edge to face π-interaction with the aromatic moieties of Tröger's base. Initially we thought it would be a good idea to test this hypothesis using computational chemistry, since computational chemistry would tell us something about how the substituent of the ligand would orient itself in relation to the receptor in the complex in addition to data obtained from NMR.

3.1.4 Using the titration series as a benchmark for determining the quality of different computational methods in predicting chemical interactions

When we first started making molecular models of the ligands and their complexes, it was decided to use molecular mechanics (MM).[146] Initially, we modeled the receptor, ligands, and the complexes using a conformational search using a solvent potential for water and a OPLS05 force field,[147-148] this gave some interesting results. The first thing that occurred to us was that the obtained values of ΔΔG calculated using the E^0 value of the lowest energy conformations obtained from the calculations did not match the experimental data, with the predicted values of ΔΔG. This was hardly surprising since we had used a solvent potential

for water and our experiments were conducted in a mixture of chloroform and methanol.

There was one slight problem and that was that the MM did not include parameters for solvent mixtures. We decided to try conducting the same conformational search using a solvent potential for chloroform and then make a linear combination of the E^0 values of the lowest energy conformations obtained using a solvent potential for chloroform and water (see paper IV for details). This gave a new set of calculated $\Delta\Delta G$ that were closer to the experimental data but not accurate enough, giving $\Delta\Delta G$ that were varying by a factor of 5-12 and at some points predicting the opposite sign. This $\Delta\Delta G$ would describe the individual contribution of the substituent to ΔG term of the binding equation and hence would tell us if the substituent would aid or hinder the binding process. At this point it was decided to see if other force fields were better at predicting the $\Delta\Delta G$ value using the same method, the MM3,[149] MMFFs,[150] OPLS3[151] force fields. Here the OPLS3 force field was the most accurate with the MM3 giving similar results both force fields were able to predict the phenyl-substituted ligand (**l3**) to be the strongest binding ligand and that the cyclohexyl-substituted ligand (**l5**) was the weakest binding ligand and with value of $\Delta\Delta G$ varying only by a factor of 2.

It occurred to us that using only the lowest energy conformations ignored a substantial amount of conformations that were viable to exist at certain times in solution. This meant that for each ligand, receptor and complex, the E^0 values obtained from the conformational search needed to be corrected with a term that was taking into account all the conformations that the chemical entity could exist as in solution (for details see paper IV). After this correction the $\Delta\Delta G$ were closer to the experimental values, and now the MM3 force field seemed to be the most accurate force field, predicting again that **53** would be the strongest binding ligand and that **Cyhex** would be weakest, it also managed to predict the values of $\Delta\Delta G$ varying only a factor of 0.5–2 from the experimentally determined values.

It occurred to us that one use of our experimental data was to evaluate various computational chemistry methods against each other. So we decided to see if we could receive more accurate results using a different computational method. We used the experimentally determined values of $\Delta\Delta G$ to investigate which of molecular mechanics (MM) and density functional theory (DFT)[152] methods would come closest to predicting the $\Delta\Delta G$ values.

An energy minimized structure of each ligand, receptor and the complex between ligand and receptor that was used to perform a separate DFT calculation using B3LYP-D3 theory[153] with a SM8 solvent model for gas phase,[154] methanol or chloroform, respectively. This resulted in an E value for each ligand, receptor or

complex. The E values were then used to calculate the ΔG for each of the complexes in gas phase, methanol or chloroform, respectively, according to the equation (1). The ΔG values were then used to calculate the ΔΔG value of the reaction using equation (2) where ΔG_{sub} indicates the substituent on the ligand and ΔG_{unsub} indicates the ligand without a substituent.

$$\Delta G = E_{complex} - E_{ligand} - E_{receptor} \qquad\qquad (1)$$

$$\Delta\Delta G_{sub} = \Delta G_{sub} - \Delta G_{unsub} \qquad\qquad (2)$$

As seen in paper IV, the attempted DFT method provided values of the difference in free energy between the ligands ΔΔG that were an order of magnitude larger, and in some cases of a different sign, than the experimental values. This could be a consequence of that in the DFT calculations, only the lowest energy conformations were used in the determination of the ΔΔG values, though when this value is compared with the values determined by MM using only the lowest energy conformation, the MM method is still superior. Neither method managed to pinpoint exactly the trend in binding affinity that the ligands have to the receptor.

Another aspect that dawned to us was that the lowest energy conformations for the free ligands obtained from both the MM and DFT calculations were not entirely consistent with the data obtained from the NOESY of the free ligands, this is hardly surprising since the NOESY provides a picture of how the ligand orients over a time lapse and is in reality showing what interactions that are present most of the time. To get a better interpretation of the observed 2D NOESY NMR spectra, we decided to conduct a molecular dynamics simulation,[155] for both the free ligands and the complexes to see how they compared with the NMR data. In these simulations, it became evident that the free ligands were indeed shifting between various conformations that provided a plausible explanation to observing the various NOE interactions that could be observed as crosspeaks in the 2D-NOESY spectra, but could not be rationalized by only examining lowest energy conformations.

3.1.5 Conclusion

From the investigation above, there were a number of conclusions that could be drawn. NMR-titration methodology is a viable method to determine association constants. Evaluation of computational models using experimental data is a viable method to test their accuracy. Some computational methods are superior to others in describing different systems, in our case the MM methods proved better at

predicting our systems than DFT methods. However, to be fair, the MM methods were investigated more thoroughly. Molecular dynamics is a very useful method to aid the interpretation of NMR data, providing explanations to interactions that can sometimes be difficult to explain otherwise.

3.2 The *meso-endo*-BisTröger's base receptor

3.2.1 Colorimetric study

Having isolated **15b**, it was decided to test if it could bind different ions and be used as a phase transfer agent. A colorimetric experiment was setup that tested the affinity of **15b** towards different ions. In the experiment, our receptor was tested to se if it could transfer an ion from an aqueous to an organic phase (dcm) using permanganate as an indicating ion. Rather surprisingly the receptor failed to transfer any ions from the aqueous to the organic phase while 18-crown-6 proved more capable. The results can be seen in the supporting information of paper I. The most interesting result here was the apparent transfer of Fe^{3+}, with the aid of **15b** to the organic phase. However there is one slight issue with this and that is that the observed color shift is not the bright violet associated with permanganate, rather an orange brown color, this color could be associated with Fe^{3+} that is also present in the solution. If this is the case, it could be an indication that Fe^{3+} binds to **15b**.

3.2.2 electropray

Seeing as the colorimetric study was inconclusive regarding some of the ions it was decided to see if **15b** exhibited any affinity to form adducts with cations in the gas phase. This was determined using electrospray mass spectroscopy. **15b** exhibited affinity to form clusters with Li^+, Na^+, and Cs^+, however one should be mindful that Na^+ is a common contaminant from glassware and will form clusters with most organic molecules in electrospray and should not be seen as a solid proof for the receptor exhibiting an affinity towards Na^+.[157]

3.2.3 Conlcusion

In our efforts to use **15b** as a receptor for cations, we conclude from the colorimetric study that the cavity is too hindered to accommodate any cations with the exception of Fe^{3+}.

Conclusion

As mentioned in the introduction, Tröger's base is a useful molecule from different aspects. The further development of the chemistry of this molecule could lead to unforeseeable future applications in various fields.

We have developed two receptors that incorporate the Tröger's base framework. Namely the bis 18-crown-6 receptor Tröger's base receptor and the bis Tröger's base endo receptor. The later has been shown to be selective towards the Fe^{2+} ion. The former receptor has shown to be able to discriminate ligands based on the substituents present on them and this data has been shown to be useful when desiring to evaluate computational models against real data.

Furthermore, we have developed an effective protocol to modify the 6 and 12 positions of Tröger's base with average to excellent yields. This method is very general and should prove of value for anyone desiring to modify Tröger's base in the 6 and 12 positions. In addition to this, we have developed the first route to endo substituted Tröger's base derivatives as well as found a second route that might prove to be an alternative if further developed and pursued.

References

1. J. Tröger, *J. Prakt. Chem.* **1187,** *36,* 225-245.

2. M. A. Spielman, *J. Am. Chem. Soc.* **1935,** *57,* 583-385.

3. E. C. Wagner, *J. Am. Chem. Soc.* **1935,** *57*, 1296-1298.

4. V. Prelog, P. Wieland, *Helv. Chem. Acta.* **1944,** *27,* 1127-1134.

5. S. B. Larson, C. S. Wilcox, *Acta. Crystallogr. Sect. C.* **1986,** *42,* 224-227.

6. S. H. Wilen, J. Z. Qi, P. G. Williard, *J. Org. Chem.* **1991,** *56*, 465-487.

7. C. S. Wilcox, *Tetrahedron Lett.* **1985,** *26*, 5749-5752.

8. B. M. Wepster, *Recl. Trav. Chim. Pays-Bas.* **1953,** *72*, 661-672.

9. A. J. de Koning, *J. Chem. Soc. Perk. Trans. 2* **1984,** *341-343*.

10. A. Greenberg, N Molinero, M. Lang, *J. Org. Chem.* **1984,** *49*, 1127-1130.

11. Y. Hamada, S. Mukai, *Tetrahedron: Asymmetry* **1996,** *7*, 2671-2674.

12. D. A. Lenev, D. G. Golovanov, K. A. Lyssenko, R. G. Kostyanovsky, *Tetrahedron Asymmetry* **2006,** *17*, 2191-2194.

13. C. Michon, A. Sharma, G. Bernardinelli, E. Francotte, J. Lacour, *Chem. Commun.* **2010,** *46,* 2206-2208.

14. D. A. Lenev, K. A. Lyssenko, D. G. Golovanov, V. Buss, R. G. Kostyanovsky, *Chem. Eur. J.* **2006,** *12,* 6412-6418.

15. O. Trapp, V. Schurig, *J. Am. Chem. Soc.* **2000**, *122*, 1424-1430.

16. Á. Révész, D. Schröder, T. A. Rokob, M. Havlik, B. Dolenský, *Angew. Chem. Int. Ed.* **2011,** *50*, 2401-2404.

17. T. R. Miller, E. C. Wagner, *J. Am. Chem. Soc.* **1941,** *63,* 832-836.

18. M. Häring, *Helv. Chim. Acta* **1963,** *46,* 2970-2982.

19. B. G. Bag, U. Maitra, *Synth. Commun.* **1995,** *25,* 1849-1856.

20. J. C. Adrian, C. S. Wilcox, *J. Am. Chem. Soc.* **1992,** *114*, 1398-1403.

21. H. Salez, A. Wardani, M. Demeunynck, A. Tatibouet, J. Lhomme, *Tetrahedron Lett.* **1995,** *36,* 1271-1274.

22. Z. Li, X. Xu, Y. Peng, Z. Jiang, C. Ding, X. Qian, *Synthesis* **2005**, 1228-1230.

23. S. Satishkumar, M. Periasamy, *Tetrahedron: Asymmetry* **2006**, *17*, 1116-1119.

24. S. Satishkumar, M. Periasamy, *Tetrahedron: Asymmetry* **2009**, *20,* 2257-2262.

25. H. Wu, P. Zhang, Y. Shen, F.-R. Zhang, Y. Wan, D.-Q. Shi, *Synlett* **2007,** 336-338.

26. M. D. H. Bhuiyan, A. B. Mahon, P. Jensen, J. K. Clegg, A. C. Try, *Eur. J. Org. Chem.* **2009,** 687-698.

27. L. Cerrada, J. Cudero, J. Elguero, C. Pardo, *J. Chem. Soc. Chem. Commun.* **1993,** 1713-1714.

28. J. Cudero, C. Pardo, M. Ramos, E. Gutierrez-Puebla, A. Monge, J. Elguero, *Tetrahedron* **1997**, *53,* 2233-2240.

29. J. Jensen, K. Wärnmark, *Synthesis* **2001**, 1873-1877.

30. S.Sergeyev, M. Schär, P. Seiler, O. Lukoyanova, L. Echegoyen, F. Diederich, *Chem. Eur. J.* **2005**, *11*, 2284-2294.

31. D. Didier, B. Tylleman, N. Lambert, C. M. L. Vande Velde, F. Blockhuys, A. Collas, S. Sergeyev, *Tetrahedron* **2008**, *64,* 6252-6262.

32. A. Hansson, J. Jensen, O. F. Wendt, K. Wärnmark, *Eur. J. Org. Chem.* **2003**, 3179-3188.

33. J. Jensen, M. Strozyk, K. Wärnmark, *J. Heterocycl. Chem.* **2003,** *40,* 373-375.

34. S. P. Bew, L. Legentil, V. Scholier, S.V. Sharma, *Chem. Commun.* **2007**, 389-391.

35. M. D. H. Bhuiyan, K.-X. Zhu, P. Jensen, A. C. Try, *Eur. J. Org. Chem.* **2010,** 4662-4670.

36. Q. M. Malik, S. Ijaz, D. C. Craig, A. C. Try, *Tetrahedron* **2011**, *67,* 5798-5805.

37. U. Kiehne, T. Weilandt, A. Lützen, *Org. Lett.* **2007,** *9,* 1283-1286.

38. M. B. Reddy, M. Shailaja, A. Manjula, J. R. Premkumar, G. N. Sastry, K. Sirisha, A. V. S. Sarma, **2015**, *13*, 1141-1149.

39. S. Banerjee, S. A. Bright, J. A. Smith, J. Burgeat, M. Martinez-Calvo, D. C. Williams, J. M. Kelly, T. Gunnlaugsson, *J. Org. Chem.* **2014,** *79,* 9272-9283.

40. D.Didier, S. Sergeyev, *Eur. J. Org. Chem.* **2007,** 3905-3910.

41. E. C. Wagner, *J. Org. Chem.* **1954,** *19,* 1862-1881.

42. W. V. Farrar, *Journal of Applied Chemistry* **1964**, *14,* 389-399.

43. R. A. Johnson, R. R. Gorman, R. J. Wnuk, N. J. Crittenden, J. W. Aiken, *J. Med. Chem.* **1993,** *36,* 3202-3206.

44. C. A. M. Abella, M. Benassi, L. S. Santos, M. N. Eberlin, F. Coelho, *J. Org. Chem.* **2007,** *72,* 4048-4054.

45. Y. Wan, R. Yuan, W.-E. Zhang, Y.-H. Shi, W. Lin, W. Yin, R-C. Bo, J.-J. Shi, H. Wu, *Tetrahedron* **2010,** *66*, 3405-3409.

46. T. H. Webb, C. S. Wilcox, *J. Org. Chem.* **1990,** *55*, 363-365.

47. D. P. Becker, P. M. Finnegan, P. W. Collins, *Tetrahedron Lett.* **1993,** *33,* 1889-1892.

48. F. C. Cooper, M. W. Partridge, *J. Chem. Soc.* **1955,** 991-994.

49. F. C. Cooper, M. W. Partridge, *J. Chem. Soc.* **1957,** 2888-2893.

50. U. Maitra, B. G. Bag, *J. Org. Chem.* **1992,** *57,* 6979-6981.

51. U. Maitra, B. G. Bag, P. Rao, D. Powell, *J. Chem. Soc., Perkin Trans. 1* **1995,** 2049-2056.

52. J. C. Adrian, C. S. Wilcox, *J. Am. Chem. Soc.* **1989,** *111,* 8055-8057.

53. S. Goswami, K. Ghosh, *Tetrahedron Lett.* **1997,** 38, 4503-4506.

54. S. Goswami, K. Ghosh, S. Dasgupta, *J. Org. Chem.* **2000,** *65,* 1907-1914.

55. A. P. Hansson, P-O. Norrby, K. Wärnmark, *Tetrahedron Lett.* **1998,** *39,* 4565-4568.

56. M. Fukae, T. Inazu, *J. Inclusion Phenom.* **1984,** *2,* 223-229.

57. A. A. Ibrahim, M. Matsumoto, Y. Miyahara, K. Izumi, M. Suenaga, N. Shimizu, T. Inazu, *J. Heterocycl. Chem.* **1998,** *35,* 209-215.

58. C. S. Wilcox, M. D. Cowart, *Tetrahedron Lett.* **1986,** *27,* 5563-5566.

59. M. D. Cowart, I. Sucholeiki, R. R. Bukownik, C. S. Wilcox, *J. Am. Chem. Soc.* **1988,** *110,* 6204-6210.

60. T. H. Webb, H. Suh, C. S. Wilcox, *J. Am. Chem. Soc.* **1991,** *113,* 8554-8555.

61. C. S. Wilcox, J. C. Adrian, T. H. Webb, F. J. Zawacki, *J. Am. Chem. Soc.* **1992,** *114,* 10189-10197.

62. M. Miyake, C. S. Wilcox, *Heterocycles* **2002,** *57,* 515-522.

63. P. D. Smith, B. R. James, D. H. Dolphin, *Coordination Chemistry Reviews,* **1981,** *39,* 31-75.

64. M. J. Crossley, T. W. Hambley, L. G. Mackay, A. C. Try, R. Walton, *J. Chem. Soc. Chem. Commun.* **1995,** 1077-1079.

65. M. J. Crossley, L. G. Mackay, A. C. Try, *J. Chem. Soc. Chem. Commun.* **1995,** 1925-1927.

66. J. N. H. Reek, M. J. Crossley, A. P. H. J. Schenning, A. W. Bosman, E. W. Meijer, *Chem. Commun.* **1998,** 11-12.

67. P. R. Brotherhood, R. A. S. Wu, P. Turner, M. J. Crossley, *Chem. Commun.* **2007,** 225-227.

68. S. Paliwal, S. Geib, C. S. Wilcox, *J. Am. Chem. Soc.* **1994,** *116,* 4497-4498.

69. E-I. Kim, S. Paliwal, C. S. Wilcox, *J. Am. Chem. Soc.* **1998,** *120,* 11192-11193.

70. B. Bhayana, C. S. Wilcox, *Angew. Chem. Int. Ed.* **2007,** *46,* 6833-6836.

71. F. Hof, D. M. Scofield, W. B. Schweizer, F. Diederich, *Angew. Chem. Int. Ed,* **2004,** *43,* 5056-5059.

72. F. R. Fisher, W.B. Schweizer, F. Diederich, *Angew. Chem. Int. Ed,* **2007,** *46,* 8270-8273.

73. H. Gardarsson, W. B. Schweizer, N. Trapp, F. Diederich, *Chem. Eur. J.* **2014,** *20,* 4608-4616.

74. E. Yashima, M. Akashi, N. Miyauchi, *Chem. Lett.* **1991,** 1017-1020.

75. A. Tatibouët, M. Demeunynck, J. Lhomme, *Synth. Commun.* **1996,** *26,* 4375-4395.

76. A. Tatibouët, M. Demeunynck, H. Salez, R. Arnaud, J. Lhomme, C.Courseille, *Bull. Soc. Chim. Fr.* **1997,** *134,* 495-501.

77. A. Tatibouët, M. Demeunynck,, C. Andraud, A. Collet, J. Lhomme, *Chem. Commun.* **1999,** 161-162.

78. C. Bailly, W. Laine, M. Demeunynck, J. Lhomme, *Biochem. Biophys, Res. Commun.***2000,** *273,* 681-685.

79. B. Baldeyrou, C. Tardy, C. Bailly, P. Colson, C. Houssier, F. Charmantray, M. Demeunyck, *Eur. J. Med. Chem.* **2002,** *37,* 315-322.

80. E. B. Veale, D. O. Frimannsson, M. Lawler, T. Gunnlaugsson, *Org. Lett.* **2009,** *11,* 4040-4043.

81. E. B. Veale, T. Gunnlaugsson, *J. Org. Chem.* **2010,** *75,* 5513-5525.

82. Y. Goldeberg, H. Alper, *Tetrahedron Lett.* **1995,** *36,* 369-372.

83. B. Minder, M. Schürch, T. Mallat, A. Baiker, *Catal. Lett.* **1995,** *31,* 143-151.

84. Y.-M. Shen, M.-X. Zhao, J. Xu, Y. Shi, *Angew. Chem. Int. Ed.* **2006,** *45,* 8005-8008.

85. F. Xu, R. D. Tillyer, D. M. Tschaen, E. J. J. Grabowski, P. J. Reider, *Tetrahedron: Asymmetry* **1998,** *9,* 1651-1655.

86. M. Harmata, M. Kahraman, *Tetrahedron: Asymmetry* **2000,** *11,* 2875-2879.

87. H. Wu, X.-M. Chen, Y. Wan, L. Ye, H.-Q. Xin, H.-H. Xu, C.-H. Yue, L-L. Pang, R. Ma, D.-Q. Shi, *Tetrahedron Lett.* **2009,** *50,* 1062-1065.

88. F. Cuenú, R. Abonia, A. Bolaños, A. Cabrera, *J. Organometa. Chem.* **2011,** *696,* 1834-1839.

89. D. Didier, S. Sergeyev, *ARKIVOC,* 124-134.

90. X. Du, Y. Sun, B. Tan, Q. Teng, X. Yao, C. Su, W. Wang, *Chem. Commun.* **2010,** *46,* 970-972.

91. J. R. Cabrero-Antonino, T. Garcia, P. Rubio-Marqués, J. A. Vidal-Moya, A. Leyva-Pérez, S. S. Al-Deyab, S. I. Al-Resayes, U. Diaz, A. Corma, *ACS Catal.* **2011,** *1,* 147-158.

92. D. R. Bond, J. L. Scott, *J. Chem. Soc. Perkin Trans. 2* **1991,** 47-51.

93. O. Trapp, G. Trapp, J. Kong, U. Hahn, F. Vögtle, V. Schurig, *Chem. Eur. Jour.* **2002,** *8*, 3629-3634.

94. C. Michon, M-H. Gonçalves-Farbos, J. Lacour, *Chirality,* **2009,** *21,* 809-817.

95. K. Y. Lee, S.Gowridankar, J. N. Kim, *SYNLETT* **2006,** *9,* 1389-1393.

96. D. A. Lenev, I. I. Chervin, K. A. Lyssenko, R. G. Kostyanovsky, *Tetrahedron Lett.* **2007,** *48,* 3363-3366.

97. A. B. Mahon, D. C. Craig, A. C. Try, *ARKIVOC* **2008,** *12*, 148-163.

98. C. S. Hampton, M. Harmata, *Tetrahedron* **2016,** *72,* 6064-6077.

99. M. Faroughi, A. C. Try, J. Klepetko, P. Turner, *Tetrahedron Lett.* **2007,** *48,* 6548-6551.

100. A. B. Mahon, D. C. Craig, A. C. Try, *Synthesis* **2009,** 4, 636-642.

101. A. Sharma, L. Guénée, J.-V. Naubron, J. Lacour, *Angew. Chem. Int. Ed.* **2011,** *50,* 3677-3680.

102. A. Sharma, C. Besnard, L. Cuénée, J. Lacour, *Org. Biomol. Chem.* **2012,** *10,* 966-969.

103. S. A. Pujari, L. Guénée, J. Lacour, *Org. Lett* **2013,** *15*, 3930-3933.

104. M. B. Reddy, A. Manjula, B. V. Rao, B. Sridar, **2012,** *2*, 312-319.

105. Q. M. Malik, A. B. Mahon, D. C. Craig, A. C. Try, *Tetrahedron* **2011,** *67,* 8509-8514.

106. B. R. MAnda, M. Alla, R. J. Ganji, A. Addlagatta, *Euro. Jour. Medi. Chem.* **2014,** *86,* 39-47.

107. M. Periasamy, S. Suresh, S. Satishkumar, *Tetrahedron: Asymmetry* **2012,** *23*, 108-116.

108. X. Gao, C. S. Hampton, M. Harmata, *Euro. Jour. Org. Chem,* **2012,** 7053-7056.

109. M. Faroughi, P. Jensen, A. C. Try, *ARKIVOC* **2009,** *2*, 269-280.

110. E.Vardelle, A. Martin-Mingot, M.-P. Jouannetaud, J.-C. Jacquesy, J. Marrot, *Tetrahedron Lett.* **2009,** *50,* 1093-1096.

111. J. Šturala, R. Cibulka, *Euro. Jour. Org. Chem,* **2012,** 7066-7074.

112. J. Artacho, E. Ascic, T. Rantanen, J. Karlsson, C.-J. Wallentin, R. Wang, O. F. Wendt, M. Harmata, V. Snieckus, K. Wärnmark, *Chem. Eur. Jour.* **2012,** *18,* 1038-1042.

113. J. Artacho, E. Ascic, T. Rantanen, C.-J. Wallentin, S. Dawaigher, K.-E. Bergquist, M. Harmata, V. Snieckus, K. Wärnmark, **2012,** *18,* 4706-4709.

114. R. Pereira, P. Ondrisek, A. Kubincová, E. Otth, J. Cvengroš *Adv. Synth. Catal.* **2016,** *358*, 2739-2744.

115. A. Bosamni, S. A. Pujari, C. Besnard, L. Guénée, A. I. Poblador-Bahamonde, J. Lacour, *Chem. Eur. Jour.* **2017,** *23*, 8678-8684.

116. S. P. Bew,L. Legentil, V. Scholier, S. V. Sharma, *Chem. Commun.* **2007**, 389-391.

117. J. Jensen, M. Strozyk, K. Wärnmark, *Synthesis* **2002**, 2761-2765.

118. U. Kiehne, A. Lützen, *Synthesis,* **2004**, 1687.

119. U. Kiehne, A. Lützen, *Synthesis*, **2004**, 1695.

120. F. Hof, M. Schär, D. M. Scofield, F. Fischer, F. Diedrich, S. Sergeyev, *Helv. Chim. Acta.* **2005**, *88*, 2333-2344.

121. C. Solano, D. Svensson, Z. Olomi, J. Jensen, O. F. Wendt, K. Wärnmark, *Eur. J. Org. Chem.* **2005**, 3510-3517.

122. D. Didier, S. Sergeyev, *Tetrahedron* **2007**, *63*, 3864-3869.

123. J. Artacho, K. Wärnmark, *Synthesis*, **2009**, 3120-3126.

124. U. Kiehne, T. Bruhn, G. Schnakenburg, R. Fröhlich, G.Bringmann, A.Lützen, *Chem. Eur. J.* **2008**, *14*, 4246-4255.

125. M. Harmata, K. W. Carter, D. E. Jones, M. Kahraman, *Tetrahedron Lett*. **1996**, 37, 6267-6270.

126. M. Harmata, K. –O. Ryanil, C. L. Barnes, *Supramol. Chem.* **2006**, *18*, 581-585.

127. V. R. Somayaji, S. Breown, *J. Org. Chem*, **1986**, *51*, 2676.

128. A. J. Kirby, I. V. Komarov, P. D. Wothers, N. Feeder, *Angew. Chem. Int. Ed.* **1998**, *37*, 785.

129. K. Tani, B. M. Stoltz, *Nature* **2006**, *441*, 731.

130. W. Flitsch, H. Peters, *Tetrahedron Lett.* **1969,** *10*, 1161.

131. V. Snieckus, *Chem. Rev.* **1990**, *90*, 879-933.

132. R. C. Larock, *Comprehensive Organic Transformations,* 2nd ed, Wiley-VCH, NY, **1999**, pp. 869-872.

133. H. C. Brown, S. C. Kim, *Synthesis,* **1977**, 635.

134. M. E. Kuehne, P. J. Shannon, *J. Org. Chem.* **1977**, *42*, 2082.

135. M. Szostak, M. Spain, A. J. Eberhart, D. J. Procter, *J. Am. Chem. Soc.* **2014**, *136*, 2268−2271.

136. S. H. Pine, R. J. Pettit, G. D. Geib, S. G. Cruz, C. H. Gallego, T. Tijerina, R. D. Pine, *J.Org. Chem.* **1985**, *50,* 1212-1216.

137. J. T. Spletstoser, J. M. White, A. R. Tunoori, G. I. Georg *J. Am. Chem. Soc.* **2007**, *129,* 3408-3419.

138. M. Yamaguchi, T. Waseda, I. Hirao, *Chem. Lett.* **1983**, 35.

139. F. Tinnis, A. Volkov, T. Slagbrand, H. Adolfsson, *Angew. Chem. Int. Ed.* **2016**, *55*, 4562-4566.

140. P.-Q. Huang, W. Ou, K.-J. Xiao, A. Wang, *Chem. Commun.* **2014,** *50*, 8761-8763.

141. A. W. Czarnik, *Tetrahedron lett* **1984**, *25*, 4875.

142. S. Laval, W. Dayoub, A. Favre-Reguillon, P. Demonchaux, G. Mignani, M. Lemaire, *Tetrahedron Lett.* **2010**, *51*, 2092-2094.

143. A. G. Shultz, M. Macielag, *J. Org. Chem*, **1986,** *51*, 4983-4987.

144. C. S. Wilcox, *Front. Supramol. Org. Chem. Photochem.* **1991**, 123-143.

145. L. Fielding, *Tetrahedron,* **2000**, *56*, 6151-6170.

146. Chapter 2 in *Introduction to Computational Chemistry 2nd Edition*, (Ed.: F. Jensen), Wiley-VCH, Weinheim, **2007**, pp. 22-77.

147. G. A. Kaminski, R. A. Friesner, J. Tirado-Rives, W. Jorgensen, *J. Phys. Chem B* **2001**, *105*, 6474-6487.

148. J. L. Banks, H. S. Beard, Y. Cao, A. E. Cho, W. Damm, R. Farid, A. K. Felts, T. A. Halgren, D. T. Mainz, J. R. Maple, R. Murphy, D. M. Philipp, M. P.Repasky, L. Y. Zhang, B. J. Berne, R. A. Friesner, E. Gallicchio, R. M. Levy. Integrated Modeling Program, *J. Comp. Chem.* **2005**, *26*, 1752.

149. N. L. Allinger, Y. H. Yuh, J-H. Lii, *J. Am. Chem. Soc.* **1989**, *111*, 8551-8565.

150. T. A. Hallgren, *J. Comp. Chem.* **1996**, *17*, 490-519.

151. E. Harder, W. Damm, J. Maple, C. Wu, M. Reboul, J. Y. Xiang, L. Wang, D. Lupyan, M. K. Dahlgren, J. L. Knight, J. W. Kaus, D. S. Cerutti, G. Krilov, W. L. Jorgensen, R. Abel, R. A. Friesner, *J. Chem. Theory. Comput.* **2016**, *12*, 281-296.

152. Chapter 6 in *Introduction to Computational Chemistry 2nd Edition*, (Ed.: F. Jensen), Wiley-VCH, Weinheim, **2007**, pp. 231-264.

153. S. Grimme, J. Antony, S. Ehrlich, H. Krieg, *J. Chem. Phys,* **2010**, *132,* 154104.

154. C. J. Cramer, D. G. Truhlar, *Acc. Chem. Res.* **2008**, *41,* 760-768.

155. Chapter 14 in *Introduction to Computational Chemistry 2nd Edition*, (Ed.: F. Jensen), Wiley-VCH, Weinheim, **2007**, pp. 445-8.

156. N. B. Cech, C. G. Enke, *Mass Spectrom. Rev.* **2001**, *20*, 362-387.

157. B. O. Keller, J. Sui, A. B. Young, R. M. Whittal, *Analytica Chimica Acta,* **2008**, *627*, 71-81.

Paper I

Tröger's Base Twisted Amides: *Endo* Functionalization and Synthesis of an Inverted Crown Ether

Josep Artacho,[†] Erhad Ascic,[†] Toni Rantanen,[§] Carl-Johan Wallentin,[†] Sami Dawaigher,[†] Karl-Erik Bergquist,[†] Michael Harmata,*[‡] Victor Snieckus,*[§] and Kenneth Wärnmark*[†]

Centre for Analysis and Synthesis, Department of Chemistry, Lund University, P.O. Box 124, 22100 Lund, Sweden, Department of Chemistry, University of Missouri—Columbia, Columbia, Missouri 65211, United States, and Snieckus Innovations and Department of Chemistry, Queen's University, Kingston, ON K7L 3N6, Canada

kenneth.warnmark@organic.lu.se; snieckus@chem.queensu.ca; harmatam@missouri.edu

ABSTRACT
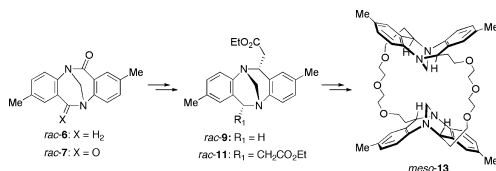
Taking advantage of the unconventional reactivity of twisted mono- and bis-amides of Tröger's base (TB), *rac*-6 and *rac*-7, respectively, the first synthesis of a 6-*endo*-monosubstituted TB analogue, *rac*-9, and the first rational synthesis of a 6,12-*endo,endo*-disubstituted TB analogue, *rac*-11, have been achieved. The bis-TB crown ether, *meso*-13, was prepared starting from *rac*-7. *Meso*-13 constitutes a rare example of a crown ether with an inverted methylene bridge-to-bridge bis-TB conformation both in solution and in the solid state, resulting in a reluctance to act as a receptor for cations.

Tröger's base (TB),[1] *rac*-1 (Figure 1), is a fascinating molecule with a controversial and lengthy history of structural and stereochemical assignment.[2] TB represents a chiral diamine with two stereogenic N-atoms and is one of the first chiral compounds resolved by chiral stationary phase chromatography (on (+)-α-lactose hydrate).[3] This textbook molecule and its functionalized analogues have received considerable attention as building blocks in diverse areas such as molecular recognition, catalysis, enzyme inhibition, and optical materials.[4,5]

These applications of the structural features of TB have elicited substantial synthetic efforts that include (1) a facile synthesis of halogenated TB analogues,[6−8] which allows its aromatic ring functionalization,[9,10] (2) *N*-mono and -dialkylations,[11] and (3) replacement of the methylene bridge.[12,13] Although C-6 and C-12 functionalized TB analogues have been synthesized from substituted dibenzodiazocines,[14] the preparation of such *exo*-mono-substituted (**2**) or *exo,exo*-disubstituted (**3**) derivatives from the readily available TB has been feasible only by the metalation strategy developed in our laboratories (Figure 1).[15] We have previously reported on the use of *exo*-substituted analogues of TB in the catalytic asymmetric addition of diethylzinc to substituted benzaldehydes in up to 86% ee.[15b] However, it may be argued that *endo*-monosubstituted (**4**) or *endo,endo*-disubstituted (**5**) analogues of TB (Figure 1) are potentially more useful since the

[†] Lund University.
[§] Queen's University.
[‡] University of Missouri—Columbia.
(1) Tröger, J. *J. Prakt. Chem.* **1887**, *36*, 225.
(2) (a) Spielman, M. A. *J. Am. Chem. Soc.* **1935**, *57*, 583. (b) Larson, S. B.; Wilcox, C. S. *Acta Crystallogr., Sect. C* **1986**, *42*, 224. (c) Wilen, S. H.; Qi, J. Z.; Williard, P. G. *J. Org. Chem.* **1991**, *56*, 485.
(3) Prelog, V.; Wieland, P. *Helv. Chim. Acta* **1944**, *27*, 1127.
(4) Wilcox, C. S. *Tetrahedron Lett.* **1985**, *26*, 5749.
(5) For the latest reviews, see: (a) Sergeyev, S. *Helv. Chim. Acta* **2009**, *92*, 415. (b) Dolenský, B.; Elguero, J.; Král, V.; Pardo, C.; Valík, M. *Adv. Heterocycl. Chem.* **2007**, *93*, 1. (c) Yuan, C. X.; Xin, Q.; Liu, H.J.; Wang, L.; Jiang, M. H.; Tao, X.T. *Sci. China Chem.* **2011**, *54*, 587.

diazocine ring substituents are directed toward the chiral cavity of TB and are therefore especially suitably positioned for asymmetric catalysis and molecular recognition.
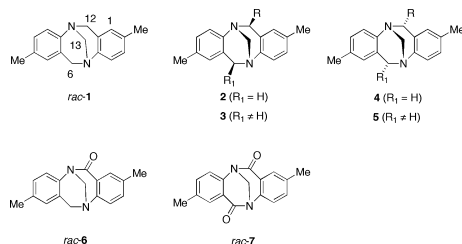
Figure 1. Possible diazocine ring substituted analogues of Tröger's base (TB) *rac*-**1**: *exo*-monosubstituted (**2**), *exo*,*exo*-disubstituted (**3**), *endo*-monosubstituted (**4**), *endo*,*endo*-disubstituted (**5**), twisted mono- (*rac*-**6**) and twisted bis- (*rac*-**7**) amides.

With these factors in mind, we prepared, by direct C-6 and C-12 oxidation reactions, mono- (*rac*-**6**) and bis-amide (*rac*-**7**) TB analogues (Figure 1),[16] the latter being the first

twisted bis-amide reported to date. Twisted amides are compounds having their carbonyl π-systems out of conjugation with the nitrogen lone pairs.[17] For *rac*-**7**, the twist angle, τ,[18] describing the deviation from coplanarity between the carbonyl π orbital and the nitrogen lone pair, was determined to be −43.7° as compared to being near 0° and 180° as commonly found in unconstrained *cisoid* and *transoid* amides, respectively. The twisted amide structural feature in *rac*-**7** was also reflected by its rapid acid hydrolysis.[16,19] This property suggested further possibilities for the benzylic functionalization of monoamide (*rac*-**6**) and bis-amide (*rac*-**7**) TB analogues.

Herein we report on the Wittig olefination of *rac*-**6** and *rac*-**7**, which has led to the first synthesis of *endo*-monosubstituted (*rac*-**9**) (Scheme 1) and the first rational synthesis of *endo*,*endo*-disubstituted (*rac*-**11**) TB analogues (Scheme 2). In addition, the availability of *rac*-**11** allowed the synthesis of crown ether *meso*-**13** (Scheme 2), which showed unexpected conformational properties.

While Wittig olefinations do not take place on regular amides, examples of olefinations of twisted amides[17b,c] and phthalimides[20] are known. Taking advantage of the protocol described for phthalimides,[20] *rac*-**6** was readily olefinated at 130−140 °C using the commercially available (ethoxycarbonylmethylene)-triphenylphosphorane to give the monoenamino TB adduct *rac*-**8** in high yield (Scheme 1) as an 83:17 *E*/*Z* mixture according to ^{1}H NMR analyses (see Supporting Information (SI)). The assignment of the geometrical isomers of *rac*-**8** was established by ROESY experiments (see SI), which showed a correlation between H-7 and the vinyl H (Scheme 1) for the isolated sample of the minor isomer, thus demonstrating the *Z*-geometry of this isomer. Since the outcome of the next synthetic step was indifferent to the configuration of the olefin, the *E*/*Z* mixture was subjected to hydrogenation using Pd/C at 1 atm and rt, resulting in the formation of *rac*-**9** in 83% yield after 16 h. The relative stereochemistry of *rac*-**9** was

(6) Halogenated TB analogues: (a) Jensen, J.; Wärnmark, K. *Synthesis* **2001**, 1873. (b) Hansson, A.; Jensen, J.; Wendt, O. F.; Wärnmark, K. *Eur. J. Org. Chem.* **2003**, 3179.

(7) Multigram scale synthesis of halogenated TB analogues: (a) Jensen, J.; Strozyk, M.; Wärnmark, K. *J. Heterocycl. Chem.* **2003**, *40*, 373. (b) Sergeyev, S.; Schär, M.; Seiler, P.; Lukoyanova, O.; Echegoyen, L.; Diederich, F. *Chem.—Eur. J.* **2005**, *11*, 2284. (c) Bew, S. P.; Legentil, L.; Scholier, V.; Sharma, S. V. *Chem. Commun.* **2007**, 389.

(8) Direct halogenation of TB: (a) Didier, D.; Sergeyev, S. *Eur. J. Org. Chem.* **2007**, 3905. (b) Faroughi, M.; Jensen, P.; Try, A. C. *ARKIVOC* **2009**, *2*, 269.

(9) Halogen–lithium exchange: (a) Jensen, J.; Teijler, J.; Wärnmark, K. *J. Org. Chem.* **2002**, *67*, 6008. (b) Sergeyev, S.; Diederich, F. *Angew. Chem., Int. Ed.* **2004**, *43*, 1738. (c) Ishida, Y.; Ito, H.; Mori, D.; Saigo, K. *Tetrahedron Lett.* **2005**, *46*, 109. (d) Hansson, A.; Wixe, T.; Bergquist, K.-E.; Wärnmark, K. *Org. Lett.* **2005**, *7*, 2019. (e) Artacho, J.; Nilsson, P.; Bergquist, K.-E.; Wendt, O. F.; Wärnmark, K. *Chem.—Eur. J.* **2006**, *12*, 2692. (f) Jin, Z.; Guo, S.-X.; Gu, X.-P.; Qiu, L.-L.; Wu, G.-P.; Fang, J.-X. *ARKIVOC* **2009**, *10*, 25.

(10) Transition-metal catalyzed cross coupling: (a) Reference 6a. (b) Jensen, J.; Strozyk, M.; Wärnmark, K. *Synthesis* **2002**, 2761. (c) Kiehne, U.; Lützen, A. *Synthesis* **2004**, 1687. (d) Solano, C.; Svensson, D.; Olomi, Z.; Jensen, J.; Wendt, O. F.; Wärnmark, K. *Eur. J. Org. Chem.* **2005**, 3510. (e) Hof, F.; Schär, M.; Scofield, D. M.; Fischer, F.; Diederich, F.; Sergeyev, S. *Helv. Chim. Acta* **2005**, *88*, 2333. (f) Didier, D.; Sergeyev, S. *Tetrahedron* **2007**, *63*, 3864. (g) Kiehne, U.; Bruhn, T.; Schnakenburg, G.; Fröhlich, R.; Bringmann, G.; Lützen, A. *Chem.—Eur. J.* **2008**, *14*, 4246. (h) Artacho, J.; Wärnmark, K. *Synthesis* **2009**, 3120.

(11) (a) Häring, M. *Helv. Chim. Acta* **1963**, *46*, 2970. (b) Weber, E.; Müller, U.; Worsch, D.; Vögtle, F.; Will, G.; Kirfel, A. *J. Chem. Soc., Chem. Commun.* **1985**, 1578. (c) Lenev, D. A.; Golovanov, D. G.; Lyssenko, K. A.; Kostyanovsky, R. G. *Tetrahedron: Asymmetry* **2006**, *17*, 2191. (d) Michon, C.; Gonçalves-Farbos, M.-E.; Lacour, J. *Chirality* **2009**, *21*, 809.

(12) (a) Cooper, F. C.; Partridge, M. W. *J. Chem. Soc.* **1957**, 2888. (b) Greenberg, A.; Molinaro, N.; Lang, M. *J. Org. Chem.* **1984**, *49*, 1127. (c) Johnson, R. A.; Gorman, R. R.; Wnuk, R. J.; Crittenden, N. J.; Aiken, J. W. *J. Med. Chem.* **1993**, *36*, 3202. (d) Hamada, Y.; Mukai, S. *Tetrahedron Lett.* **1996**, *7*, 148.

(13) (a) Lenev, D. A.; Chervin, I. I.; Lyssenko, K. A.; Kostyanovsky, R. G. *Tetrahedron Lett.* **2007**, *48*, 3363. (b) Mahon, Q. B.; Craig, D. A.; Try, A. C. *Synthesis* **2009**, 636. (c) Michon, C.; Sharma, A.; Bernadinelli, G.; Francotte, E.; Lacour, J. *Chem. Commun.* **2010**, *46*, 2206. (d) Sharma, A.; Guénée, L.; Naubron, J.-V.; Lacour, J. *Angew. Chem., Int. Ed.* **2011**, *50*, 3677.

Scheme 1. Synthesis of *endo*-Substituted TB Analogue *rac*-**9**

assigned by NOESY experiments (see SI), which showed a correlation between the H-6 and one of the methylene

(14) (a) Metlesics, W.; Tavares, R.; Sternbach, L. H. *J. Org. Chem.* **1966**, *31*, 3356. (b) Albert, A.; Yamamoto, H. *J. Chem. Soc. B* **1966**, 956.

(15) (a) Harmata, M.; Carter, K. W.; Jones, D. E.; Kahraman, M. *Tetrahedron Lett.* **1996**, *37*, 6267. (b) Harmata, M.; Kahraman, M. *Tetrahedron: Asymmetry* **2000**, *11*, 2875. (c) Harmata, M.; Rayanil, K.-O.; Barnes, C. L. *Supramol. Chem.* **2006**, *18*, 581.

(16) Artacho, J.; Ascic, E.; Rantanen, T.; Karlsson, J.; Wallentin, C.-J.; Wang, R.; Wendt, O. F.; Harmata, M.; Snieckus, V.; Wärnmark, K. *Chem.—Eur. J.* **2012**, *18*, 1038.

bridge protons (Scheme 1), thus establishing the *endo* configuration of the ethoxycarbonylmethylene group. The stereochemical outcome of the hydrogenation may be rationalized by consideration of the convex face of *rac*-**8** being more accessible to the catalyst surface compared to the more hindered concave face.

Next, the methodology for the synthesis of *endo*-mono-substituted TB analogue *rac*-**9** was successfully applied to the preparation of the *endo,endo*-disubstituted TB analogue *rac*-**11** (Scheme 2). Thus, *rac*-**7** was readily olefinated at 150 °C using (ethoxycarbonylmethylene)-triphenylphosphorane to give *rac*-**10** in 77% yield as a mixture of the three possible geometrical isomers in a 51:39:10 (*E,E/E,Z/Z,Z*) ratio, according to ^{1}H NMR analyses (see SI), differing from a 69:28:3 statistical ratio expected if the *E/Z* selectivity of the olefination of *rac*-**6** and *rac*-**7** had been the same. The assignment of the geometrical isomers of *rac*-**10** was established by ROESY experiments, as in the case of *rac*-**8**. This mixture of isomers was subjected to hydrogenation using Pd/C at 80 bar and rt for 24 h to give *rac*-**11**[21] in 73% yield.[22] As for *rac*-**9** (*vide supra*), the relative stereochemistry was assigned by NOESY experiments (see SI and Scheme 2).

With *rac*-**11** in hand, we recognized the potential for the preparation of derivatives with functional groups oriented toward the aromatic cavity of TB. One possibility was the introduction of an oligoethylene glycol strap. Toward this end, reduction of *rac*-**11** with LAH smoothly gave the diol *rac*-**12** in 78% yield (Scheme 2). Although attempts to bridge the two hydroxyl groups with tri- and tetraethylene glycol ditosylates to form the corresponding mono-TB crown ether failed, the use of diethylene glycol ditosylate resulted in a dimerization to give the bis-TB crown ether **13** in 30% yield as a 1:1 mixture of *meso*-**13** and *rac*-**13** (Scheme 2),

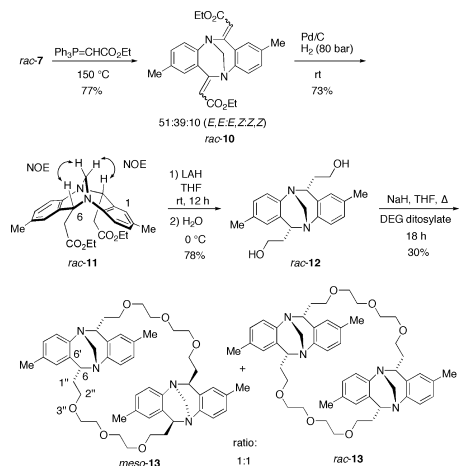as revealed by ^{1}H NMR spectroscopy (see SI). The rest of the isolated material was assumed to be oligomeric due to the observed broad peaks in its ^{1}H NMR spectrum. Macrocycle *meso*-**13** was obtained in 9% yield by a double recrystallization of the reaction mixture, first from hexane/*i*PrOH (8:2) and then from EtOAc. Alternatively, each of the three stereoisomers was separated by semi-preparative HPLC using a cellulose-derived chiral stationary phase, giving (−)-**13**, (+)-**13**, and *meso*-**13** (see SI), respectively, as isolated pure compounds.

The structure of *meso*-**13** was unambiguously assigned by X-ray crystallography, thereby conclusively establishing the *endo,endo*-configuration of precursor TB derivatives **11**–**13**. To our surprise, the solid state structure of *meso*-**13** (Figure 2) showed that the methylene bridges of the TB framework were both directed toward and not away from each other as expected from the *endo,endo*-configuration of the starting TB analogue *rac*-**12**, resulting in an "inverted" crown ether. All efforts to grow suitable crystals for X-ray diffraction analysis of both racemic and enantiopure **13** were unsuccessful.

The conformation of *meso*-**13** was investigated by *in silico* modeling using molecular dynamics with CHCl$_3$ as solvent (see SI). The C6′−C6−C1″−C2″ structural component (Scheme 2) of the simulated structure of *meso*-**13** showed a very good correlation with the solid state structure (compare Figures S29 and S30, SI), supporting the methylene bridge-to-bridge bis-TB conformation. The conformations obtained by the X-ray crystal structure and the geometry-optimized calculated structure both agreed well with the ROESY correlations achieved for *meso*-**13** in CDCl$_3$ (see SI). The *in silico* modeling data established a dihedral angle of 160° for C6′−C6−C1″−C2″ and a dihedral angle of −70° for C6−C1′−C2″−O3″ for the (*S,S*)-Tröger's base structural component, and the opposite sign for the corresponding dihedral angles for the (*R,R*)-Tröger's base of *meso*-**13**, respectively, agreeing well with the X-ray structure. The measured ROESY cross peaks for hydrogen atoms at C1″ and C2″ to aromatic hydrogen atoms at C4 and C7 are in accordance with this geometry (see Figures S30−31, SI).

Scheme 2. Synthesis of *endo,endo*-Disubstituted TB Analogues *rac*-**11**, *rac*-**12**, and bis-TB Crown Ethers **13**

(17) Examples of twisted amides: (a) Somayaji, V. R.; Brown, S. *J. Org. Chem.* **1986**, *51*, 2676. (b) Kirby, A. J.; Komarov, I. V.; Wothers, P. D; Feeder, N. *Angew. Chem., Int. Ed.* **1998**, *37*, 785. (c) Kirby, I. V.; Komarov, I. V.; Feeder, N. *J. Chem. Soc., Perkin Trans. 2* **2001**, 522. (d) Tani, K.; Stoltz, B. M. *Nature* **2006**, *441*, 731. (e) Szotak, M.; Yao, L.; Aubé, J. *J. Am. Chem. Soc.* **2010**, *132*, 2078. (f) Szotak, M.; Yao, L.; Aubé, J. *ibid.* **2010**, *132*, 8836. (g) Greenberg, A.; Moore, D. T.; DuBois, T. D. *ibid.* **1996**, *118*, 8658. (h) Greenberg, A.; Venanzi, C. A. *ibid.* **1993**, *115*, 6951. (i) Mujika, J. I.; Formoso, E.; Mercero, J. M.; Lopez, X. *J. Phys. Chem. B* **2006**, *110*, 15000. (j) Sliter, B.; Morgan, J.; Greenberg, A. *J. Org. Chem.* **2011**, *76*, 2770.

(18) Defined first by: Winkler, F. K.; Dunitz, J. D. *J. Mol. Biol.* **1971**, *59*, 169.

(19) Yamada, S. *The Amide Linkage: Structural Significance in Chemistry, Biochemistry, and Materials Science*; Greenberg, A., Breneman, C. M., Liebman, J. F., Eds.; Wiley: New York, 2000; p 239.

(20) Flitsch, W.; Peters, H. *Tetrahedron Lett.* **1969**, *10*, 1161.

(21) One *endo,endo*-substituted TB analogue has been obtained in low yield from a 2,5-disubstituted diazocine: see ref 14a.

(22) This experiment was performed before the conditions for the 1 atm hydrogention to give *rac*-**9** had been carried out.

Notably, macrocycle **13** is an uncommon example of crown ether analogues of TB.[23] It is also structurally similar to "Trögerophanes"[24] and a bis(*endo,endo*-dihydroxymethyl)dibenzobicyclo[3.3.1]-nonane crown ether.[25] These compounds show interesting recognition properties as receptors for benzenoid and alicyclic systems in aqueous solvents[24a,b] and are useful as chiral resolving reagents in phase-transfer systems,[25b] and as potential enzyme models.[24c]
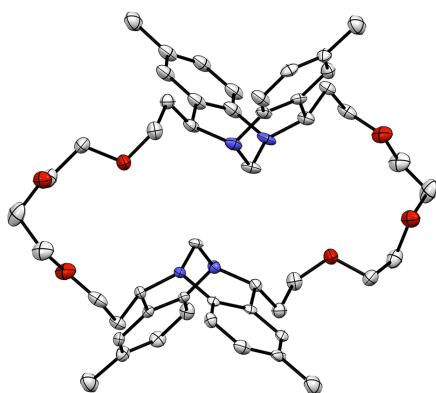
Figure 2. ORTEP representation of the crystal structure of *meso*-**13**. H-atoms have been removed for clarity.

Knowledge of these facts led to the examination of the cation recognition properties of *meso*-**13**, both in colorimetric phase transfer and in ESI-MS screening protocols,[26] which included 19 metal and ammonium salts (see SI). In the colorimetric phase transfer screening, no evidence for interactions between the salts and *meso*-**13** was found with the possible exception for Fe^{3+}. In the gas phase ESI-MS screening, only interactions between Li^+, Na^+, and Cs^+, respectively, and *meso*-**13** were established. The lack of recognition properties of *meso*-**13** strongly suggests a closed cavity in the macrocycle resulting from its methylene bridge-to-bridge bis-TB conformation as a contributing factor.

In summary, taking advantage of the enhanced reactivity of twisted mono- and bis-amide TB analogues, *rac*-**6** and *rac*-**7**, we have synthesized the first *endo*-monosubstituted and *endo,endo*-disubstituted TB analogues, *rac*-**9** and *rac*-**11**, respectively.[21] The diol *rac*-**12**, readily available from *rac*-**11**, was converted into *meso*-**13**, a rare example of an "inverted" crown ether, exhibiting an unexpected methylene bridge-to-bridge bis-TB conformation in both the solid state and in solution. As evidenced by phase transfer and gas phase screening experiments, the methylene bridge-to-bridge conformation of *meso*-**13** hampers the recognition of a range of cations in solution. The chemistry leading to *rac*-**9** and *rac*-**11** is expected to be general, thereby providing an opportunity for the generation of a number of *endo*-substituted TB analogues whose application in supramolecular chemistry and catalysis may be anticipated. Modification of the design of macrocycle *meso*-**13**, in which both "closed" and "open" conformations are accessible, has potential for the construction of gated hosts.[27] Further results will be reported in due course.

Supporting Information Available. Detailed experimental procedures, characterization data for all compounds (including relevant NMR spectra), and CIF files of compound *meso*-**13**. This material is available free of charge via the Internet at http://pubs.acs.org.

(23) (a) Manjula, A.; Nagarajan, M. *Tetrahedron* **1997**, *53*, 11859. (b) Ibrahim, A. A.; Matsumoto, M.; Miyahara, Y.; Izumi, K.; Suenaga, M.; Shimizu, N.; Inazu, T. *J. Heterocycl. Chem.* **1998**, *35*, 209. (c) Hansson, A. P.; Norrby, P.-O.; Wärnmark, K. *Tetrahedron Lett.* **1998**, *39*, 4565.

(24) (a) Cowart, M. D.; Sucholeiki, I.; Bukownik, R. R.; Wilcox, C. S. *J. Am. Chem. Soc.* **1988**, *110*, 6204. (b) Webb, T. H.; Suh, H.; Wilcox, C. S. *ibid.* **1991**, *113*, 8554. (c) Miyake, M.; Wilcox, C. S. *Heterocycles* **2002**, *57*, 515.

(25) (a) Naemura, K.; Fukunaga, R.; Yamanaka, M. *J. Chem. Soc., Chem. Commun.* **1985**, 1560–1561. (b) Naemura, K.; Fukunaga, R.; Komatsu, M.; Yamanaka, M.; Chikamatsu, H. *Bull. Chem. Soc. Jpn.* **1989**, *62*, 83.

(26) For a recent paper on the complexation between the tetramethylammonium cation and 18-crown-6 in the gas phase, see: Fránski, R.; Giersky, B. *J. Incl. Phenom. Macrocycl. Chem.* **2008**, *62*, 339.

(27) For an early example of a gated crown ether "ON-OFF-receptor" based on conformational changes crown ethers, see: Shinkai, S.; Ogawa, T.; Kusano, Y.; Manabe, O. *Chem. Lett.* **1980**, 283.

The authors declare no competing financial interest.

Paper II

A Protocol for the *exo*-Mono and *exo,exo*-Bis Functionalization of the Diazocine Ring of Tröger's Base

Sami Dawaigher,[†] Kristoffer Månsson,[†] Erhad Ascic,[†,‡] Josep Artacho,[†] Roger Mårtensson,[†] Nagarajan Loganathan,[†] Ola F. Wendt,[†] Michael Harmata,*,[§] Victor Snieckus,*,[‡] and Kenneth Wärnmark*,[†]

[†]Centre for Analysis and Synthesis, Department of Chemistry, Lund University, P.O. Box 124, 221 00 Lund, Sweden
[‡]Department of Chemistry, Queen's University, Kingston, ON K7L 3N6, Canada
[§]Department of Chemistry, University of Missouri—Columbia, Columbia, Missouri 65211, United States

Ⓢ *Supporting Information*
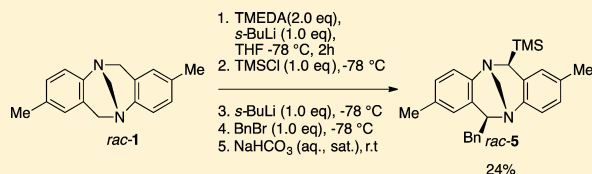
ABSTRACT: An efficient protocol has been developed for the *exo*-mono and *exo,exo*-bis functionalization of Tröger's base in the benzylic 6 and 12 positions of the diazocine ring. The lithiation of Tröger's base using *s*-BuLi/TMEDA followed by electrophilic quench affords *exo*-mono- and *exo,exo*-bis-substituted derivatives of Tröger's base in good to excellent yields. The variation of the number of equivalents of *s*-BuLi/TMEDA and the order of addition of the electrophile strongly govern the outcome of the reaction for each electrophile.

■ INTRODUCTION

Tröger's base (TB, *rac*-**1**) was first synthesized in 1887 by the condensation of *p*-toluidine and methylal in hydrochloric acid.[1] TB exhibits interesting properties: it is a chiral C_2-symmetric rigid molecule with a diazocine core forming a hydrophobic cavity between its two aromatic rings that are situated at roughly 90° in relation to each other. It is chiral because of the presence of stereogenic nitrogen atoms.[2] The structural properties make TB and its analogues useful for applications as building blocks in the fields of molecular recognition, catalysis, and enzyme inhibition.[2]

The synthesis of TB analogues containing electron-poor substituents on their aromatic rings has been impractical because of the poor reactivity of starting anilines. This was overcome by the development of the synthesis of halogenated analogues of *rac*-**1** using paraformaldehyde and TFA,[3] which triggered the development of general methodologies for functionalizing the aryl rings of TB.[3,4] However, the same development has not been observed with the functionalization of its diazocine ring, for which new methodologies are still required. To date, the diazocine ring has been *N*-mono- or *N,N′*-dialkylated and modified on the methylene bridge either by cleavage and replacement or by direct exchange using various methods.[2c,5]

As part of ongoing work, we now report a new synthetic method for the functionalization of the 6-*exo* and 6,12-*exo,exo* positions of TB. Addressing the *exo* position of the TB

framework is important because it may allow the development of new enantiomerically pure ligands for use in transition metal asymmetric catalysis as we have previously shown.[6b] The improved metalation conditions reported herein, compared to those previously reported,[6,7] allow not only the synthesis of the monosubstituted (*rac*-**2a**–**e**) and disubstituted (*rac*-**3a**–**e**) TB derivatives in good to excellent yield but also the synthesis of hetero-disubstituted derivatives, such as *rac*-**5**, in simple one-pot procedures (Figure 1).

In previous work by our groups toward the *exo* substitution of the diazocine ring of *rac*-**1**, it was shown that the treatment of *rac*-**1** with $BF_3 \cdot OEt_2$ followed by *n*-BuLi and then quenching with an electrophile gave the *exo*-monosubstituted products in good yields,[6] whereas the preparation of the *exo,exo*-disubstituted derivatives required two sequential steps resulting in low overall yields.[6,7] In view of these limitations, the question of conducting the reaction with a different lithiating agent was raised. There are several reports of the use of alternative lithiating reagents on other molecules giving rise to differences in product distributions or yields.[9] In particular, it seemed likely that the reaction might proceed in a better manner under strong basic conditions in the absence of a Lewis acid, for example, with *s*-BuLi/TMEDA as a base
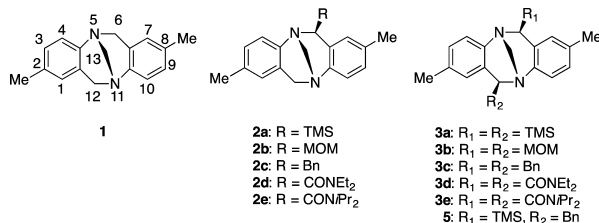
Figure 1. Tröger's base (*rac*-1) and synthesized derivatives described in this article.

Scheme 1. Product Distribution from the Reaction of *rac*-1 with TMEDA/*s*-BuLi Followed by Quenching with CH$_3$OH-d_4 or D$_2$O

Table 1. Synthesis of 6-*exo*-Monosubstituted and 6,12-*exo,exo*-Substituted TB Derivatives *rac*-2a−e and *rac*-3a−e by the Direct-Addition Method

entry	*s*-BuLi/TMEDA (equiv)	electrophile	product	yield %[a]	yield using BF$_3$·Et$_2$O (%)[b]
1[c]	1.1	TMSCl (1.2)	*rac*-2a	76	66
2[c]	1.1	BnBr	*rac*-2b	51[e]	68
3[c]	1.1	MOMCl (1.2)	*rac*-2c	85	
4[c]	0.8	Et$_2$NCOCl (1.2)	*rac*-2d	42	
5[c]	1.0	iPr$_2$NCOCl (1.2)	*rac*-2e	32	
6[d]	2.2	TMSCl (2.5)	*rac*-3a	62	
7[d]	2.2	BnBr (2.5)	*rac*-3b	74	36
8[d]	2.2	MOMCl (2.5)	*rac*-3c	81	
9[d]	2.0	Et$_2$NCOCl (2.4)	*rac*-3d	42	
10[d]	2.0	iPr$_2$NCOCl (2.4)	*rac*-3e	44	

[a]Yield of the isolated analytically pure compound. [b]BF$_3$·OEt$_2$/*n*-BuLi method.[6b,7] [c]For entries 1−5, 1.2 equiv of electrophile was used. [d]In entries 6−10, 2.4 equiv of electrophile was used. [e]Approximately 20% of the disubstituted product and 20% of unreacted starting material were isolated. On the basis of 1.00 and 0.20 g of starting TB, optimal product yields of 51 and 58%, respectively, were obtained.

instead of *n*-BuLi, because of the former exhibiting a basicity 10^3 times stronger than that of the latter.[10]

RESULTS AND DISCUSSION

We first undertook *s*-BuLi/electrophile quench experiments to determine if a high *exo/endo* product ratio could be established. Thus, subjecting *rac*-1 to 1.1 equiv of *s*-BuLi/TMEDA for 1−2 h at −78 °C in THF followed by quenching with 1.2 equiv of CD$_3$OD-d_4 or D$_2$O gave the *exo* monodeuterated TB derivative *rac-deutero*-1$_{exo}$ in 80% yield and the *endo* monodeuterated TB derivative *rac-deutero*-1$_{endo}$ in 20% yield, the same for both deuterium sources, as determined by ^{1}H NMR of the reaction mixture (Scheme 1). The *exo*-6-deuterio stereochemistry was established by the characteristic upfield shift of the remaining *endo*-6-H resonance.[11] The preference for *exo* selectivity is most likely the result of the approach of the electrophile to the incipient

carbanion from the less sterically demanding convex surface of the bicyclic[3.3.1] framework.[6a]

On the basis of successful deuteration experiments, we investigated the scope and limitations of the reaction with respect to different electrophiles (Table 1). Hence, subjecting *rac*-1 to 1.1 equiv of *s*-BuLi/TMEDA for 1 h at −78 °C followed by an electrophilic quench with 1.2 equiv of TMSCl (16 h) (see the reaction in Table 1) gave the *exo* monosilylated Tröger's base derivative *rac*-2a in a 76% yield of isolated and analytically pure product (Table 1, entry 1). This is an improvement on the 66% yield previously reported using the BF$_3$·OEt$_2$-mediated conditions[6a] and as such provides evidence of the superior performance of the new method.

However, repeating the metalation conditions, but now quenching the lithiated intermediate with BnBr (6 h), resulted in the formation of compound *rac*-2b in 51% yield, lower

compared to that obtained by the BF$_3$·OEt$_2$ method.[6a] Roughly 20% of the recovered material was unreacted TB, and roughly 20% was the disubstituted derivative *rac*-3b as determined by ^{1}H NMR spectroscopy. The 6-*exo* stereochemistry of the *rac*-2b was supported by the characteristic upfield shift of remaining *endo*-6-proton resonance, by comparison to TB itself, for which the 6- and 12-*endo*-proton resonances are shifted upfield compared to the 6- and 12-*exo*-proton resonances.[11] The *exo* stereochemistry of *rac*-2b was firmly confirmed by an X-ray diffraction (XRD) analysis (Figure 2). This comparison between the 6-*exo* stereo-
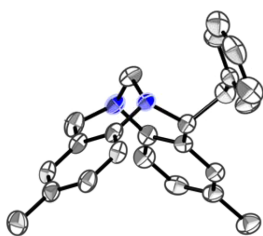
Figure 2. Molecular structure of compound *rac*-2b with thermal ellipsoids at the 30% probability level. Hydrogen atoms have been omitted for the sake of clarity.

chemistry of *rac*-2b as determined by XRD analysis and the upfield shift of the 6-*exo*-proton resonance in the ^{1}H NMR spectrum supports the use of ^{1}H NMR spectroscopy for determining the 6-*exo/endo* stereochemistry of TB derivatives as previously done for TB itself.[11]

As the next experiment, subjecting *rac*-1 to 1.1 equiv of *s*-BuLi/TMEDA for 1 h at −78 °C followed by quenching with

1.2 equiv of MOMCl (16 h) resulted in the formation of *rac*-2c in an excellent 85% yield (Table 1, entry 3).

It was noted that along with the desired TB derivative *rac*-2a (76%) and unreacted *rac*-1 (11%), a small amount (9%) of *exo,exo*-6,12-disilylated TB derivative *rac*-3a was present in the lithiation/TMSCl quench reaction described above. The latter result suggested that the *s*-BuLi/TMEDA method would allow for the bis-functionalization of the diazocine ring of *rac*-1.

Hence, doubling the number of equivalents of *s*-BuLi/TMEDA to 2.0−2.2 equiv in the reactions with BnBr, TMSCl, and MOMCl, respectively, led to the synthesis of the *exo,exo*-disubstituted TB derivatives *rac*-3a−c in good to very good yields (Table 1, entries 6−8). The lithiation time of 1 h followed by electrophile quenching and allowing for the reaction mixture to slowly reach rt over 16−20 h were used as optimal conditions, although longer or shorter times were of little consequence for the observed yields. Particularly satisfying was the near doubling of the yield of the *exo,exo*-dibenzyl derivative (*rac*-3b) compared to that observed using the *n*-BuLi/BF$_3$·OEt$_2$ method (Table 1, entry 7).[6a] The 6,12-*exo,exo* stereochemistry of *rac*-3c was confirmed by XRD analysis (Figure S-2 of the Supporting Information).

The yields obtained from the reactions using diethylcarbamoyl chloride (Et$_2$NCOCl) and *N,N*-diisopropylcarbamoyl chloride (*i*Pr$_2$NCOCl) as electrophiles, on the other hand, were disappointing (Table 1, entries 4, 5, 9, and 10). Duplicate reactions using *s*-BuLi/TMEDA (1 h, 1.1 equiv) and *N,N*-Et$_2$NCOCl (15 h, 1.2 equiv) and working up the reaction mixture with a saturated aqueous NaHCO$_3$ solution revealed that, in addition to the expected *exo*-monosubstituted product *rac*-2d (∼25%), unreacted starting material (∼35%), traces of *rac*-3d (∼5%), and a compound that was identified as the *endo*-monosubstituted addition product *rac*-4 (∼20%) were obtained (Scheme 2a) (see the Supporting Information).

Scheme 2. Product Distribution from the Reaction of TB (*rac*-1) with *s*-BuLi/TMEDA Followed by (a) Et$_2$NCOCl and (b) Successive Quenching with Et$_2$NCOCl and CD$_3$OD
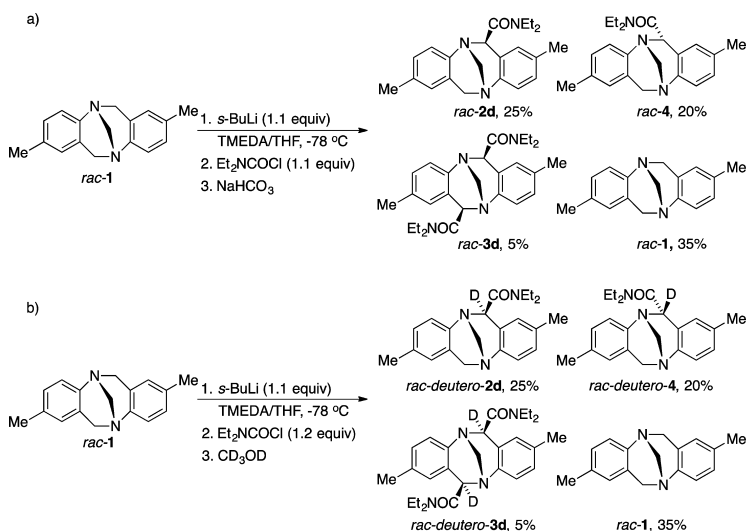
Scheme 3. Mechanistic Rationalization of the Reaction of TB (*rac*-1) with *s*-BuLi/TMEDA Followed by Et$_2$NCOCl and CD$_3$OD

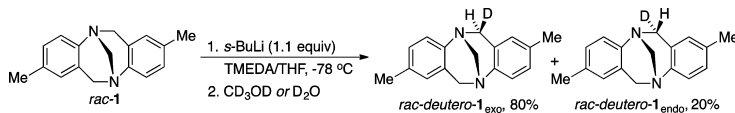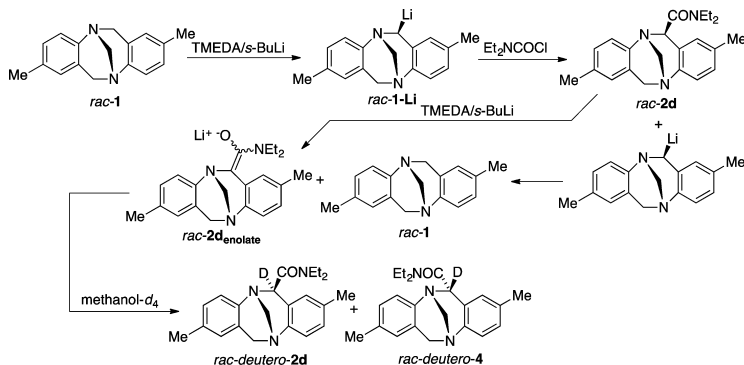**Table 2. Synthesis of 6-*exo* Mono and 6,12-*exo*,*exo*-Substituted TB Derivatives 2a–e and 3a–e by the Inverse-Addition Method**
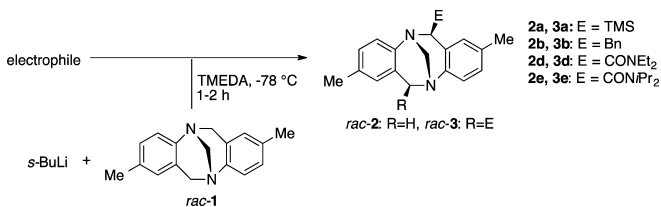
entry	*s*-BuLi/TMEDA (equiv)	electrophile (equiv)	product	yield (%)[a]	yield using BF$_3$·Et$_2$O (%)[b]
1	0.95	TMSCl (>10)	*rac*-2a	72	
2	0.95	BnBr (>10)	*rac*-2b	0[c]	68
3	0.95	Et$_2$NCOCl (>10)	*rac*-2d	70	
4	0.95	iPr$_2$NCOCl (7.5)	*rac*-2e	73	
5	3.0	TMSCl (>10)	*rac*-3a	89	
6	3.0	BnBr (>10)	*rac*-3b	96	34
7	3.0	Et$_2$NCOCl (>10)	*rac*-3d	97	
8	3.0	iPr$_2$NCOCl (7.5)	*rac*-3e	98	

[a]Yields of isolated products after column chromatography and/or crystallization. [b]Yields using the *n*-BuLi/BF$_3$·OEt$_2$ method, via direct addition.[7] [c]Traces of starting material (<5%) and polymeric material were obtained.

Using the same conditions but now quenching with CD$_3$OD resulted in part deuteration at the α-position of the amide group, yielding the TB amide derivatives *rac-deutero*-2d, *rac-deutero*-3d, and *rac-deutero*-4 in the same ratios as described above as determined by ^{1}H NMR spectroscopy of the crude product (Scheme 2b) (see the Supporting Information). However, no deuterated TB (*rac*-1) was isolated from the same reaction quenched with CD$_3$OD, indicating that the enolization of *rac*-2d has at least partly proceeded via metalated *rac*-1, because the lithiation of *rac*-1 using *s*-BuLi/TMEDA goes to completion (Scheme 1). Hence, from the product distribution and the deuteration experiments, it became apparent that either the lithiated TB or the excess *s*-BuLi/TMEDA species effects the deprotonation of the newly formed amide *rac*-2d in the reaction mixture, forming the corresponding enolate *rac*-2d$_{enolate}$ (Scheme 2). Hence, quenching with CD$_3$OD affords *endo* and *exo* isomers *rac*-2d and *rac*-4, respectively, in approximately equal amounts.

Because the inverse-addition method *vide infra* (Scheme 3) solved this epimerization problem, this reaction was not further investigated.

To counter the setback described above, a method was developed on the basis of inverse addition that involved treating *rac*-1 with *s*-BuLi/TMEDA in THF at −78 °C followed by the addition of the resulting lithiated TB species *rac*-1-Li to an excess of electrophile (>10 equiv) in THF at −78 °C (see Scheme 3 and the reaction in Table 2), then allowing the mixture to reach room temperature slowly (1–2 h), and finally quenching the reaction with a saturated aqueous solution of sodium bicarbonate. As established by the inverse-addition protocol, the presence of a large excess of an electrophile traps lithiated *rac*-1 as it is formed, thus preventing its action as a base in deprotonating the newly formed product *rac*-2d. The results of the inverse-addition method are summarized in Table 2.

Scheme 4. Synthesis of the *exo,exo*-6,12-Heterosubstituted TB Derivative *rac*-5
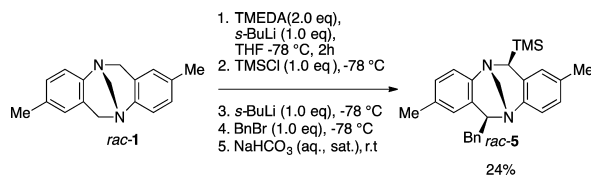
In the process of the optimization of the inverse-addition method, it became apparent, as expected, that increasing the amount of *s*-BuLi/TMEDA for the lithiation step had an effect on the observed yields. Hence, treating *rac*-1 with 1.1– 2.2 equiv of *s*-BuLi/TMEDA resulted in reaction mixtures containing both mono- and disubstituted products *rac*-2d and *rac*-3d, respectively. Using 0.95 equiv of *s*-BuLi/TMEDA eliminated the formation of disubstituted product *rac*-3d with the drawback that some unreacted starting material (10−20%) was isolated. The starting material was, however, recovered by column chromatography and reused. Increasing the amount of *s*-BuLi/TMEDA to 3.0 equiv completely eliminated the formation of the monosubstituted product *rac*-2d and the starting material and also the necessity of column chromatography in the purification process.

Addition of the lithiated TB species *rac*-1-Li to an excess (>10 equiv) of the electrophile increased the overall yield of both mono- and difunctionalized TB derivatives *rac*-2a, *rac*-2d, *rac*-2e, *rac*-3a, *rac*-3b, *rac*-3d, and *rac*-3e (Table 2, entries 1 and 3−8, respectively), compared to adding a stoichiometric amount of the electrophile directly to the lithiated species (Table 1). Monosubstituted products *rac*-2a, *rac*-2d, and *rac*-2e (Table 2, entries 1, 3, and 4, respectively) were obtained in good to very good yields; however, some unreacted *rac*-1 (20−30%) was always isolated from the crude reaction mixture, indicating incomplete metalation of *rac*-1 under the <1.0 equiv of *s*-BuLi/TMEDA conditions. Notably, using the inverse-addition method, the yield of products *rac*-2d and *rac*-2e (Table 2, entries 3 and 4, respectively) was improved over the direct-addition method by as much as 35−40%. Oddly, this method proved to be ineffective in producing *rac*-2b (Table 2, entry 2); in addition to trace amounts of *rac*-1, only polymeric material was obtained. Because *rac*-2b was produced in an acceptable yield by the direct-addition method, this reaction was not further investigated. It can be suggested that during the conditions of the inverse-addition method, in which the lithiated TB encounters a large excess of benzyl bromide, the lithiated TB generates a benzyl radical by a single electron transfer to benzyl bromide, a reaction similar to what has been observed for the reaction of lithium reagents with alkyl halides.[8] It can, for example, be further suggested that the so-formed benzyl radical reacts quickly with benzyl bromide, leading to the depletion of the latter so that no benzyl benzylated TB can form. Notably, the yields of the disubstituted products *rac*-3a, *rac*-3b, *rac*-3d, and *rac*-3e ranged from very good to excellent, improving the yields compared to the direct-addition method by as much as 55 and 54% in the case of *rac*-3d and *rac*-3e, respectively. Rewardingly, the yield of the *exo,exo*-6,12-dibenzylated compound *rac*-3b was higher than that obtained by the BF$_3$·OEt$_2$/*n*-BuLi method.[7]

To extend the use of our developed synthetic method to obtain *exo,exo*-6,12-heterodisubstituted TB derivatives, a one-pot direct-addition methodology was developed. Thus, a solution of *rac*-1 containing 2.2 equiv of TMEDA was sequentially treated with 1.0 equiv of *s*-BuLi and TMSCl, respectively, followed, after 1 h, by 1.0 equiv of *s*-BuLi and BnBr, respectively, in succession to give the *exo*-6-benzyl-*exo*-12-trimethylsilyl TB derivative *rac*-5 in 24% yield (Scheme 4). The low yield obtained is due to the formation of byproducts such as *rac*-3a that hampered the purification due to their R$_f$ values being very close to that of *rac*-5.

In conclusion, two efficient methods for the synthesis of *exo*-6-monosubstituted and *exo,exo*-6,12-bis-substituted derivatives *rac*-2a−e and *rac*-3a−e of Tröger's base *rac*-1 have been developed: a straightforward and simple one-pot, direct-addition method and a somewhat more cumbersome inverse-addition method. Both of these methods rely on using different amounts of *s*-BuLi/TMEDA as the metalating reagent and have distinct advantages. The direct-addition method does not require the use of excess electrophile, may be used to produce heterosubstituted TB derivatives *rac*-5, and is preferred for the synthesis of monosubstituted TB *rac*-2a, *rac*-2b, and *rac*-2c. The inverse-addition method shows yields vastly superior to those of the direct-addition method and other previously reported methods[6,7] for the preparation of the *exo,exo*-disubstituted TB derivatives. The inverse-addition method precludes the formation of enolate, thereby securing a high yield of the *exo* diastereomer of *rac*-2d, *rac*-2e, *rac*-3d, and *rac*-3e, compounds containing an acidic α-hydrogen atom. Another advantage of both the direct- and inverse-addition methods developed in the work is the use of the TMEDA additive that is less costly and more bench stable than BF$_3$·OEt$_2$. Finally, our work has generated new TB derivatives or increased the availability of known TB derivatives with defined *exo* stereochemistry via a more efficient synthesis. These compounds constitute or may be modified into new building blocks that can be used in supramolecular chemistry and catalysis.

■ EXPERIMENTAL SECTION

General Methods. All chemicals were used as received from commercial sources without further purification unless stated otherwise. TMEDA was dried with KOH overnight and distilled under house vacuum prior to use. Benzyl bromide and *N,N*-diethylcarbamoyl chloride were distilled under house vacuum prior to use. *N,N*-Diisopropylcarbamoyl chloride was sublimed and kept under nitrogen prior to use. THF was dried with sodium and distilled under nitrogen. PE refers to petroleum ether (bp 40−60 °C). *s*-BuLi was titrated prior to use according to a literature method.[12] Precoated Merck silica gel 60 F$_{254}$ plates were used for TLC analysis. Column chromatography was performed on silica gel (Davisil 35−70 μm). ¹H and ¹³C NMR spectra were recorded on a 400 NMR spectrometer. Chemical shifts (δ) are reported relative to shift scale calibrated with residual NMR solvent peak CDCl$_3$ (δ 7.26

for ^{1}H NMR and δ 77.23 for ^{13}C NMR). Melting points were recorded on a Fischer-Jones apparatus, using plate technology. IR spectra were recorded on a FTIR spectrophotometer. HRMS data were obtained on a Q-TOF micro instrument.

Crystallography. Crystals of *rac*-**2b** were grown by dissolving 50 mg of *rac*-**2b** in ethyl acetate (1.0 mL), adding heptane (1.0 mL), and allowing the mixture to evaporate slowly at room temperature. Crystals of *rac*-**3c** were grown by dissolving 50 mg of *rac*-**3c** in diethyl ether (1.0 mL), adding heptane (1.0 mL), and allowing the mixture to evaporate slowly at room temperature. Intensity data were collected with an Oxford Diffraction Excalibur 3 system, using ω-scans and Mo Kα (λ = 0.71073 Å) radiation.[13] The data were extracted and integrated using Crysalis RED.[14] The structure was determined by direct methods and refined by full-matrix least-squares calculations on F^2 using SHELXL[15] and SIR-92.[16] Molecular graphics were generated using CrystalMaker version 8.3.5.[17] CCDC deposition numbers CCDC 1416673−1416674.

General Procedure for the Direct-Addition Method. The general procedure consists of 1.00 g of *rac*-**1** being dissolved in dry THF under N$_2$. TMEDA (amount indicated in entry) is added, and the solution is cooled to −78 °C. *s*-BuLi (amount indicated in entry) is added dropwise over 10−20 min at −78 °C. The solution is maintained at −78 °C for 1−2 h. The electrophile (amount specified in each entry) is then added dropwise at −78 °C, and the reaction mixture is allowed to reach room temperature. The reaction is then quenched by successively adding a saturated aqueous solution of NaHCO$_3$ (10 mL), CH$_2$Cl$_2$ (30 mL), and water (20 mL), and the phases are separated. The aqueous phase is extracted with additional CH$_2$Cl$_2$ (3 × 50 mL). The combined organic phase is washed with brine, dried with Na$_2$SO$_4$, and subjected to filtration and the solvent removed *in vacuo*. The crude material is purified as described in each individual entry.

exo-2,8-Dimethyl-6-trimethylsilyl-6H,12H-5,11-methanodibenzo-[b,f][1,5]diazocine (2a). To a stirred solution of TB *rac*-**1** (0.998 g, 3.99 mmol) in anhydrous THF (30 mL) under an inert atmosphere was added TMEDA (0.66 mL, 4.4 mmol), and the resulting faint yellow solution was stirred at rt for 30 min before being cooled to −78 °C for 15 min. *s*-BuLi (1.31 M, 3.40 mL, 4.45 mmol) was then added dropwise over 30 min, and the resulting reaction mixture was stirred for an additional 1 h before the TMSCl (0.63 mL, 5.0 mmol) was slowly added over 30 min. The cooling bath was removed, and the reaction mixture was allowed to warm to rt (20 h) and the reaction quenched with saturated aqueous NaHCO$_3$ (10 mL) followed by addition of CH$_2$Cl$_2$ (30 mL) and water (30 mL). The resulting layers were separated, and the aqueous phase was further extracted with CH$_2$Cl$_2$ (3 × 50 mL). The combined organic layer was washed with brine, dried over Na$_2$SO$_4$, subjected to filtration, and evaporated *in vacuo* to dryness. The resulting residue was purified by column chromatography (3 cm × 10 cm, 9:1 PE/EtOAc) to give *rac*-**2a** as colorless crystals in 76% yield (0.98 g): R_f = 0.25 (9:1 PE/EtOAc); mp 128−130 °C (heptane/EtOAc); IR (CH$_2$Cl$_2$) 2953, 1488, 1322, 1244, 832 cm^{-1}; ^{1}H NMR (400 MHz, CDCl$_3$) δ 7.00 (d, J = 8.1 Hz, 1H, H-10), 6.93 (dd, J = 8.4, 1.4 Hz, 1H, H-3), 6.91−6.87 (m, 2H, H-4 and H-9), 6.67 (s, 1H, H-1), 6.61 (s, 1H, H-7), 4.63 (d, J = 16.6 Hz, 1H, H-12x), 4.22 (dd, J = 12.7, 1.1 Hz, 1H, H-13), 4.16 (dd, J = 12.7, 1.0 Hz, 1H, H-13′), 4.07 (d, J = 16.5 Hz, 1H, H-12n), 3.84 (s, 1H, H-6), 2.20 (s, 6H, Ar-CH$_3$), 0.24 (s, 9H, -Si(CH$_3$)$_3$); ^{13}C NMR (100 MHz, CDCl$_3$) δ 148.8, 144.9, 133.01, 132.97, 131.1, 128.1, 127.6, 127.3, 127.0, 126.9, 125.2, 124.9, 65.6, 63.7, 59.4, 21.2, 21.0, −1.2 (3C); HRMS-EI$^+$ *m/z* [M]$^+$ calcd for C$_{20}$H$_{26}$N$_2$Si 322.1865, found 322.1867. Anal. Calcd for C$_{20}$H$_{26}$N$_2$Si: C, 74.48; H, 8.13; N, 8.69. Found: C, 74.44; H, 8.11; N, 8.65.

exo-2,8-Dimethyl-6-benzyl-6H,12H-5,11-methanodibenzo[b,f]-[1,5]diazocine (2b). TB *rac*-**1** (1.00 g, 3.99 mmol) was subjected to the general procedure using TMEDA (0.66 mL, 4.4 mmol), *s*-BuLi (1.30 M, 3.40 mL, 4.42 mmol), and benzyl bromide (0.570 mL, 4.79 mmol). A 1 h lithiation time was used before the addition of the electrophile. The reaction was quenched after the mixture had been stirred for 6 h at rt. Purification by column chromatography (5 cm × 10 cm, 9:1 PE/EtOAc) gave *rac*-**2b** as an amorphous solid in 51%

yield (0.70 g): R_f = 0.28 (9:1 PE/EtOAc); mp 134−136 °C (heptane/diethyl ether); ^{1}H NMR (400 MHz, CDCl$_3$) δ 7.50−7.43 (m, 4H, Ar-*H*), 7.35 (tt, J = 7.0, 1.9 Hz, 1H, Ar-*H*), 7.10 (d, J = 8.1 Hz, 1H, H-10), 7.03 (dd, J = 8.2, 1.8 Hz, 1H, H-9), 6.87 (s, 1H, H-1), 6.83 (dd, J = 8.1, 1.4 Hz, 1H, H-3), 6.68 (s, 1H, H-7), 6.46 (d, J = 8.1 Hz, 1H, H-4), 4.69 (d, J = 16.6 Hz, 1H, H-12x), 4.53 (dd, J = 12.9, 1.6 Hz, 1H, H-13), 4.26−4.21 (m, 2H, H-6 and H-13′), 4.14 (d, J = 16.6 Hz, 1H, H-12n), 3.22 (dd, J = 14.2, 4.4 Hz, 1H, -CH$_2$-Ph), 3.16 (dd, J = 14.1, 10.2 Hz, 1H, -CH$_2$-Ph), 2.28 (s, 3H, Ar-CH$_3$), 2.20 (s, 3H, Ar-CH$_3$); ^{13}C NMR (100 MHz, CDCl$_3$) δ 146.6, 145.7, 140.2, 133.3, 133.2, 130.9, 129.7 (2C), 128.51, 128.47 (2C), 128.1, 127.5, 127.2, 126.4, 125.0, 124.6, 77.2, 69.3, 61.5, 58.6, 43.1, 21.1, 21.0; HRMS-ESI$^+$ *m/z* [M + H]$^+$ calcd for C$_{24}$H$_{25}$N$_2$ 341.2018, found 341.2031. Anal. Calcd for C$_{24}$H$_{24}$N$_2$·0.25H$_2$O: C, 83.56; H, 7.16; N, 8.12. Found: C, 83.90; H, 7.39; N, 8.34.

exo-2,8-Dimethyl-6-methoxymethyl-6H,12H-5,11-methanodibenzo[b,f][1,5]diazocine (2c). TB *rac*-**1** (1.00 g, 3.99 mmol) was subjected to the general procedure using TMEDA (0.66 mL, 4.4 mmol), *s*-BuLi (0.530 M, 8.32 mL, 4.40 mmol), and MOMCl (0.360 mL, 4.74 mmol). A 1 h lithiation time was used before the addition of the electrophile. The reaction was quenched after the mixture had been stirred for 16 h at rt. Purification by column chromatography (5 cm × 10 cm, 3:2 PE/EtOAc) gave *rac*-**2c** as an off-white highly viscous liquid in 85% yield (1.01 g): R_f = 0.30 (3:2 PE/EtOAc); ^{1}H NMR (400 MHz, CDCl$_3$) δ 7.04 (d, J = 8.0 Hz, 1H, H-10), 7.02 (d, J = 7.9 Hz, 1H, H-4), 6.98 (dd, J = 8.2, 1.8 Hz, 1H, H-3), 6.95 (dd, J = 8.2, 1.4 Hz, 1H, H-9), 6.84 (s, 1H, H-1), 6.68 (s, 1H, H-7), 4.67 (d, J = 16.6 Hz, 1H, H-12x), 4.43 (dd, J = 12.9, 1.6 Hz, 1H, H-13), 4.25−4.18 (m, 2H, H-6 and H-13′), 4.09 (d, J = 16.5 Hz, 1H, H-12n), 3.83 (dd, J = 10.3, 9.1 Hz, 1H, -CH$_2$O-), 3.72 (dd, J = 10.4, 3.8 Hz, 1H, -CH$_2$O-), 3.54 (s, 6H, -OCH$_3$), 2.23 (s, 3H, Ar-CH$_3$) 2.23 (s, 6H, Ar-CH$_3$); ^{13}C NMR (100 MHz, CDCl$_3$) δ 146.34, 146.28, 133.50, 133.31, 128.8, 128.6, 128.3, 127.6, 127.5, 127.3, 125.2, 125.1, 76.2, 66.9, 62.1, 59.4, 58.5, 21.04, 21.00; HRMS-ESI$^+$ *m/z* [M + H]$^+$ calcd for C$_{19}$H$_{23}$N$_2$O 295.1810, found 295.1785. Anal. Calcd for C$_{19}$H$_{22}$N$_2$O: C, 77.52; H, 7.53; N, 9.52. Found: C, 77.48; H, 7.48; N, 9.46.

exo-2,8-Dimethyl-6-(N,N-diethylamide)-6H,12H-5,11-methanodibenzo[b,f][1,5]diazocine (2d). TB *rac*-**1** (1.00 g, 3.99 mmol) was subjected to the general procedure using TMEDA (0.48 mL, 3.2 mmol), *s*-BuLi (1.29 M, 2.50 mL, 3.22 mmol), and *N,N*-diethylcarbamoyl chloride (0.610 mL, 4.80 mmol). A 1 h lithiation time was used before the addition of the electrophile. The reaction was quenched after the mixture had been stirred for 15 min at rt. Purification by column chromatography (5 cm × 9 cm, 3:2 PE/EtOAc) gave *rac*-**2d** as colorless crystals in 42% yield (0.589 g): R_f = 0.21 (7:3 PE/EtOAc); mp 149−151 °C (heptane/EtOAc); IR (CH$_2$Cl$_2$) 3391, 3052, 2936, 1700, 1646, 1609, 1445, 1363, 1324, 1266, 733 cm^{-1}; ^{1}H NMR (400 MHz, CDCl$_3$) δ 7.05 (d, J = 8.1 Hz, 1H, H-10), 7.02 (d, J = 8.1 Hz, 1H, H-4), 7.00−6.93 (m, 2H, H-3 and H-9), 6.72 (d, J = 0.8 Hz, H-1), 6.62 (d, J = 1.5 Hz, H-7), 4.91 (s, 1H, H-6), 4.83 (dd, J = 12.8, 1.8 Hz, 1H, H-13), 4.64 (d, J = 16.7 Hz, 1H, H-12x), 4.13−4.02 (m, 3H, H-13′, H-12n and N-CH$_2$-CH$_3$), 3.75 (dq, J = 14.7, 7.3 Hz, 1H, N-CH$_2$-CH$_3$), 3.54 (dq, J = 13.7, 6.9 Hz, 1H, N-CH$_2$-CH$_3$), 3.44 (dq, J = 13.7, 6.9 Hz, 1H, N-CH$_2$-CH$_3$), 2.22 (s, 3H, Ar-CH$_3$), 2.20 (s, 3H, Ar-CH$_3$), 1.46 (t, J = 7.1 Hz, 3H, -CH$_2$-CH$_3$), 1.21 (t, J = 7.1 Hz, 3H, -CH$_2$-CH$_3$); ^{13}C NMR (100 MHz, CDCl$_3$) δ 170.2, 145.8, 145.3, 133.8, 133.1, 128.9, 128.3, 128.2, 128.2, 127.9, 126.4, 124.8, 123.2, 66.5, 63.0, 58.6, 42.3, 41.1, 21.0, 20.8, 14.9, 13.0; HRMS-EI$^+$ *m/z* [M]$^+$ calcd for C$_{22}$H$_{27}$N$_3$O 349.2154, found 349.2156. Anal. Calcd for C$_{22}$H$_{27}$N$_3$O: C, 75.61; H, 7.79; N, 12.02. Found: C, 75.64; H, 7.74; N, 11.97.

exo-2,8-Dimethyl-6-(N,N-diisopropylamide)-6H,12H-5,11-methanodibenzo[b,f][1,5]diazocine (2e). TB *rac*-**1** (1.00 g, 3.99 mmol) was subjected to the general procedure using TMEDA (0.60 mL, 4.0 mmol), *s*-BuLi (1.31 M, 3.00 mL, 3.93 mmol), and *N,N*-diisopropylcarbamoyl chloride (0.790 g, 4.83 mmol) dissolved in THF (5 mL). A 1 h lithiation time was used before the addition of the electrophile. The reaction was quenched after the mixture had been stirred for 2 h at rt. Purification by column chromatography (5

cm × 10 cm, 3:2 PE/EtOAc) gave *rac*-**2e** as colorless crystals in 32% yield (0.49 g): R_f = 0.35 (7:3 PE/EtOAc); mp 201−203 °C (heptane/EtOAc); IR (neat) 1638, 1490, 1437, 1214 cm^{-1}; ^{1}H NMR (400 MHz, CDCl$_3$) δ 7.03 (d, J = 8.2 Hz, 1H, H-10), 6.99−6.94 (m, 3H, H-3, H-4 and H-9), 6.71 (s, 1H, H-1), 6.60 (s, 1H, H-7), 4.97 (septet, J = 6.7 Hz, 1H, -CH(CH$_3$)$_2$), 4.90 (s, 1H, H-6), 4.65−4.60 (m, 2H, H-12x and H-13), 4.12−4.08 (m, 2H, H-12n and H-13′), 3.47 (septet, J = 6.7 Hz, 1H, -CH(CH$_3$)$_2$), 2.21 (s, 3H, Ar-CH$_3$), 2.21 (s, 3H, Ar-CH$_3$), 1.47−1.40 (m, 12H, -CH(CH$_3$)$_2$); ^{13}C NMR (100 MHz, CDCl$_3$) δ 169.6, 145.9, 145.3, 133.8, 132.9, 129.1, 129.0, 128.28, 128.25, 128.0, 126.7, 124.7, 122.8, 68.5, 63.3, 58.9, 49.2, 46.5, 21.4, 21.14, 20.96 (2C), 20.8, 20.4; HRMS-ESI$^+$ m/z [M + H]$^+$ calcd for C$_{24}$H$_{32}$N$_3$O 378.2545, found 378.2547. Anal. Calcd for C$_{24}$H$_{31}$N$_3$O: C, 76.35; H, 8.28; N, 11.13; Found: C, 76.31; H, 8.26; N, 11.07.

exo,exo-2,8-Dimethyl-6,12-bis(trimethylsilyl)-6H,12H-5,11-methanodibenzo[b,f][1,5]diazocine (**3a**). TB *rac*-**1** (1.00 g, 3.99 mmol) was subjected to the general procedure using TMEDA (1.31 mL, 8.79 mmol), *s*-BuLi (1.30 M, 6.66 mL, 8.79 mmol), and TMSCl (1.27 mL, 9.99 mmol). A 2.5 h lithiation time was used before the addition of the electrophile. The reaction was quenched after the mixture had been stirred for 2 h at rt. Purification by column chromatography (5 cm × 20 cm, 20:1 PE/EtOAc) gave *rac*-**3a** as colorless crystals in 62% yield (0.980 g): R_f = 0.28 (40:1 PE/EtOAc); mp 139−141 °C (heptane/diethyl ether); IR (CH$_2$Cl$_2$) 2961, 1485, 1248, 1217, 832 cm^{-1}; ^{1}H NMR (400 MHz, CDCl$_3$) δ 6.88 (d, J = 8.1 Hz, 2H, H-4 and H-10), 6.84 (dd, J = 8.1, 1.7 Hz, 2H, H-3 and H-9), 6.58 (s, 2H, H-1 and H-7), 4.07 (s, 2H, H-13), 3.80 (s, 2H, H-6 and H-12), 2.19 (s, 6H, Ar-CH$_3$), 0.23 (s, 18H, -Si(CH$_3$)$_3$); ^{13}C NMR (100 MHz, CDCl$_3$) δ 148.4, 132.4, 131.1, 127.0, 126.7, 125.1, 64.2, 64.1 (1C), 21.2, −1.1 (6C); HRMS-EI$^+$ m/z [M]$^+$ calcd for C$_{23}$H$_{34}$N$_2$Si$_2$ 394.2261, found 394.2272. Anal. Calcd for C$_{23}$H$_{34}$N$_2$Si$_2$: C, 69.99; H, 8.68; N, 7.10. Found: C, 69.87; H, 8.58; N, 7.10.

exo,exo-2,8-Dimethyl-6,12-bis(benzyl)-6H,12H-5,11-methanodibenzo[b,f][1,5]diazocine (**3b**). TB *rac*-**1** (1.00 g, 3.99 mmol) was subjected to the general procedure using TMEDA (1.34 mL, 9.00 mmol), *s*-BuLi (1.30 M, 6.90 mL, 8.97 mmol), and benzyl bromide (1.20 mL, 10.1 mmol). A 1 h lithiation time was used before the addition of the electrophile. The reaction was quenched after the mixture had been stirred for 16 h at rt. Purification by column chromatography (5 cm × 10 cm, 4:1 PE/EtOAc) gave *rac*-**3b** as white crystals in 74% yield (1.28 g): R_f = 0.30 (4:1 PE/EtOAc); mp 220−222 °C (heptane/diethyl ether); ^{1}H NMR (400 MHz, CDCl$_3$) δ 7.45−7.39 (m, 8H, Ar-H), 7.31 (tt, J = 6.8, 2.1 Hz, 2H, Ar-H), 6.80 (dd, J = 8.1, 1.9 Hz, 2H, H-3 and H-9), 6.77 (s, 2H, H-4 and H-7), 6.40 (d, J = 8.1 Hz, 2H, H-3 and H-10), 4.37 (s, 2H, H-13), 4.16 (dd, J = 10.3, 4.2 Hz, 2H, H-6 and H-12), 3.16 (dd, J = 14.1, 4.2 Hz, 2H, -CH$_2$-Ph), 3.09 (dd, J = 14.1, 10.4 Hz, 2H, -CH$_2$-Ph), 2.17 (s, 6H, Ar-CH$_3$); ^{13}C NMR (100 MHz, CDCl$_3$) δ 146.6, 140.3, 132.9, 130.8, 129.7, 128.5, 128.4, 128.3, 126.4, 124.6, 69.1, 56.1 (1C), 43.2, 21.1; HRMS-ESI$^+$ m/z [M + H]$^+$ calcd for C$_{31}$H$_{31}$N$_2$ 431.2487, found 431.2502. Anal. Calcd for C$_{31}$H$_{30}$N$_2$· 0.25H$_2$O: C, 85.58; H, 7.07; N, 6.44. Found: C, 85.73; H, 7.05; N, 6.60.

exo,exo-2,8-Dimethyl-6,12-bis(methoxymethyl)-6H,12H-5,11-methanodibenzo[b,f][1,5]diazocine (**3c**). TB *rac*-**1** (1.00 g, 3.99 mmol) was subjected to the general procedure using TMEDA (1.32 mL, 8.86 mmol), *s*-BuLi (0.530 M, 16.6 mL, 8.80 mmol), and MOMCl (0.730 mL, 9.61 mmol). A 1 h lithiation time was used before the addition of the electrophile. Purification by column chromatography (5 cm × 32 cm, 7:3 hexanes/EtOAc) gave *rac*-**3c** as a highly viscous liquid in 81% yield (1.10 g): R_f = 0.16 (7:3 hexanes/EtOAc); ^{1}H NMR (400 MHz, CDCl$_3$) δ 7.04 (d, J = 8.2 Hz, 2H, H-4 and H-10), 6.97 (dd, J = 8.2, 1.9 Hz, 2H, H-3 and H-9), 6.81 (d, J = 1.5 Hz, 2H, H-1 and H-7), 4.32 (s, 2H, H-13), 4.21 (dd, J = 9.0, 3.8 Hz, 2H, H-6 and H-12), 3.81 (dd, J = 10.4, 9.1 Hz, 2H, -CH$_2$O-), 3.72 (dd, J = 10.5, 3.8 Hz, 2H, -CH$_2$O-), 3.54 (s, 6H, -OCH$_3$), 2.21 (s, 6H, Ar-CH$_3$); ^{13}C NMR (100 MHz, CDCl$_3$) δ 146.9, 133.3, 128.9, 128.4, 127.4, 125.3, 76.1, 66.6, 59.4, 57.2 (1C), 21.0; HRMS-

ESI$^+$ m/z [M + H]$^+$ calcd for C$_{21}$H$_{27}$N$_2$O$_2$ 339.2073, found 339.2093. Anal. Calcd for C$_{21}$H$_{26}$N$_2$O$_2$: C, 74.52; H, 7.74; N, 8.28. Found: C, 74.52; H, 7.77; N, 8.19.

exo,exo-2,8-Dimethyl-6,12-bis(N,N-diethylcarbamide)-6H,12H-5,11-methanodibenzo[b,f][1,5]diazocine (**3d**). TB *rac*-**1** (1.00 g, 3.99 mmol) was subjected to the general procedure using TMEDA (1.20 mL, 8.05 mmol), *s*-BuLi (1.29 M, 6.20 mL, 8.00 mmol), and N,N-diethylcarbamoyl chloride (1.30 mL, 10.2 mmol). A 15 min lithiation time was used before the addition of the electrophile. The reaction was quenched after the mixture had been stirred for 20 h at rt. Purification by column chromatography (5 cm × 10 cm, 3:2 PE/EtOAc) gave *rac*-**3d** as colorless crystals in 42% yield (0.766 g): R_f = 0.12 (7:3 PE/EtOAc); mp 224−226 °C recrystallized from heptane/diethyl ether; IR (NaCl) 2976, 1638, 1490, 1138 cm^{-1}; ^{1}H NMR (400 MHz, CDCl$_3$) δ 7.04 (d, J = 8.2 Hz, 2H, H-4 and H-10), 6.98 (dd, J = 8.2, 2.0 Hz, 2H, H-3 and H-9), 6.63 (d, J = 1.6 Hz, 2H, H-1 and H-7), 4.89 (s, 2H, H-6 and H-12), 4.49 (s, 2H, H-13), 4.11 (dq, J = 14.6, 7.3 Hz, 2H, N-CH$_2$-CH$_3$), 3.76 (dq, J = 14.6, 7.3 Hz, 2H, N-CH$_2$-CH$_3$), 3.55 (dq, J = 13.6, 6.9 Hz, 2H, N-CH$_2$-CH$_3$), 3.38 (dq, J = 13.6, 6.9 Hz, 2H, N-CH$_2$-CH$_3$), 2.20 (s, 6H, Ar-CH$_3$), 1.44 (t, J = 7.0 Hz, 6H, -CH$_2$-CH$_3$), 1.18 (t, J = 7.0 Hz, 6H, -CH$_2$-CH$_3$); ^{13}C NMR (100 MHz, CDCl$_3$) δ 170.0, 145.5, 133.3, 129.5, 129.1, 127.0, 122.8, 67.3, 59.1 (1C), 42.3, 41.3, 21.0, 14.9, 13.0; HRMS-EI$^+$ m/z [M]$^+$ calcd for C$_{27}$H$_{36}$N$_4$O$_2$ 448.2837, found 448.2838. Anal. Calcd for C$_{27}$H$_{36}$N$_4$O$_2$·0.33H$_2$O: C, 71.33; H, 8.13; N, 12.32. Found: C, 71.05; H, 8.30; N, 12.07.

exo,exo-2,8-Dimethyl-6,12-bis(N,N-diisopropylamide)-6H,12H-5,11-methanodibenzo[b,f][1,5]diazocine (**3e**). TB *rac*-**1** (1.00 g, 3.99 mmol) was subjected to the general procedure using TMEDA (1.20 mL, 8.05 mmol), *s*-BuLi (1.29 M, 6.20 mL, 8.00 mmol), and N,N-diisopropylcarbamoyl chloride (1.64 g, 10.0 mmol) dissolved in THF (5 mL). A 1 h lithiation time was used before the addition of the electrophile. The reaction was quenched after the mixture had been stirred for 20 h at rt. Purification by column chromatography (5 cm × 10 cm, 4:1 PE/EtOAc) gave *rac*-**3e** as colorless crystals in 44% yield (0.902 g): R_f = 0.20 (4:1 PE/EtOAc); mp 261−262 °C (heptane/diethyl ether); IR (NaCl) 2970, 1638, 1492, 1443, 1334, 1265, 739 cm^{-1}; ^{1}H NMR (400 MHz, CDCl$_3$) δ 6.98 (d, J = 8.3 Hz, 2H, H-4 and H-10), 6.95 (dd, J = 8.3, 1.8 Hz, 2H, H-3 and H-9), 6.61 (s, 2H, H-1 and H-7), 5.03 (septet, J = 6.6 Hz, 2H, -CH(CH$_3$)$_2$), 4.87 (s, 2H, H-6 and H-12), 4.37 (s, 2H, H-13), 3.46 (septet, J = 6.7 Hz, 2H, -CH(CH$_3$)$_2$), 2.20 (s, 6H, Ar-CH$_3$), 1.47−1.37 (m, 24H, -CH(CH$_3$)$_2$); ^{13}C NMR (100 MHz, CDCl$_3$) δ 169.5, 145.3, 132.9, 130.0, 129.0, 127.0, 122.3, 69.2, 59.2 (1C), 49.1, 46.5, 21.4, 21.1, 21.0, 20.7, 20.3; HRMS-EI$^+$ m/z [M]$^+$ calcd for C$_{31}$H$_{44}$N$_4$O$_2$ 504.3464, found 504.3469. Anal. Calcd for C$_{31}$H$_{44}$N$_4$O$_2$·0.5H$_2$O: C, 72.48; H, 8.83; N, 10.91. Found: C, 72.68; H, 9.06; N, 10.56.

endo-6-(N,N-Diethylcarbamoyl)-2,8-dimethyl-6H,12H-5,11-methanodibenzo[b,f][1,5]diazocine (**4**). TB *rac*-**1** (1.00 g, 3.99 mmol) was subjected to the general procedure using TMEDA (1.30 mL, 8.72 mmol), *sec*-BuLi (1.30 M, 6.80 mL, 8.84 mmol), and N,N-diethylcarbamoyl chloride (0.610 mL, 4.81 mmol). A 1 h lithiation time was used before the addition of the electrophile. The reaction was quenched with 10 mL of NaHCO$_3$ [aq, 10% (w/w)] after the mixture had been stirred for 4 h at rt. Purification by column chromatography (5 cm × 18 cm, 3:2 PE/EtOAc) gave *rac*-**4** as colorless crystals in 31% yield (0.439 g): R_f = 0.25 (3:2 PE/EtOAc); mp 155−157 °C (heptane/diethyl ether); IR (neat) 1641, 1489, 1428, 1375 cm^{-1}; ^{1}H NMR (400 MHz, CDCl$_3$) δ 7.02 (d, J = 8.1 Hz, 1H, H-10), 7.00 (dd, J = 8.2, 1.9 Hz, 1H, H-9), 6.81 (dd, J = 8.1, 1.4 Hz, 1H, H-3), 6.76 (brs, 1H, H-7), 6.72 (d, J = 8.2 Hz, 1H, H-4), 6.70 (brs, 1H, H-1), 5.40 (s, 1H, H-6), 4.64 (d, J = 16.8 Hz, 1H, H-12x), 4.41 (dd, J = 12.6, 1.5 Hz, 1H, H-13), 4.41−4.32 (m, 3H, N-CH$_2$-CH$_3$), 4.33 (d, J = 12.6 Hz, 1H, H-13′), 4.19 (d, J = 16.7 Hz, 1H, H-12n), 3.85−3.76 (m, 1H, N-CH$_2$-CH$_3$), 3.46 (dq, J = 14.9, 7.3 Hz, 1H, N-CH$_2$-CH$_3$), 3.26 (dq, J = 13.7, 6.9 Hz, 1H, N-CH$_2$-CH$_3$), 2.23 (s, 3H, Ar-CH$_3$), 2.18 (s, 3H, Ar-CH$_3$), 1.38 (t, J = 7.2 Hz, 3H, -CH$_2$-CH$_3$), 1.29 (t, J = 7.1 Hz, 3H, -CH$_2$-CH$_3$); ^{13}C NMR (100 MHz, CDCl$_3$) δ 167.9, 145.8, 141.4, 134.6, 133.4, 129.5,

128.8, 128.4, 127.2, 127.1, 126.94, 126.91, 125.0, 68.5, 65.9, 58.7, 41.7, 40.7, 21.2, 21.0, 15.2, 12.6; HRMS-ESI⁺ *m/z* [M + Na]⁺ calcd for C₂₂H₂₇N₃ONa 372.2099, found 372.2052. Anal. Calcd for C₂₂H₂₇N₃O·0.14EtOAc: C, 74.88; H, 7.83; N, 11.61. Found: C, 74.97; H, 7.44; N, 11.41.

exo,exo-2,8-Dimethyl-12-benzyl-6-trimethylsilyl-6H,12H-5,11-methanodibenzo[b,f][1,5]diazocine (5). To a solution of TB *rac-*1 (1.00 g, 3.99 mmol) in anhydrous THF (30 mL) was added TMEDA (8.05 mmol, 1.20 mL), and the resulting pale yellow solution was stirred at rt for 30 min under an inert atmosphere before being cooled to −78 °C for 15 min. *s*-BuLi (1.30 M, 4.03 mmol, 3.10 mL) was then added dropwise over 15 min, and the resulting reaction mixture was additionally stirred for 1 h before TMSCl (4.02 mmol, 0.510 mL) was added dropwise over 15 min. The resulting reaction mixture was allowed to stir for 1 h. *s*-BuLi (4.03 mmol, 3.10 mL) was then added dropwise over 15 min, and the resulting reaction mixture was stirred for an additional 1 h before benzyl bromide (4.20 mmol, 0.500 mL) was added over 15 min. The reaction mixture was left in the cooling bath to slowly reach rt, and after the mixture had been stirred for 15 min, the reaction was quenched with saturated aqueous NaHCO₃ (10 mL) followed by CH₂Cl₂ (30 mL) and water (30 mL). The resulting layers were separated, and the aqueous phase was further extracted with CH₂Cl₂ (3 × 50 mL). The combined organic layer was washed with brine, dried over Na₂SO₄, filtered, and evaporated *in vacuo* to dryness. The resulting residue was purified by column chromatography (5 cm × 20 cm, 20:1 PE/EtOAc) to give *rac-*5 as colorless crystals in 24% yield (0.403 g): R_f = 0.28 (60:1 PE/EtOAc); mp 156−158 °C recrystallized from heptane/diethyl ether; ¹H NMR (400 MHz, CDCl₃) δ 7.44−7.37 (m, 4H, Ar-*H*), 7.32−7.27 (m, 1H, Ar-*H*), 6.96−6.91 (m, 2H, H-3 and H-4), 6.78 (s, 1H, H-1), 6.70 (dd, *J* = 8.1, 1.7 Hz, 1H, H-9), 6.54 (s, 1H, H-7), 6.39 (d, *J* = 8.1 Hz, 1H, H-10), 4.35 (dd, *J* = 12.9, 1.5 Hz, 1H, H-13), 4.16 (dd, *J* = 10.2, 4.2 Hz, 1H, H-12), 4.08 (d, *J* = 13.0 Hz, 1H, H-13′), 3.81 (s, 1H, H-6), 3.14 (dd, *J* = 14.1, 4.3 Hz, 1H, -C*H₂*-Ph), 3.08 (dd, *J* = 14.1, 10.2 Hz, 1H, -C*H₂*-Ph), 2.22 (s, 3H, Ar-C*H₃*), 2.13 (s, 3H, Ar-C*H₃*), 0.24 (s, 9H, -Si(C*H₃*)₃); ¹³C NMR (100 MHz, CDCl₃) δ 148.9, 146.0, 140.4, 132.7, 132.6, 131.0, 130.9, 129.7, 128.47, 128.42, 128.3, 126.8, 126.7, 126.4, 124.9, 124.8, 69.6, 63.4, 60.1, 43.4, 21.2, 21.1, −1.1; HRMS-ESI⁺ *m/z* [M + H]⁺ calcd for C₂₇H₃₃N₂Si 413.2413, found 413.2413. Anal. Calcd for C₂₇H₃₂N₂Si·0.25H₂O: C, 77.74; H, 7.88; N, 6.72. Found: C, 77.71; H, 7.82; N, 6.79.

General Procedure for the Inverse-Addition Method. *exo-2,8-Dimethyl-6-trimethylsilyl-6H,12H-5,11-methanodibenzo[b,f]-[1,5]diazocine (2a).* TB *rac-*1 (1.00 g, 3.99 mmol) was dissolved in dry THF at rt, and TMEDA (0.57 mL, 3.8 mmol) was added to the stirred solution. The solution was cooled to −78 °C for 15 min, after which *s*-BuLi (1.40 M, 2.70 mL, 3.78 mmol) was added dropwise over 30 min at −78 °C. The solution was left at −78 °C for 1 h, after which it was added rapidly via a cannula to a flask of vigorously stirred TMSCl (10.0 mL, 79.0 mmol) cooled to −39 °C (1 °C above the freezing point). The reaction mixture was cooled to −78 °C and left to stir to slowly reach rt over 15 h. The reaction was quenched with saturated aqueous NaHCO₃ (15 mL), after which diethyl ether (50 mL) and water (30 mL) were added. The phases were separated. The aqueous phase was extracted with an additional 2 × 30 mL of diethyl ether. The combined organic phase was washed with brine, dried with Na₂SO₄, filtered, and evaporated *in vacuo* to dryness. The resulting residue was purified by column chromatography (3 cm × 10 cm, 9:1 PE/EtOAc) gave *rac-*2a as colorless crystals in 72% yield (0.93 g): R_f = 0.25 (9:1 PE/EtOAc); mp 128−130 °C (heptane/EtOAc). Spectral data were identical to those observed using the direct-addition method.

exo-2,8-Dimethyl-6-(N,N-diethylamide)-6H,12H-5,11-methanodibenzo[b,f][1,5]diazocine (2d). TB *rac-*1 (1.00 g, 3.99 mmol) was dissolved in dry THF at rt, and TMEDA (0.57 mL, 3.8 mmol) was added to the stirred solution. The solution was cooled to −78 °C for 15 min, after which *s*-BuLi (1.40 M, 2.70 mL, 3.78 mmol) was added dropwise over 30 min at −78 °C. The solution was left at −78 °C for 1 h, after which it was added rapidly via a

cannula to a flask of vigorously stirred Et₂NCOCl (109 mmol, 10 mL) in dry THF (10 mL) cooled to −78 °C. The reaction mixture was left to stir to reach rt over 15 h. The reaction mixture was quenched and worked up as in the general procedure for the inverse-addition method. The excess Et₂NCOCl was removed by vacuum distillation (bp 42−48 °C, 5 mbar). Purification by column chromatography (5 cm × 10 cm, 3:2 PE/EtOAc) gave *rac-*2d as colorless crystals in 70% yield (0.97 g): R_f = 0.12 (7:3 PE/EtOAc); mp 224−226 °C (heptane/diethyl ether). Spectral data were identical to those observed using the direct-addition method.

exo-2,8-Dimethyl-6-(N,N-diisopropylamide)-6H,12H-5,11-methanodibenzo[b,f][1,5]diazocine (2e). TB *rac-*1 (1.00 g, 3.99 mmol) was dissolved in dry THF at rt, and TMEDA (0.57 mL, 3.8 mmol) was added to the stirred solution. The solution was cooled to −78 °C for 15 min, after which *s*-BuLi (1.40 M, 2.71 mL, 3.79 mmol) was added dropwise over 30 min at −78 °C. The solution was left at −78 °C for 1 h, after which it was added rapidly via cannula to a flask of vigorously stirred *i*Pr₂NCOCl (5.00 g, 30.6 mmol) in dry THF (10 mL) cooled to −78 °C. The cooling system (dry ice bath) was removed, and the reaction mixture was left to stir to reach rt over 2 h. The reaction mixture was quenched and worked up as in the general procedure for the inverse-addition method. Purification by column chromatography (5 cm × 10 cm, 3:2 PE/EtOAc) gave *rac-*2e as colorless crystals in 73% yield (1.07 g): R_f = 0.35 (7:3 PE/EtOAc); mp 201−203 °C (heptane/EtOAc). Spectral data were identical to those observed using the direct-addition method.

exo,exo-2,8-Dimethyl-6,12-bis(trimethylsilyl)-6H,12H-5,11-methanodibenzo[b,f][1,5]diazocine (3a). TB *rac-*1 (1.00 g, 3.99 mmol) was dissolved in dry THF at rt, and TMEDA (1.8 mL, 12.0 mmol) was added to the stirred solution. The solution was cooled to −78 °C for 15 min, after which *s*-BuLi (1.40 M, 8.60 mL, 12.0 mmol) was added dropwise over 30 min at −78 °C. The solution was left at −78 °C for 1 h, after which it was added rapidly via cannula to a flask of vigorously stirred TMSCl (79 mmol, 10 mL) cooled to −39 °C (1 °C above the freezing point). The reaction mixture was cooled to −78 °C and left to stir to slowly reach rt over 15 h. The reaction was quenched with saturated aqueous NaHCO₃ (15 mL), and diethyl ether (50 mL) and water (30 mL) were added. The phases were separated. The aqueous phase was extracted with an additional 2 × 30 mL of diethyl ether. The combined organic phase was washed with brine, dried with Na₂SO₄, filtered, and evaporated *in vacuo* to dryness. Purification by column chromatography (5 cm × 20 cm, 20:1 PE/EtOAc) gave *rac-*3a as colorless crystals in 89% yield (1.4025 g): R_f = 0.28 (40:1 PE/EtOAc); mp 139−141 °C (heptane/diethyl ether). Spectral data were identical to those observed using the direct-addition method.

exo,exo-2,8-Dimethyl-6,12-bis(benzyl)-6H,12H-5,11-methanodibenzo[b,f][1,5]diazocine (3b). TB *rac-*1 (1.00 g, 3.99 mmol) was dissolved in dry THF at rt, and TMEDA (1.8 mL, 12.0 mmol) was added to the stirred solution. The solution was cooled to −78 °C for 15 min, after which *s*-BuLi (1.40 M, 8.60 mL, 12.0 mmol) was added dropwise over 30 min at −78 °C. The solution was left at −78 °C for 2 h, after which the solution was added rapidly via cannula to a solution of BnBr (10.0 mL, 84.2 mmol) in dry THF (10 mL) cooled to −78 °C. The reaction mixture was left to stir to reach rt over 15 h. The solvent and excess BnBr were removed by vacuum distillation, and the residue was dissolved in 50 mL of dichloromethane and 50 mL of water. The phases were separated. The aqueous phase was extracted with an additional 2 × 50 mL of dichloromethane. The combined organic phase was washed with brine, dried with Na₂SO₄, filtered, and evaporated *in vacuo* to dryness. Purification by column chromatography (5 cm × 10 cm, 4:1 PE/EtOAc) gave *rac-*3b as white crystals in 96% yield (1.65 g): R_f = 0.30 (4:1 PE/EtOAc); mp 220−222 °C (heptane/diethyl ether). Spectral data were identical to those observed using the direct-addition method.

exo,exo-2,8-Dimethyl-6,12-bis(N,N-diethylamide)-6H,12H-5,11-methanodibenzo[b,f][1,5]diazocine (3d). TB *rac-*1 (1.00 g, 3.99 mmol) was dissolved in dry THF at rt, and TMEDA (1.80 mL, 12.0

mmol) was added to the stirred solution. The solution was cooled to −78 °C for 15 min, after which *s*-BuLi (1.40 M, 8.6 mL, 12.0 mmol) was added dropwise over 30 min at −78 °C. The solution was left at −78 °C for 2 h, after which the solution was added rapidly via cannula to a solution of Et$_2$NCOCl (10.0 mL, 109 mmol) in THF (10 mL) cooled to −78 °C. The reaction mixture was left to stir to reach rt over 15 h. The reaction mixture was quenched and worked up as in the general procedure for the inverse-addition method. The excess Et$_2$NCOCl was removed by vacuum distillation (bp 42−48 °C, 5 mbar). The crude could either be recrystallized from heptane and diethyl ether to yield 58% (1.05 g) pure *rac*-**3d** as colorless crystals: mp 224−226 °C. Alternatively, purification by column chromatography (5 cm × 10 cm, 3:2 PE/EtOAc) would yield *rac*-**3d** as colorless crystals in 97% yield (1.73 g): R_f = 0.12 (7:3 PE/EtOAc); mp 224−226 °C (heptane/diethyl ether). Spectral data were identical to those observed using the direct-addition method.

exo,exo-2,8-Dimethyl-6,12-bis(N,N-diisopropylamide)-6H,12H-5,11-methanodibenzo[b,f][1,5]diazocine (**3e**). TB *rac*-**1** (1.00 g, 3.99 mmol) was dissolved in dry THF at rt, and TMEDA (1.80 mL, 12.0 mmol) was added to the stirred solution. The solution was cooled to −78 °C for 15 min, after which *s*-BuLi (1.40 M, 8.6 mL, 12.0 mmol) was added dropwise over 30 min at −78 °C. The solution was left at −78 °C for 2 h, after which the solution was added rapidly via cannula to a solution of *i*Pr$_2$NCOCl (5.00 g, 30.6 mmol) in THF (10 mL) cooled to −78 °C. The reaction mixture was left to stir to reach rt over 15 h. The reaction mixture was quenched and worked up as in the general procedure for the inverse-addition method. Crystallization from heptane and diethyl ether yielded 1.41 g (70.0% yield) of *rac*-**3e** as colorless crystals. The mother liquor was evaporated, and the residue was purified by column chromatography (5 cm × 10 cm, 4:1 PE/EtOAc), giving an additional 0.44 g (0.87 mmol, 22.0% yield) of *rac*-**3e** as colorless crystals: R_f = 0.20 (4:1 PE/EtOAc); mp 261−262 °C recrystallized from heptane/diethyl ether. Spectral data were found to be identical to those observed using the direct-addition method.

■ ASSOCIATED CONTENT

Ⓢ Supporting Information
The Supporting Information is available free of charge on the ACS Publications website at DOI: 10.1021/acs.joc.5b01921.

  X-ray crystallographic file for *rac*-**2b** (CIF)
  X-ray crystallographic file for *rac*-**3c** (CIF)
  Copies of ^{1}H NMR and ^{13}C NMR spectra of all compounds and NOESY spectra for compounds **2d** and **4** (PDF)

■ AUTHOR INFORMATION

Corresponding Authors
*E-mail: harmatam@missouri.edu.
*E-mail: viktor.snieckus@chem.queensu.ca.
*E-mail: kenneth.warnmark@chem.lu.se.
Notes
The authors declare no competing financial interest.

■ REFERENCES

(1) Tröger, J. *Journal für Praktische Chemie* **1887**, *36*, 225−245.
(2) (a) Dolensky, B.; Elguero, J.; Král, V.; Pardo, C.; Valík, M. *Adv. Heterocycl. Chem.* **2007**, *93*, 1−56. (b) Sergeyev, S. *Helv. Chim. Acta* **2009**, *92*, 415−444. (c) Runarsson, Ö. V.; Artacho, J.; Wärnmark, K. *Eur. J. Org. Chem.* **2012**, *2012*, 7015−7041 and references cited therein. (d) Valík, M.; Strongin, R. M.; Král, V. *Supramol. Chem.* **2005**, *17*, 347.

(3) Jensen, J.; Wärnmark, K. *Synthesis* **2001**, *2001*, 1873−1877.
(4) (a) Hansson, A.; Jensen, J.; Wendt, O. F.; Wärnmark, K. *Eur. J. Org. Chem.* **2003**, *2003*, 3179−3188. (b) Jensen, J.; Strozyk, M.; Wärnmark, K. *J. Heterocycl. Chem.* **2003**, *40*, 373−375. (c) Sergeyev, S.; Schär, M.; Seiler, P.; Lukoyanova, O.; Echegoyen, L.; Diederich, F. *Chem. - Eur. J.* **2005**, *11*, 2284−2294. (d) Bew, S. P.; Legentil, L.; Scholier, V.; Sharma, S. V. *Chem. Commun.* **2007**, 389−391.
(5) (a) Michon, C.; Sharma, A.; Bernardinelli, G.; Francotte, E.; Lacour, J. *Chem. Commun.* **2010**, *46*, 2206−2208. (b) Sharma, A.; Guenee, L.; Naubron, J.-V.; Lacour, J. *Angew. Chem., Int. Ed.* **2011**, *50*, 3677−3680.
(6) (a) Harmata, M.; Carter, K. W.; Jones, D. E.; Kahraman, M. *Tetrahedron Lett.* **1996**, *37*, 6267−6270. (b) Harmata, M.; Kahraman, M. *Tetrahedron: Asymmetry* **2000**, *11*, 2875−2879.
(7) Harmata, M.; Rayanil, K.-O.; Barnes, C. L. *Supramol. Chem.* **2006**, *18*, 581−586.
(8) (a) Reich, H. J. *Chem. Rev.* **2013**, *113*, 7130−7178. (b) Ashby, E. C.; Pham, T. N. *J. Org. Chem.* **1987**, *52*, 1291. (c) Sazanov, P. K.; Artamkina, G. A.; Beletskaya, I. P. *Russ. Chem. Rev.* **2012**, *81*, 317−335.
(9) (a) Gómez-SanJuan, A.; Sotomayor, S.; Lete, E. *Beilstein J. Org. Chem.* **2013**, *9*, 313−322. (b) Smith, K.; El-Hiti, G. A.; Alshammari, M. B. *J. Org. Chem.* **2012**, *77*, 11210−11215. (c) Page, A.; Clayden, J. *Beilstein J. Org. Chem.* **2011**, *7*, 1327−1333.
(10) Snieckus, V. *Chem. Rev.* **1990**, *90*, 879−933.
(11) Pardo, C.; Ramos, M.; Fruchier, A.; Elguero, J. *Magn. Reson. Chem.* **1996**, *34*, 708−710.
(12) Burchat, A. F.; Chong, J. M.; Nielsen, N. J. *J. Organomet. Chem.* **1997**, *542*, 281−283.
(13) *Crysalis CCD*; Oxford Diffraction Ltd.: Abingdon, U.K., 2005.
(14) *Crysalis RED*; Oxford Diffraction Ltd.: Abingdon, U.K., 2005.
(15) Sheldrick, G. M. *Acta Crystallogr., Sect. A: Found. Crystallogr.* **2008**, *A64*, 112−122.
(16) Altomare, A.; Cascarano, G.; Giacovazzo, C.; Guagliardi, A.; Burla, M. C.; Polidori, M.; Camalli, M. *J. Appl. Crystallogr.* **1994**, *27*, 435−436.
(17) *CrystalMaker*; Begbroke Science Park: Sandy Lane, Yarnton, Oxfordshire, OX5 1PF, United Kingdom, 2010.

Paper III

The Synthesis of Mono *endo*-6- and Bis *endo,endo*-12 *N,N*-Diethyl Carbamoyl Derivatives of Tröger's Base – The Isomerization Approach

Sami Dawaigher[a]
Emil Lindbäck[a]
Daniel Strand[a]
Michael Harmata*[b]
Victor Snieckus*[c]
Kenneth Wärnmark*[a]

[a] Centre for Analysis and Synthesis, Department of Chemistry, Lund University, P.O Box 124, 221 00 Lund, Sweden.

[b] Department of Chemistry, University of Missouri-Columbia, Columbia, Missouri 65211, United States

[c] Department of Chemistry, Queen's University, Kingston, ON K7L 3N6, Canada.

Kenneth.warnmark@chem.lu.se.

Click here to insert a dedication.
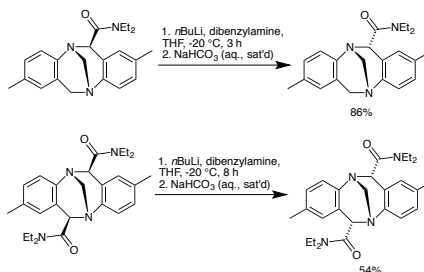
Abstract A method to introduce amide substituents in the *endo*-6, or *endo,endo*-6,12 positions of Tröger's base in only two synthetic steps has been developed. Starting from Tröger's base, the *exo-N,N*-diethylcarbamoyl substituent was introduced in the 6 position and the 6 and 12 positions using a lithiation-isomerisation protocol. The corresponding kinetic mono-*endo* product could be obtained in 86% isolated yield using optimized isomerization conditions (*n*BuLi 1.1 equiv.), dibenzylamine (1.1 equiv.), THF (-20 °C), 2 h and quench with NaHCO₃. The bis-*endo* product could be obtained in 54% isolated yield using similar conditions, but with a longer reaction time. It was shown that an enolate was involved as the key intermediate in the reaction.

Key words Tröger's base,

Tröger's base (**1**), first synthesized in 1887,[1] is a molecule that has received a fair amount of attention in recent years due to its properties: Compound **1** is a V-shaped C_2- symmetric compound that lends itself to several applications. Several investigators have found **1** and its derivatives and analogues to be useful in various applications and studies. Examples include application as a dopant for liquid crystals used in display screens,[2] as a building block for receptors used in molecular recognition,[3] as a ligand in the hydrosilylation of alkanes and as a chiral ligand in the addition of diethylzinc to aromatic aldehydes.[4] Some of its derivatives and analogues have even been found to be cytotoxic,[5] and in the field of chromatography, **1** is used as a standard to evaluate the performance of chiral columns.[6] The Tröger's base scaffold has also been used by Wilcox in the development of a torsion balance used to evaluate aromatic edge-to-face interactions.[7]

Due to the versatility of **1**, many groups[8] including ours[9], have developed an array of procedures to modify Tröger's base and create derivatives and analogues. Having moieties pointing towards the inside the chiral pocket of **1** would be useful since this would allow the installment of new binding sites on the concave face of TB. TB derivatives with such *endo* functionality could prove valuable in the fields of molecular recognition and catalysis. To date, the only method available to synthesize *endo*-6 and *endo*-12 substituted derivatives of **1** is by its oxidation of the benzylic position next to the nitrogen bridgehead, resulting in a TB twisted amide[9b, 10] followed by a Wittig reaction resulting in an olefin that then is selectively catalytically hydrogenated to the *endo* isomer.[9b] The major drawback with this method are that the benzylic oxidation is a low yielding step, 28% for the dioxidized Tröger's base derivative. Furthermore, removal of phosphorus byproducts resulting from the Wittig reaction are difficult to remove. [9b, 10]

We have a long-term interest in the lithiation of Tröger's base.[4b, 9a, 11] Using our methodology to achieve mono- and bisfunctionalization of the 6- and 12-positions of **1** could result in a variety of analogues in which one or both of the benzylic methlenes of TB are functionalized with various groups in the *endo* orientation. The attachment of an amide functionality in one- or in both endo-postion(s) of Tröger's base (**1**) is especially attractive because of its ability to coordinate metal ions,[12] thus opening for the possibility to attach a catalytically active metal in the chiral cavity of Tröger's base as well as a possible further transformation. Hence, when *rac*-Tröger's base (**1**) was treated with s-BuLi (1.1 or 2.2 equiv.) and TMEDA (1.1 or 2.2 equiv.) followed by an electrophilic quench (1.2 or 2.4 equiv),[9a] a deviation from the expected product distribution was encountered when using diethylcarbamoyl chloride or diisopropylcarbamoyl chloride as electrophiles (see Scheme 1) compared to results seen with other electrophiles such as TMSCl and BnBr. It appeared that the excess organolithium was acting as a base on the product amide, forming an enolate that upon quenching gave rise to the product distribution, ca.

50% starting material (**1**), 20% mono *exo*-6 product (**2**) 10% *exo,exo*-6,12-disubstituted product (**4**), and 15% of a compound that proved to be mono-*endo* substituted product (**3**), resulting in yields of roughly 70% for the monosubstituted product and 15% for the disubstituted product (using 1.2 equiv of the electrophile). As mentioned above, the other known synthetic path to *endo*-substituted Tröger's base analogs was a some tedious and low-yielding process,[9b] we decided to further investigate this amide synthesis to see if the product distribution could be optimized to generate *endo*-substituted Tröger's base derivatives by controlled isomerization via the corresponding enolate.
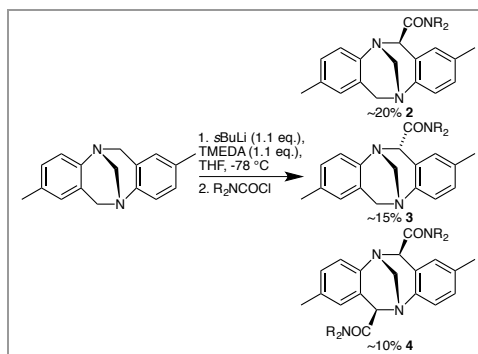
Scheme 1 Observed product distribution of the reaction of **1** with *s*BuLi (1.1 equiv.) and TMEDA and quenching with R$_2$NCOCl, note that roughly 50% of **1** was retained. Yields shown for R=Et.

We began this study with the aim to better understand the mechanism(s) of product formation in our earlier study,[9a] in order to optimize the reactions conditions such that both yield and *endo/exo* stereocontrol could be achieved. To this end, it was essential to determine which of the two isomers **2** (*exo*) or **3** (*endo*) constituted the thermodynamic product of the reaction. This investigation was first conducted experimentally. Thus, each of the stereoisomers Tröger's base amide, **2** and **3**, (see Table 1 entries a and b) was separately treated with a catalytic amount of sodium methoxide (0.15 equiv) in methanol for a period of 2 weeks. We observed that under these conditions the *endo* isomer **3** isomerized completely to **2** (Table 1, entry b). Conversely, the *exo* isomer **2** did not undergo isomerization into the *endo* isomer **3** (Table 1, entry a). The proton NMR spectrum was used to determine the *endo/exo* isomer ratio by comparing the relative integrals of the peaks at δ = 5.40 and δ = 4.91 ppm, which correspond to the α-protons of the *endo* (**3**) and *exo* (**2**) amide, respectively. Repeating the isomerization experiments of **2** and **3** in methanol-d_4, we observed the exchange of the α-proton in the both cases for deuterium (Table 1, entries c and d). This observation suggested that the isomerization of **3** into **2** takes place via a carbanion intermediate, most likely an enolate.

In addition, as enantiomerically pure **1** is known to racemize under weakly acidic conditions,[13] treating each of **2** or **3** with

an acid should also result in isomer equilibration (Table 1, entries e and f). This was indeed the case; treating each of **2** and **3** separately with a catalytic amount of aqueous HCl resulted in the isolation of **2** both cases. Performing the experiment in methanol-d_4 and using a catalytic amount of DCl (Table 1, entries g and h), showed no exchange of any protons in **2**. This is consistent with an isomerization mechanism involving opening of the methylene bridge in **1** *and not* an enolization mechanism.[11]

Table 1 Determination of the thermodynamic product between *endo*- and *exo*-6-*N,N*-diethyl amide substituted Tröger's base.

2: R$_1$ = CONEt$_2$, R$_2$ = H
3: R$_1$ = H, R$_2$ = H

Entry	Starting Amide	Conditions	Resulting amide and yield[a]
a	**2**	MeONa(0.05 eq.), MeOH, rt, 2 weeks	**2** (100%)
b	**3**	MeONa(0.05 eq.), MeOH, rt, 2 weeks	**2** (100%)
c	**2**	CD$_3$ONa (0.05 eq.), CD$_3$OD, rt, 2 weeks	**2** R$_2$ =D (100%)
d	**3**	CD$_3$ONa (0.05 eq.), CD$_3$OD, rt, 2 weeks	**2** R$_2$ =D (100%)
e	**2**	HCl (0.05 eq.), MeOH, rt, 24 *h*	**2** (100%)
f	**3**	HCl (0.05 eq.), MeOH, rt, 24 *h*	**2** (100%)
g	**2**	DCl (0.05 eq.), CD$_3$OD, rt, 24	**2** (100%)
h	**3**	DCl (0.05 eq.), CD$_3$OD, rt, 24	**2** (100%)

[a]Yield determined through H-NMR of Crude.

A computational investigation regarding the stability of **2** vs **3** was conducted. Thus, DFT calulations using at the B3LYP/6-31G level of theory showed **2** to be 2.8 kcal/mol lower in energy than **3**.... (see supporting information. As both the experimental and computational investigations show *exo* isomer **2** to be a *thermodynamically* more stable product than **3**, we decided to investigate whether **2** could be converted to **3** by treating **2** with a base of sufficient strength under *kinetic control*. An initial investigation showed that treating **2** with 1.1 equiv of LDA at -78 °C and then allowing the reaction mixture to slowly reach room temperature overnight resulted in the formation of both **3** and **2** (**3**(*endo*):**2**(*exo*); 84:16) after quenching. LDA was preffed to *n*BuLi as base since the later converted **2** back to Tröger's base (**1**) in quantitative yield. We presume this occurred by a mechanism similar to that of the Haller-Bauer reaction.[14] Indeed, some side products that could be observed in the mass of the crude reaction mixture were the butyl tröger's base ketone (**4**), ethyl tröger's base ketone (**5**), diethyl amine, and possible hemiaminal (**6**) as seen in Scheme 2.
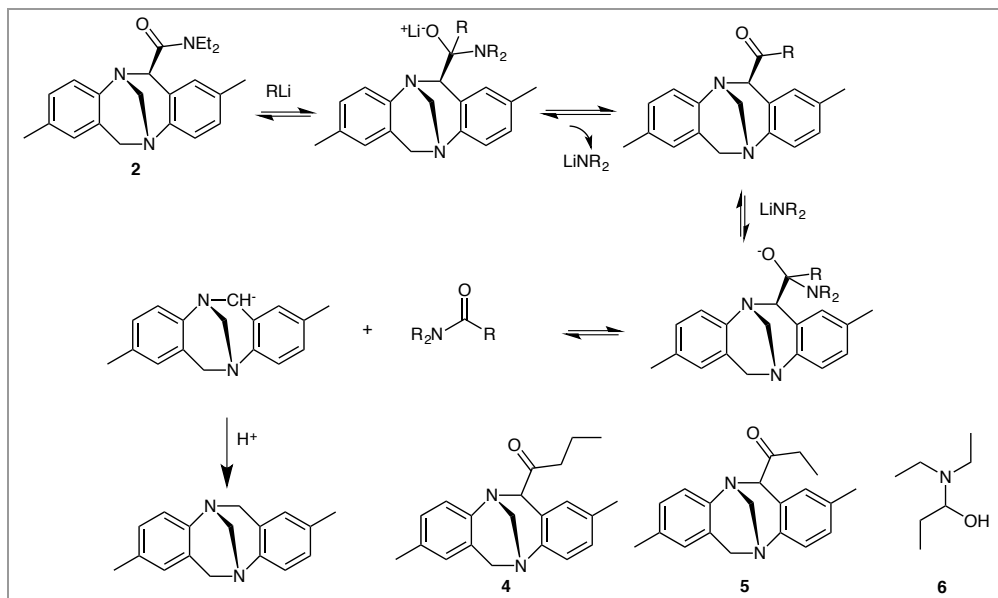
Scheme 2 A Possible mechanism for the amide splitting when treating with *n*BuLi. Molecules **4**, **5**, and **6** are observed in the reaction mixture.

The above initial observations led us to conclude that there were four variables to be investigated in order to optimize the reaction conditions to maximize the yield of the reaction: the reaction temperature, the reaction time, the amount and type of base, and the type of quencher used.

The first parameter to be optimized was the reaction temperature. Hence, compound **2** (50.5 mg, 0.145 mmol) was dissolved in THF (2 mL). DIPA (0.022 ml, 0.160 mmol) was then added and the mixture was cooled to the desired temperature. This was followed by the slow dropwise addition of *n*BuLi (0.064 ml, 2.5 M, 0.160 mmol). Following that, the reaction mixture was kept at the desired temperature for 2 h. The residue was dissolved in chloroform-*d* and a ¹H NMR spectrum was recorded to determine the ratio *endo:exo* of the product mixture. The results are summarized in Table 2. As seen in Table 2, the ideal temperature to perform the reaction appeared to be at -20 °C (entry 5). At -10 °C, on the other hand, a majority of **1** was obtained demonstrating that any higher temperature would not result in a high yield of **3** (entry 6). We presume that at low temperature, deprotonation of DIPA by *n*BuLi is rapid relative to nucleophilic attack on the amide. A change in relative rates at -10 °C is clear from the data.

Table 2 Optimization of the reaction temperature .
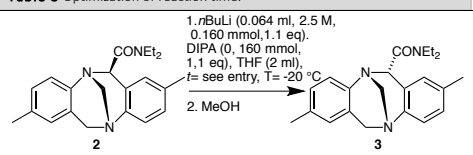
Entry	Temperature °C	Product distribution[a] *endo* (**3**):*exo* (**2**)
1	-78	0:100
2	-50	27:73
3	-40	8:92
4	-30	2:98
5	-20	49:51
6	-10	46:54

[a]Derived from ¹H spectrum after work up of reaction mixture. [b]The ratio is that of the remainder **3:2** observed by ¹H NMR even though more than 90% of the **2** was converted to **1**.

After finding the optimum reaction temperature, attention was turned to identifying the optimum reaction time. This was done by using the same method used for finding the optimum temperature, however this time the temperature was kept at a constant -20 °C and the reaction time was varied from 1 minute up to 6 hours (see Table 3). The optimum reaction time in order to obtain the *endo* product appeared to be 3 h (entry 3), after which the product distribution remained constant (entries 5-7). We conclude from this data that LDA formation is rapid but deprotonate of 2 is relatively slow, requiring upwards of 3 h to go to completion. This was confirmed in an experiment (entry 8) using d₄ methanol for quenching that resulted in that the traces

of **3** had their α-proton displaced by deuterium while α-proton on the remaining **2** was untouched.

Table 3 Optimization of reaction time.

1.*n*BuLi (0.064 ml, 2.5 M, 0.160 mmol,1.1 eq). DIPA (0, 160 mmol, 1.1 eq), THF (2 ml), *t*= see entry, T= -20 °C

2. MeOH

Entry	reaction time	Product distribution[a] endo(**3**):exo(**2**)
1	1 min	2:98
2	1 h	35:65
3	2 h	49:51
4	3 h	82:18
5	4 h	82:18
6	6 h	82:18
7	18 h	84:16
8	1 min	2:98[b]

[a]Derived from ^{1}H NMR spectrum after work up of reaction mixture. [b]Quenching with d$_4$ methanol resulted in all **3** being deuterated.

We next investigated whether the quencher used had any significant effect on the *exo* versus *endo* distribution. Different quenching reagents were tried, namely methanol, water, NaHCO$_3$ (aq, sat.) and isopropanol in THF. There were no significant differences between the different quenchers (see supporting information).

The next parameter to be altered was the base used and the amine used in conjunction with *n*BuLi, when the latter was employed as base. We used a small selection of different amines as seen in Table 4. The general reaction conditions were as described above. As before, with *n*BuLi alone or with a tertiary amine, **2** was converted to **1**. (entries 2, 3 and 7). Using LiHMDS (entry 6), the observed product distribution was inferior to that of *n*BuLi/secondary amine. Among the secondary amines investigated, the product distribution was comparable, with the best results observed for dibenzylamine (DBA, Entry 5), also adding *n*BuLi to a mixture of **2** and DIPA in THF resulted in exactly the same results as adding LDA to a solution of **2** in THF (Table 4, entries 1 and 8).

Table 4 Optimization of type of amine used in conjunction with *n*BuLi as base .

1.see entry for base , THF (2 ml), *t*= 4 h, T= -20 °C

2. NaHCO$_3$ (Aq, sat'd)
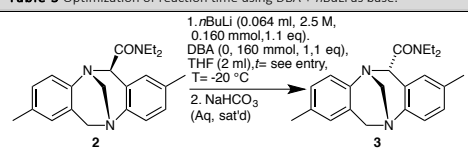
Entry	Base used	Product distribution[a] endo(**3**):exo(**2**)
1	*n*BuLi (0.064 ml, 2.5 M, 0.160 mmol, 1.1 eq.) DIPA (0.160 mmol, 1.1 eq.)	82:18
2	*n*BuLi (0.064 ml, 2.5 M, 0.160 mmol, 1.1 eq.) TMEDA (0.160 mmol, 1.1 eq.)	0:0[b]
3	*n*BuLi (0.064 ml, 2.5 M, 0.160 mmol, 1.1 eq.) DIPEA (0.160 mmol, 1.1 eq.)	0:0[b]
4	*n*BuLi (0.064 ml, 2.5 M, 0.160 mmol, 1.1 eq.) DEA (0.160 mmol, 1.1 eq.)	80:20
5	*n*BuLi (0.064 ml, 2.5 M, 0.160 mmol, 1.1 eq.) DBA (0.160 mmol, 1.1 eq.)	86:14
6	LiHMDS (0.16 mL, 1.0 M, 0.160 mmol, 1.1 eq.)	32:68
7	*n*BuLi (0.064 ml, 2.5 M, 0.160 mmol, 1.1 eq.)	0:0[b]
8	LDA (0.080 ml, 2.0 M, 0.160 mmol, 1.1 eq.)	82:18

[a] Derived from ^{1}H-NMR spectrum after work up of reaction mixture. [b]Compound **1** is the only material isolated.

Since *n*BuLi/DBA showed the best results we decided to further optimize the reaction time using this reagent mixture. The results are presented in Table 5. Rewardingly, the optimum reaction time for *n*BuLi/DBA combination was shorter than the reaction time for *n*BuLi/DIPA, (2 hours being ideal), as no not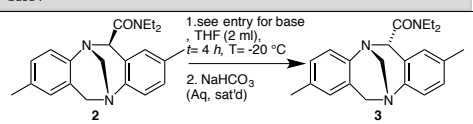able change in product distribution could be seen after this (Table 5, Entry 3). That the combination of lithium base and amine generates an amide that is the active base is supported by the fact that essentially the same results are obtained using *n*BuLi + DEA and LDA, respectively (Table 4, Entries 4 and 8).

Table 5 Optimization of reaction time using DBA + *n*BuLi as base.

1.*n*BuLi (0.064 ml, 2.5 M, 0.160 mmol,1.1 eq). DBA (0, 160 mmol, 1,1 eq), THF (2 ml),*t*= see entry, T= -20 °C

2. NaHCO$_3$ (Aq, sat'd)

Entry	Reaction time	Product distribution endo(**3**):exo(**2**)
1	1 min	15:85
2	1 h	81:19
3	2 h	86:14
4	3 h	83:17
5	4 h	83:17
6	18 h	84:16

[a]Derived from ^{1}H NMR spectrum after work up of reaction mixture.

Finally, the number of equivalents of base used was investigated. Increasing the amount of base from 1.1 to 2 or 3 equivalents (of *n*BuLi/DBA) did not change the product distribution, keeping the general reaction conditions as above. This implies complete deprotonation of 2 and a kinetic quench that does not prefer the convex face of the enolate intermediate exclusively, only predominantly.

In a scale up of the reaction with optimal conditions using 500 mg of **2**, we were able to synthesize **3** in a very good isolated yield of 86% (Scheme 3). The stereochemistry the *N,N*-diethylcarbamoyl group in position 6 of **3** was unambiguously assigned by X-ray diffraction (Figure 1)
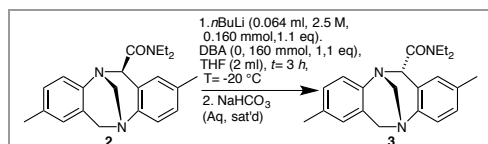
Scheme 3 The synthesis of mono-*endo* Tröger's base derivative **3** from mono-*exo* Tröger's base derivate **2** using optimized conditions.
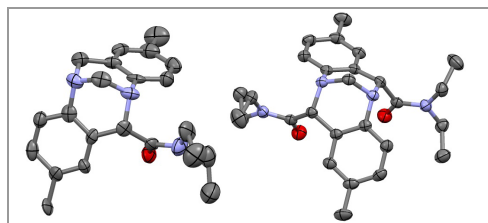
Figure 1 x-ray representation of **3** and **5**. Unambiguously comfirming the stereochemistry of the compounds determined from the ^{1}H-NMR spectra.

Having optimized the conditions for the isomerization of the monosubstituted Tröger's base derivative **2**,we decided to see if the same reaction conditions would have a similar effect on the *exo,exo*-diamide Tröger's base derivative **7** (see Scheme 4). The initial reaction conditions proved quite effective and only required longer reaction time to yield the *endo, endo* bisamide **5** in an isolated yield of 54%. The stereochemistry of the 6 and 12 position of **8** was unambiguously assigned by X-ray diffraction analysis to be *endo* (Figure 1). A second compound was also observed, **9** (<15% yield). Given the difficulty of separating **7** and **9** on a chromatographic column, pure **6** was not isolated. An additional amount of remaining **7** (~25%) was also obtained from the reaction mixture.
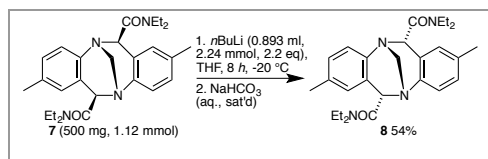
Scheme 4 The synthesis of bis-*endo* Tröger's base derivative **5** from bis-*exo* Tröger's base derivate **4** using optimized conditions for the corresponding mono-*exo* to mono-*endo* reaction.

One can speculate why quenching at -20 °C results in predominantly the *endo* isomer. It is highly likely that since the isomerization only occurs in the presence of a secondary amine, that the amine and the *n*BuLi form a lithium amide that is the active base for the deprotonation of the α-proton. The resulting lithium amide must approach the carbonyl from the endo direction, resulting in the formation of the enolate shown in Scheme 5. This would be a result of the *exo*-face being too sterically hindered for the amide base to approach from that

direction. Any quencher would hence approach from the *exo*-face and would result in an *endo* configuration.
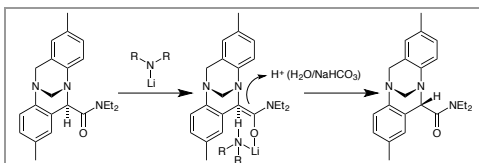
Scheme 5 The lithium amide base approaches the α-carbon of the carbonyl from the *endo* position, in the process of deprotonation an enolate is formed that forms a tight ion pair together with the protonated lithium amide that limits the approach of the quencher from the *endo* direction.

We have investigated the isomerization of the *exo*-substituted Tröger's base derivatives **2** (mono *exo*-subsitituted amide) and **7** (bis *exo, exo*-substituted amide) to their *endo*-substituted isomers as depicted in Schemes 3 and 4. The reactions conditions have been systematically optimized so that the maximum yield of the desired isomer is obtained. This new route of *exo*- to *endo*-substituted Tröger's base derivatives improves the overall yield over the previously reported method. This method exhibits an overall yield of 60 % for **3** and 53% for **8** over 2 steps. Moreover, in this case, with the so- installed *endo* substituents being amides, a functionality able to coordinate metal ions,[15] metal ions could now be placed directly in the cavity of Tröger's base. There have been reports in the chemical literature that mention the use of tertiary amides as ligands in catalysis[16] and since the Tröger's base amide derivatives are chiral; they may prove useful as ligands. Finally, our study paves the way for the use of other functional groups as side chains that are able to induce enolization (carbanion formation), to yield *endo* substituents at the Trögers base skeleton.

The experimental section has no title; please leave this line here.

General Methods

2 and **7** were synthesized according to the protocol reported in our previous publication.[9a] All chemicals were used as received from commercial sources without further purification. DIPA, DBA, TMEDA, DIPEA, DEA were dried with KOH overnight and distilled under house vacuum prior to use. THF was dried with sodium and distilled under nitrogen. PE refers to petroleum ether (bp 40-60 °C). Precoated Merck silica gel 60 F_{254} plates were used for TLC analysis. Column chromatography was performed on silica gel (Davisil 35-70 μm). ^{1}H and ^{13}C NMR spectra were recorded on a 400 NMR spectrometer. Chemical shifts (δ) are reported relative to shift-scale calibrated with residual NMR solvent peak CDCl$_3$ (7.26 ppm for ^{1}H NMR and 77.23 for ^{13}C NMR). Melting points were recorded on a Fischer-Jones apparatus, using plate technology. IR spectra were recorded on a FTIR spectrophotometer. HRMS were obtained on a Q-TOF micro instrument.

Isomerization study of 2 and 3

MeOH/MeONa: Compound **2** or **3** (50 mg, 0.143 mmol) was dissolved in methanol (2 ml). Sodium (0.5 mg, 0.0217 mmol) was added. The mixture was allowed to stir for 24 h. The mixture was made neutral by slow addition of HCl in methanol-d_4 (1.0 M). The solvent was removed on a rotavap. The residue was dissolved in deuterated chloroform and a ^{1}H NMR spectrum was recorded on the resulting solution to determine the product ratio (see above).

CD$_3$OD/CD$_3$ONa: Compound **2** or **3** (50 mg, 0.143 mmol) was dissolved in methanol-d_4 (2 ml). Sodium (0.5 mg, 0.0217 mmol) was added and the resultant mixture was kept stirring for 24 h. The mixture was made neutral by slow addition of DCl in methanol-d_4 (1.0 M). The solvent was

removed on a rotavap. The residue was dissolved in deuterated chloroform and a ^{1}H-NMR spectrum was recorded of the resulting solution.

HCl/MeOH: Compound **2** or **3** (50 mg, 0.143 mmol) was dissolved in MeOH (5 ml). Aqueous HCl (1 mL, 1 M) was added and the mixture was kept stirring overnight at r.t. The mixture was made basic (pH 10) by adding aqueous NaOH (1.0 M). Dichloromethane (5 ml) was added and the phases were separated, the aqueous phase was extracted with additional dichloromethane (2×5 ml). The organic phases were collected and dried with Na$_2$SO$_4$, filtered and the solvent was removed *in vacuo*. The residue was dissolved in deuterated chloroform and a ^{1}H-NMR spectrum was recorded on the resulting solution.

DCl/CD$_3$OD: Compound **2** or **3** (50 mg, 0.143 mmol) was dissolved in 1 ml DCl in deuterated(d4) methanol-d_4 (1.0 M). The mixture was allowed to stir for 24h. The mixture was made neutral by slow addition of NaMeO in deuterated methanol (1.0 M). The solvent was removed on a rotavap. The residue was dissolved in deuterated methanol and a ^{1}H NMR spectrum was recorded of the resulting solution.

Optimized isomerization protocols

Compound **2** (0.050 g, 0.14 mmol), was dissolved in 2 ml freshly distilled THF under N$_2$ in a twin necked round bottomed flask equipped with a low temperature thermometer and sealed with a rubber septum. Amine (1.1 equiv) was added and the solution was cooled to the desired temperature. *n*BuLi (1.1 equiv) was added drop wise over 10 min. The reaction mixture was left the amount of time required and then quenched with the desired quenching medium. 5 ml water and 5 ml dichloromethane were then added and the phases were separated. The aqueous phase was washed with additional dichloromethane (2×5 ml). The combined organic phases were washed with brine (5 ml) and dried with Sodium Sulfate. The solvent was removed *in vacuo* to dryness. The residue was dissolved in deuterated chloroform and a ^{1}H NMR spectrum was recorded of the resulting solution.

Compound **7** (0.050 g, 0.11 mmol), was dissolved in 2 ml freshly distilled THF under N$_2$. Amine (2.2 equiv) was added and the solution was cooled to the desired temperature. *n*BuLi (2.2 equiv) was added drop wise over 30 min. The reaction mixture was left the amount of time required and then quenched with the desired quenching medium. 5 ml water and 5 ml dichloromethane were then added and the phases separated. The aqueous phase was washed with additional dichloromethane (2×5 ml). The combined organic phases were washed with brine (5 ml) and dried with Sodium Sulfate. The solvent was removed *in vacuo* to dryness. The residue was dissolved in deuterated chloroform and a ^{1}H NMR spectrum was recorded of the resulting solution.

Optimized preparative protocols

Endo-2,8-dimethyl-6-(*N,N*-diethylcarbamoyl)-6*H*,12*H*-5,11-methanodibenzo[*b,f*]diazocine (3): *rac*-**2** (0.502 g, 1.44 mmol) was dissolved in 15 ml dry THF under nitrogen. Dibenzylamine (0.31 ml, 1.6 mmol) was added under stirring and the mixture was cooled to -20 °C. *n*BuLi (2.5 M, 0.64 ml, 1.6 mmol) was added dropwise under vigorous stirring over 10 mins. The solution was left stirring at -20°C for 2 hrs. The reaction was quenched with 10 mL NaHCO$_3$ (aq, sat.). Additional H$_2$O (20 mL) and CH$_2$Cl$_2$ (20 mL) were added and the phases were separated. The aqueous phase was extracted with an additional 3×25 ml CH$_2$Cl$_2$. The combined organic phases were washed with brine, dried with Na$_2$SO$_4$, filtrated and evaporated *in vacuo* to dryness. Purification by column chromatography (4×10 cm, PE:EtOAc 7:3) gave *rac*-**3** (0.432 g, 1.24 mmol, 86.1 % yield) as colorless crystals, R$_f$ = 0.20 (7:3, PE:EtOAc) mp: 155-157 °C (Heptane/Diethyl Ether).

IR (neat): 1641, 1489, 1428, 1375 cm^{-1}.

^{1}H NMR (CDCl$_3$, 400 MHz): δ = 7.02 (d, *J* = 8.1 Hz, 1H, H-10), 7.00 (dd, *J* = 8.2, 1.9 Hz, 1H, H-9), 6.81 (dd, *J* = 8.1, 1.4 Hz, 1H, H-3), 6.76 (brs, 1H, H-7), 6.72 (d, *J* = 8.2 Hz, 1H, H-4), 6.70 (brs, 1H, H-1), 5.40 (s, 1H, H-6), 4.64 (d, *J* = 16.8 Hz, 1H, H-12x), 4.41 (dd, *J* = 12.6, 1.5 Hz, 1H, H-13a), 4.41-4.32 (m, 1H, N-C*H$_2$*-CH$_3$), 4.33 (d, *J* = 12.6 Hz, 1H, H-13b), 4.19 (d, *J* = 16.7 Hz,

1H, H-12e), 3.85-3.76 (m, 1H, N-C*H$_2$*-CH$_3$), 3.46 (dq, *J* = 14.9, 7.3 Hz, 1H, N-C*H$_2$*-CH$_3$), 3.26 (dq, *J* = 13.7, 6.9 Hz, 1H, N-C*H$_2$*-CH$_3$), 2.23 (s, 3H, Ar-C*H$_3$*), 2.18 (s, 3H, Ar-C*H$_3$*), 1.38 (t, *J* = 7.2 Hz, 3H, -CH$_2$-C*H$_3$*), 1.29 (t, *J* = 7.1 Hz, 3H, -CH$_2$-C*H$_3$*).

^{13}C NMR (CDCl$_3$, 100 MHz): δ = 167.9, 145.8, 141.4, 134.6, 133.4, 129.5, 128.8, 128.4, 127.2, 127.1, 126.94, 126.91, 125.0, 68.5, 65.9, 58.7, 41.7, 40.7, 21.2, 21.0, 15.2, 12.6.

HRMS (ESI$^+$): *m/z* [M+Na]$^+$ calcd for for C$_{22}$H$_{27}$N$_3$ONa: 372.2099; found: 372.2052.

Anal. Calcd for Calcd for C$_{22}$H$_{27}$N$_3$O · 0.14EtOAc: C, 74.88; H, 7.83; N, 11.61. Found: C, 74.97; H, 7.44; N, 11.41.

Endo,endo-2,8-dimethyl-6,12-di(*N,N*-diethylcarbamoyl)-6*H*,12*H*-5,11-methanodibenzo[*b,f*]diazocine (8): *rac*-**7** (0.625 g, 1.39 mmol), was dissolved in THF (20 ml), dibenzylamine (0.60 ml, 3.1 mmol) was added. The mixture was cooled down to -78°C. *n*BuLi (2.5 M, 1.25 ml, 3.1 mmol) was added drop wise over 15 min. The mixture was left to slowly reach rt over 18 h. The reaction was quenched with 10 mL NaHCO$_3$ (aq, sat.). Additional H$_2$O (20 mL) and CH$_2$Cl$_2$ (20 mL) were added and the phases were separated. The aqueous phase was extracted with an additional 3×25 ml CH$_2$Cl$_2$. The combined organic phases were washed with brine, dried with Na$_2$SO$_4$, filtrated and evaporated *in vacuo* to dryness. Purification by column chromatography (5×10 1:1 PE:EtOAc) gave pure *rac*-**5** (0.384 g, 0.856 mmol, 54% yield) as colorless crystals. R$_f$=0,1 (1:1 PE:EtOAc); mp: 230.1-231.0 °C

IR (neat): 2974, 2930, 2871, 1633, 1487, 1430, 1215, 1136, 1059, 961, 816, 631, 557 cm^{-1}cm^{-1}.

^{1}H NMR (CDCl$_3$, 400 MHz): δ = 6.88-6.86 (d, *J* = 7.8 Hz ,2H, H-3), 6..76-6.73 (m, 4H, H-1, H-4), 5.40 (s, 2H, H-6), 4.47 (s, 2H, H-13), 4.38-4.33 (m, 2H, N-C*H$_2$*-CH$_3$), 3.84-3.76 (m, 2H, N-C*H$_2$*-CH$_3$), 3.49-3.40 (m, 2H, N-C*H$_2$*-CH$_3$), 3.29-3.21 (m, 2H, N-C*H$_2$*-CH$_3$), 2.21 (s, 6H, Ar-C*H$_3$*), 1.39-1.35 (t, *J* = 7.1 Hz, 6H, N-CH$_2$-C*H$_3$*), 1.30-1.26 (t, *J* = 7.1 Hz, 6H, N-CH$_2$-C*H$_3$*).

^{13}C NMR (CDCl$_3$, 100 MHz): δ = 167.5, 141.5, 134.2, 129.1, 128.2, 127.4, 126.6, 70.4, 66.3, 41.5, 40.5, 21.1, 15.1, 12.5.

HRMS (ESI$^+$): *m/z* [M+H]$^+$ calcd for C$_{27}$H$_{37}$N$_4$O$_2$: 449.2917; found: 449.2914.

Anal. Calcd for C$_{27}$H$_{36}$N$_4$O$_2$: C, 72.29; H, 8.09; N, 12.49. Found: C, 72.67; H, 8.39; N, 12.38.

Funding Information

Acknowledgment

Supporting Information

YES

Primary Data

NO

References

(1) Tröger, J. *Journal für Praktische Chemie* **1887**, *36*, 225-245.
(2) ChunXue, Y.; Qian, X.; HuiJun, L.; Lei, W.; MinHua, J.; XuTang, T. *Sci. China. Chem.* **2011**, *54*, 587-595.
(3) Cowart, M. D.; Sucholeiki, I.; Bukownik, R. R.; Wolcox, C. S. *J. Am. Chem. Soc.* **1988**, *110*, 6204-6210.
(4) (a) Goldberg, Y.; Alper, H. *Tetrahedron Lett.* **1995**, *36*, 369-72; (b) Harmata, M.; Kahraman, M. *Tetrahedron: Asymmetry* **2000**, *11*, 2875-2879.

(5) Paul, A.; Maji, B.; Misra, S. K.; Jain, A. K.; Muniyappa, K.; Bhattacharya, S. *J. Med. Chem.* **2012**, *55*, 7460-7471.

(6) Huang, J.; Zhang, P.; Chen, H.; Li T. *Anal. Chem.* **2005**, 77, 3301-3305.

(7) (a) Paliwal, S. ; Geib, S.; Wilcox, C. S. *J. Am. Chem. Soc.* **1994**, *116*, 4497-4498; (b) Kim, E. –I.; Paliwal, S.; Wilcox, C. S. *J. Am. Chem. Soc.* **1998**, *120*, 11192-11193.

(8) Dolensky, B.; Havlik, M.; Kral, V. *Chem. Soc. Rev.* **2012,** *41*, 3839-3858.

(9) (a) Dawaigher, S.; Månsson, K.; Ascic, E.; Artacho, J.; Mårtensson, R.; Loganathan, N.; Wendt, O. F.; Harmata, M.; Snieckus, V.; Wärnmark, K. *J. Org. Chem.* **2015**, *80*, 12006-12014; (b) Artacho, J.; Ascic, E.; Rantanen, T.; Wallentin, C. –J.; Dawaigher, S.; Bergquist, K. –E.; Harmata, M.; Snieckus, V.; Wärnmark, K. *Org. Lett.* **2012**, *14*, 4706-4709; (c) Artacho, J.; Wärnmark, K. *Synthesis* **2009**, 3120-3126; (d) Jensen, J.; Wärnmark, K. *Synthesis* **2001**, 1873–1877; (e) Hansson, A.; Jensen, J.; Wendt, O. F.; Wärnmark, K. *Eur. J. Org. Chem.* **2003**, 3179–3188; (f) Jensen, J.; Strozyk, M.; Wärnmark, K. *J. Heterocycl. Chem.* **2003**, *40*, 373–375.

(10) Artacho, J.; Ascic, E.; Rantanen, T.; Karlsson, J.; Wallentin, C. –J; Wang, R.; Wendt, O. F.; Harmata, M.; Snieckus, V.; Wärnmark, K. **2012,** *18,* 1038-1042.

(11) (a) Haramata, M.; Carter, K. W.; Jones, D. E.; Kahraman, M. *Tetrahedron Lett.* **1996**, *37.* 6267-6270; (b) Harmata, M.; Rayanil, K. –O.; Barnes, C. L. *Supramol. Chem.* **2006**, *50,* 581-586.

(12) Schneider, H. –J.; Rüdiger, V.; Cuber, U. *J. Org. Chem.* **1995**, *60*, 996-999.

(13) Greenberg, A.; Molinero, N.; Lang, M. *J. Org. Chem.* **1984**, *49*, 1127-1130.

(14) Haller, A.; Bauer, E. *Compt. Rend.* **1908**, *147,* 824-829.

(15) Sigel, H.; Martin, R. B. *Chem. Rev.* **1982,** *82*, 385-426.

(16) (a) Mason, C. M.; Schwarz, J. *Tetrahedron Lett.* **2000,** *41*, 8999-9003; (b) Ashok, M.; Ravinder, V.; Prasad, A. V. S. S. *Transition Met. Chem.* **2007**, *32,* 23-30; (c) Fache, F.; Schulz, E.; Tommasino M. L.; Lemaire, M. *Chem. Rev.* **2000**, *100*, 2159-2231.

Paper IV

FULL PAPER

Discrimination of Bisammonium Salts by a Bis(Crown-Ether) Tröger's Base as a Model for Peptide-Protein Interactions and Validation of Computational Methods

Sami Dawaigher,[a] Carlos Solano Arribas,[a] Anna Ryberg,[a] Jacob Jensen,[a], Karl Erik Bergquist,[a] Anders Sundin,[a] Per-Ola Norrby,* [b] Kenneth Wärnmark*[a]

Abstract: A system, comprised of heptane-1,7-diyl bisammonium ligands having in the 4-position an aliphatic group (hydrogen (**4**), methyl (**5**), or cyclohexyl (**8**)), or an aromatic group (phenyl (**6**) and benzyl (**7**)), and a bis(18-crown-6) receptor with an aromatic cavity (**3**) based on Tröger's base, has been developed for three different purposes: (1) as a model for the peptide-protein complexes found in living cells, (2) to study the interactions between alkyl or aromatic side chains of ligands and aromatic cavities of receptors, and (3) evaluation of the accuracy of different computational methods with respect to binding preferences of the ligand to the aromatic receptor (qualitative evaluation) as well as to the binding energies between the ligands and receptor (quantitative evaluation). The interaction between the ligands and the receptor was studied experimentally in $CDCl_3$:MeOH-d_4 (1:1) by NOESY and ROESY NMR spectroscopy, NMR titration methodologies, and theoretically by molecular mechanics (MM) and density functional theory (DFT), using different solvent models. The experimental data showed that the conformation of the aliphatic framework of the ligands had an all-*anti* conformation when accommodated between the two crown ether moieties of **3**. The substituents of the ligand were situated in the cavity (**5**), partly inside (**6** and **8**), and outside (**7**). MM using the chloroform solvent model, reproduced the experimentally found conformation of the aliphatic framework of the ligands as well as the experimentally found position of the substituent in relation to the cavity of the receptor of all of the ligands, except for **6**, when bound to receptor (**3**), whereas the water model failed for all, except **6**. The interaction between the receptor and ligands was quantified both directly and competitively by high accuracy using NMR titrations. Both methodologies showed that the ligand having a phenyl substituent binds strongest to the receptor followed by methyl, hydrogen, benzyl and cyclohexyl. The experimentally estimated relative binding values ($\Delta\Delta G$) were compared to the ones from MM and DFT, respectively. MM was better than DFT methods in reproducing the experimentally found relative binding strength of the different ligands to the receptor. However, both the relative- and

absolute binding energies obtained with the two theoretical methods diverted to a large extent from the ones obtained experimentally.

Introduction

Two constituents of living systems are proteins and peptides. The proteins are present among other things as transmembrane receptors, enzymes and antibodies. Peptides act as hormones[1], immunosuppressive agents[2], neurotransmitters[3], or as side chains in proteins.[4] It has recently been suggested that new drug candidates can be found by studying the interactions between a smaller surface of a globular protein and a short peptide fragment of another protein.[5] Hence, the construction of model systems of biological systems where the influence of such interactions on both the binding conformation of the receptor (protein) and ligand (peptide) and the strength of the binding can be studied under controlled terms is thus of importance.

A vast majority of peptides and proteins contain both hydrophilic and hydrophobic fractions present in their side chains, and their ratio in the protein/peptide is the major factor determining the strength of the interactions between the peptide and the protein[6] through the hydrophobic,[15] ion-ion- and ion-dipole effects. There are however several cases where the weaker non-polar interactions such as van der Waals forces are in majority in the fragments and due to their large number in the systems will generate strong binding.[6,7] Another important class of non-polar interactions between side chains of pepteides and proteins are involving aromic groups. [9]. There are two types of such interactions, aromatic-aromatic[11,12] and C-H aromatic interactions.[9a,13]

One common way of predicting how proteins and peptides interact between themselves and between each other is by the use of computational chemistry. In recent years, computational chemistry has been extensively used in medicinal chemistry, where it is providing a tool to inexpensively screening of a manifold of drug candidates.[22] However, one of the major problems that computational chemistry has to deal with is the quality assessment; how can the user be sure that the calculations are correctly reproducing the experimental results? When obtaining different results with different methods, one can assume that either one method is correct or all methods are wrong, but how should one decide? In contrast, if one theoretical method matches an experimental result, then one can assume that the theoretical method is correctly describing the system under study and it is highly likely that it would describe similar

[a]   S. Dawaigher, Dr. C. Solano Arribas, Dr. A. Ryberg, Dr. J. Jensen, Dr. K. E. Bergquist, Dr. A. Sundin, Prof. Dr. K. Wärnmark
       Centre for Analysis and Synthesis, Department of Chemistry
       Lund University
       P. O Box 124, S-221 00 Lund (Sweden)
       E-mail: Kenneth.warnmark@chem.lu.se
[b]   Prof. Dr. P.-O. Norrby
       Early Product Development, Pharmaceutical Sciences
       IMED Biotech Unit, AstraZeneca Gothenburg, Sweden
       Email: Per-Ola.Norrby@astrazeneca.com

       Supporting information for this article is given via a link at the end of the document.

systems correctly. Hence, the benchmarking of computational methods against experimental methods is crucial for the trust and use of computational methods in chemistry. Importantly, this requires that the experimental results against which the computational results will benchmark be are of high quality.

For all the purposes mentioned above, we have constructed a model system comprising ligands with an aliphatic framework that contains substituents attached to the main chain and a receptor having an aromatic cavity and ligands with an aliphatic framework that contains substituents attached to the main chain as a model for the interactions between the side chain of a peptide and aromatic groups of a protein constituting an aromatic cavity. By using NOESY and ROESY NMR methods, the change in the conformation of the ligand framework upon interacting with the receptor has been experimentally determined. To quantify the interaction, high quality NMR-titrations, direct- and competitive-, have been performed. This has generated a good estimation of the association constants and thus the free binding energies. Having access to high quality NOSEY and ROESY data on one hand and experimentally estimated binding free energies of high accuracy on the other, gives an opportunity to investigate how well computational methods are to reproduce experimentally found conformations and ligand-receptor binding energies in a system that models the interactions found in a hydrophobic pocket of a protein.

Our model system contains a multitude of factors that challenges computational methods; it includes supramolecular interactions such as hydrogen bonding and receptor- and/or ligand solvent interactions that are known to complicate the calculations involved.[23] It also involves charged entities of the ligands that challenge the computations. The titrations were conducted in a mixture of solvents meant to resemble aqueous solutions. This challenges the computational method even further. We tested a range of force field methods, as well as a dispersion-corrected DFT method.[24,25] Ensembles were generated by conformational searching (CS), and selected low energy structures reoptimized using DFT. Relative energies from force fields as well as from DFT were compared to relative experimental binding energies obtained from the NMR titrations. Four force fields were tested: MM3,[26] MMFFs,[27] OPLS05[28] and OPLS3.[29]

Results and Discussion

Binding mode and association constants

Conception of the titration series: We first set out to develop the model system. To simulate a hydrophobic pocket and allowing for π-π or π-CH interactions to take place between the receptor and ligand, the receptor was designed to have an aromatic cavity. In a previous study, we had developed a receptor that had a well-defined hydrophobic cavity,[30] this receptor was based on the Tröger's base (1) motif (Figure 1). For the purpose of studying the interaction between the cavity of the receptor and a well-defined substituent on the ligand, the side-group of the ligand must be placed over the aromatic surface of the cavity of the receptor. To ensure this, the crown-ether—ammonium binding motif was chosen to direct the ligand framework. Hence, to each end of the aromatic cavity (1) one 18-crown-6 moiety (2), was fused. This resulted in receptor 3

(see Figure 1).[30] Conversely, to each end of an aliphatic back-bone containing the substituent, was attached an ammonium group, resulting in heptane-1,7-diyl bisammonium dichlorides (4-8) ligands containing a substituent in the 4-position, to constitute , were selected as suitable model compounds for peptides (Figure 2). These ligands have roughly the same length as a tripeptide chain (both are roughly 10 Å in length, as suggested by molecular modelling). We had previously demonstrated that the relaxed, all-*anti* conformation of heptane-1,7-diyl bisammonium chloride, containing seven carbon atoms, possessed an ideal length to bind to each of the 18-crown-6 moieties of receptor 3.[29] Moreover, we had also seen in simpler molecular modelling that the hydrogen atoms of carbon atom 4 in the heptane chain were pointing towards the cavity in complex 3·8.[30] The nature of the substituents in the 4-position was mainly chosen as to mimic the side chains of different amino acids and the effect of aromatic and non-aromatic nature side-chains as well as of non-natural ligands. Based on this, the following side-groups were chosen: methyl, phenyl, benzyl, and cyclohexyl, leading to bisammonium heptane-1,7-diyl ligands 5, 6, 7, 8, respectively, in addition to hydrogen, the unsubstituted ligand 4, the latter being commercially available and acts as a reference compound (Figure 2). The choice of solvent was governed by two factors: since the solvent had to simulate a biological system, water would be ideal, however this was offset by the fact that the receptor was not soluble in water, hence a compromise had to be made. A 1:1 mixture of methanol and chloroform was a compromise that was settled for. The methanol in the mixture provides opportunities for the system to hydrogen bond to the solvent, and at the same time, chloroform solubilizes the receptor.
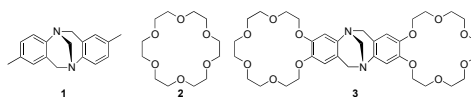
Figure 1. Tröger's base (1), 18-Crown-6 (2), 18-Crown-6 appended Tröger's base receptor (3).

4: R = H
5: R = Me
6: R = Ph
7: R = Bn
8: R = Cy
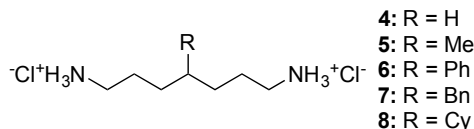
Figure 2. The bisammonium heptane chloride salts 4-8 chosen as ligands.

If the back-bone of the aliphatic chain of the ligand would have the same conformation and length between the terminal ammonium units within the series, determining the ΔG-value for the interaction between receptor 3 and each ligand 4-8, and subtracting with the ΔG-value of the unsubstituted ligand 4, the resulting $\Delta\Delta G$-values, would represent how strong the interaction of a specific "free" substituent would be with a "free" aromatic cavity of 3. However, the conception of a "uniform" conformation of the ligand framework is as expected difficult to

FULL PAPER

realize especially in our system where there is a such a large degree of conformation freedom in the ligands (vide infra). Instead, the conceptual model is that the association constant between receptor **3** and each of the ligands **4**-**8** *represents the the binding energy between a ligand framework having a side substituent and an aromatic cavity of a receptor*. This $\Delta\Delta G$ value involves *both* the binding energy between the side chain and receptor (negative value) and the rearrangement energy of the ligand framework to fit to the receptor cavity (positive value). This case is reminiscent to what could be found in nature as for instance the interaction between small peptides and a protein cavity containing aromatic side chains. However, in same cases where the change in in the conformation of the ligand framework is small upon binding to the receptor, the $\Delta\Delta G$ value can be taken as a rough estimate of the binding energy between the ligand side group itself and an aromatic surface or cavity (vide infra).

Synthesis of receptor 3 and ligands 5-8. Receptor **3** was synthesized by the condensation of commercially available 4-aminobenzo-18-crown-6 together with formaldehyde in the presence of HCl in ethanol (Scheme 1).[30] The synthetic route to the bisammonium salts is depicted in Scheme 2. It starts with the KF/18-crown-6 assisted bis-Michael addition between two equivalents of acrylonitrile and one equivalent of an α-substituted nitromethane unit in dichloromethane.[31] This was followed by the exchange of the nitro group for a hydrogen atom using tributyltin hydride in the presence of AIBN in benzene.[32] With the exception of **8c**, the reduction of dinitriles (**5c, 6c. 7c**) was conducted using BH₃ in 1,4-dioxane, and the subsequent quench with 4 M HCl resulted in the bisammonium salts.[33] In the case of **8** the dinitrile **8c** was reduced using Adam's catalyst.[34]
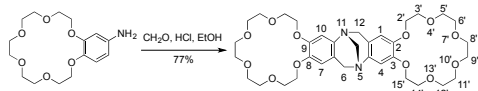
Scheme 1. Synthesis of receptor **3**.[30]

Scheme 2. Synthesis of ligands **5-8**. i) acrylonitrile, KF, 18-Crown-6, CH₂Cl₂. ii) Bu₃SnH, AIBN, benzene, reflux. iii) BH₃, THF. iv) HCl (4 M) in dioxane. v) PtO₂, H₂ (50 psi), CHCl₃, MeOH.

Experimental determination of the association constants of 3-8. To experimentally determine the free energy of the association of ligands **4** to receptor **3**, the corresponding associa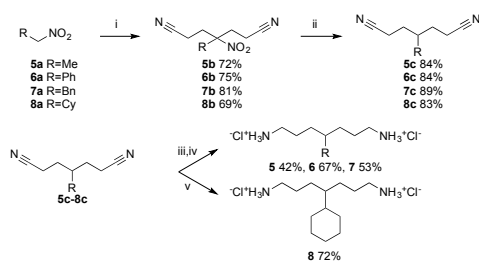tion constants were estimated by NMR titration methodology.[35] In this study we were presented with a dilemma since we want to study the association process in homogeneous solution: Polar aprotic solvents are the solvent of choice since they dissolve *both* ammonium salts and compounds containing 18-crown-6. Unfortunately, these solvents lack the possibility for some of the essential interactions with solutes present in biological systems. To counter this dilemma, we chose a solvent system comprised of CDCl₃:MeOH-d_4 (1:1) in which both the receptor and ligands were soluble and in which the desired interactions with the solute would be present. Initial studies of the association between **3** and **8** using ¹H NMR spectroscopy revealed that the chemical shifts observed for the protons were dependent on both the relative concentrations of **3** and **8** as well as the total concentration.[35] This observation meant that the association could be quantified using NMR titration methodology.

Binding stoichiometry. First, the binding stoichiometry between receptor **3** and the class of bisammonium salts **4-8** was estimated from the association of of **4** to **3** in CDCl₃:MeOH-d_4 (1:1) using a Job plot,[36] constructed using chemical shift data from ¹H NMR Job plot titrations (see supporting information).The so obtained Job plot showed a 1:1 stoichiometry for the binding and this ratio is assumed to be valid for all the complexes between receptor **3** and ligands **4-8**. This result is supported by ES-mass spectroscopy, where each of complexes **3**·(**4-8**) could be identified in equimolar solutions of **3** and each of **4-8** in CDCl₃:MeOH-d_4 (1:1) (see supporting information).

Direct titrations. When fitting the 1:1-binding model as suggested from the Job plot to binding data of **4** to **3**, it became evident that the association constant was too high to be estimated directly using ¹H NMR ($K_{3\text{-}4} > 10^4$ M⁻¹).[35] This lead to that the association constants had to be estimated relative to a weaker association. It was decided that the best choice would be to perform the titration of the bisammonium salts in the presence of a monoammonium salt; in our case methyl ammonium chloride (**9**). It was chosen for two reasons. The first reason being that **9** has a single ¹H NMR resonance that could easily be identified. The second reason was that the addition of a mono ammonium chloride salt **9** allowed us to keep the concentration of the [Cl⁻] = 74 mM throughout the whole titration, in an attempt mitigate the changes in ionic strength in the solution during the titrations.

The association between the ditopic receptor (R) and the bisammonium salt (B) leads to one complex (RB) following a 1:1 binding model and thus equation 1 below would apply.

$$R + B \rightleftharpoons RB \qquad\qquad K^{bis} = \frac{[RB]}{[R][B]} \qquad (1)$$
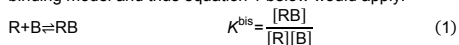
However, since the titrations were performed in competition for R with a monoammonium salt (M), the equilibria 2 and 3 are also present and need to be considered,

$$R + M \rightleftharpoons RM \qquad\qquad K_1^{mono} = \frac{[RM]}{[R][M]} \qquad (2)$$

$$RM + M \rightleftharpoons RM_2 \qquad\qquad K_2^{mono} = \frac{[RM_2]}{[RM][M]} \qquad (3)$$
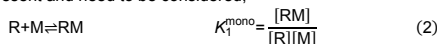
Taking into account to the above equations, the total concentration of R, B and M are given by,

$$[R]_{total}=[R]+[RM]+[RM_2]+[RB] \tag{4}$$
$$[B]_{total}=[B]+[RB] \tag{5}$$
$$[M]_{total}=[M]+[RM]+2[RM_2] \tag{6}$$

Insertion of equations 1, 2 and 3 into 4 results in the following expression for the concentrations,

$$[R]=\frac{[R]_{total}}{1+K_1^{mono}[M]\left(1+K_2^{mono}\right)+K^{bis}[B]} \tag{7}$$

$$[RM]=\frac{[R]_{total}-[R]\left(1+K^{bis}[B]\right)}{1+K_2^{mono}[M]} \tag{8}$$

$$[RM_2]=[R]_{total}-[R]\left(1+K_1^{mono}[M]+K^{bis}[B]\right) \tag{9}$$

The concentration of free monoammonium salt is given by the expression,

$$[M]=\frac{[M]_{total}}{1+K_1^{mono}[R]+2K_1^{mono}K_2^{mono}[R][M]} \tag{10}$$

The mole fractions of the R, RM, RM$_2$ and M species in solution are as follows, $x_R=\frac{[M]_{total}}{[R]_{total}}$, $x_{RM}=\frac{[RM]}{[R]_{total}}$, $x_{RM_2}=\frac{[RM_2]}{[R]_{total}}$, $x_M=\frac{[M]}{[M]_{total}}$.
The above expressions are useful, since the observed chemical shift δ_{obs}^r for a given proton resonance, r, in the NMR spectrum, in any species containing R is given by the expression,

$$\delta_{obs}^r=x_R\,\delta_R^r+x_{RM}\,\delta_{RM}^r+x_{RM_2}\,\delta_{RM_2}^r \tag{11}$$

Likewise, the observed chemical shift for a resonance *m* in any species containing M is given by,

$$\delta_{obs}^m=x_M\,\delta_M^m+x_{RM}\,\delta_{RM}^m+x_{RM_2}\,\delta_{RM_2}^m \tag{12}$$

The estimation of the association constant is described in the supporting information and the quality of the fit is demonstrated by the good correlation between calculated and observed chemical shifts (Figure 3). Thus the chemical shifts of each of the complexes (4-8)·3 fits a 1:1 binding model. This also supports the indirect assumption that the association of the monoammonium salt competitor to the receptor can be neglected as already observed for the unsubstituted ligand 4.[30] The result of the estimation of the association constants from direct titrations is given in Table 1.

Figure 3. The correlation between observed and fitted chemical shifts for all the different bisammonium salts.

Table 1. Estimated association constants for the association of ligands 4-8 to 3, obtained from direct titrations in CDCl$_3$:MeOH-d_4 (1:1) .

| Bisammonium ligand	Log *K*	Probability of binding[35]
4	7.22 (3)[a]	0.41-0.97
5	7.46 (2)	0.51-0.99
6	7.94 (1)	0.65-0.99
7	7.14 (4)	0.38-0.97
8	6.67 (5)	0.21-0.93

[a] Ranking of the ligands with respect to the binding to the receptor.

Competitive titrations. As can be seen from Table 1, the difference in the estimated association constants between the different bisammonium salts is small. This fact makes it difficult to assess the relative order of binding of ligands 4-8 to receptor 3. In order to get more reliable information about the affinity of 3 for each bisammonium salt, 4-8, prompted us to conduct competitive titrations between each of ligands 4-8 in the presence of 3. This results in the estimation of the relative association constant of each of the complexes in relation to one of the complexes, the reference compound/competitor. The phenyl-substituted ligand 6 was chosen as the common competitor in all experiments due to the low degree of overlap between its proton resonances with the other bisammonium salt ligands in the ^{1}H NMR spectra during the titrations. The competitive titrations were conducted in the presence of 9 to keep the conditions as similar as possible to the ones used in the estimation of the absolute association constants.

Hence, under the above conditions, the ratio between the association constants of two different bisammonium ligands *x* and *y* with receptor 3 are given by equation 13 below.[37]

$$\left(\delta_{obs}^{bx}-\delta_x^{bx}\right)\left(\delta_{3\cdot y}^{by}-\delta_{obs}^{by}\right)=\frac{K_{3\cdot x}^{bis}}{K_{3\cdot y}^{bis}}\left(\delta_{3\cdot x}^{bx}-\delta_{obs}^{bx}\right)\left(\delta_{obs}^{by}-\delta_y^{by}\right) \tag{13}$$

In equation 13, the terms b*x* and b*y* stand for a given NMR resonance b in ligands *x* and *y*, and complexes 3•*x* and 3•*y*, respectively. The difference in association constants between ligands 4-8 and monoammonium salt 9 is so large that the association of 9 to 3 is negligible in the presence of each of 4-8 (vide supra).[30] Hence, equation 13 can be considered a valid description of the constructed titration system.[37] Thus, for each competitive pairwise titration of bisammonium salt *x* = 4, 5, 7 or 8, with *y* = 6 in the presence of receptor 3, experimental data can be plotted in accordance with equation 13 above for a given NMR active resonance b in *x* = 4, 5, 7 or 8 and *y* = 6 respectively. The competitive titrations were conducted over a set of concentration ranges. The $\left(\delta_{obs}^{bx}-\delta_x^{bx}\right)\left(\delta_{3\cdot 6}^{b6}-\delta_{obs}^{b6}\right)$ term was plotted versus the $\left(\delta_{3\cdot x}^{bx}-\delta_{obs}^{bx}\right)\left(\delta_{obs}^{b6}-\delta_6^{b6}\right)$ term. A straight line was fitted to the data points using the "least square method" The so calculated slop slope of the line corresponds to $\frac{K_{3\cdot x}^{bis}}{K_{3\cdot 6}^{bis}}$ (Figure 4). The results are given in Table 2 for *y* = 6.
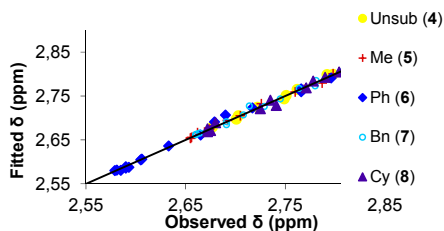
FULL PAPER
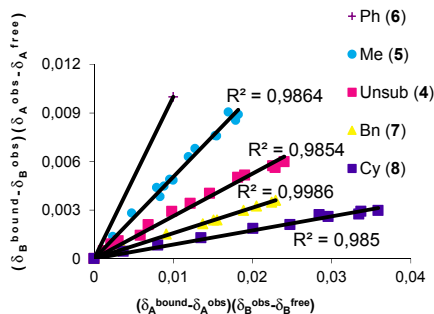
Figure 4. Visualization of the fitting of the model represented by equation 13 to experimental data for the estimation of the relative association constants, $K_{3\cdot x}/K_{3\cdot 6}$ in CDCl$_3$:MeOH-d_4 (1:1), [Cl$^-$]$_{tot}$= 74 mM, of **3·4**, **3·5**, **3·6**, **3·7**, **3·8**, respectively, relative to **3·6**. The ratio $K_{3\cdot x}/K_{3\cdot 6}$ is given by the slope of each straight line.

The good agreement between the modelled- and the experimental chemical shifts suggest that the weaker association and small degree of deprotonation of the monoammonium salt have a negligible effect on the value of the estimated association constant from both direct and competitive titrations.[30] The so-obtained relative association constants are given in Table 3, both relative to **3·6** and **3·4**, containing the unsubstituted reference ligand **4**.

Table 2. Estimated relative association constants for the association **4-8** to **3**, obtained from competitive titrations in CDCl$_3$:MeOH-d_4 (1:1).

subst	H	Me	Ph	Bn	Cy
(ligand **x**)	**(4)**	**(5)**	**(6)**	**(7)**	**(8)**
$K^{bis}_{3\cdot x}/K^{bis}_{3\cdot 6}$	0.26	0.51	1	0.15	0.09
$K^{bis}_{3\cdot x}/K^{bis}_{3\cdot 4}$	1 (3)[a]	1.96 (2)	3.85 (1)	0.58 (4)	0.35 (5)

[a] Ranking of the ligands with respect to the binding to the receptor.

One of our aims is to obtain data that could be used as a benchmark to evaluate various computational methods. For this purpose, the relative association constants were converted to Δ Δ G^0 values using equation 14 below.

$$\Delta\Delta G^0_{3\cdot x\text{-}3\cdot y} = \Delta G^0_{3\cdot x} - \Delta G^0_{3\cdot y} = -RT\ln\frac{K^{bis}_{3\cdot x}}{K^{bis}_{3\cdot y}} \qquad (14)$$

he results are given in Table 3. With the experimental values of Δ Δ G^0 determined, where each Δ Δ G^0 value in Table 3 could be interpreted as the individual contribution of each substituent in ligand **x** to the Δ G^0 value of complexation in relation to ligand **y**, the stage is set (vide infra) to evaluate the accuracy of some of the most common computational methods.

Table 3. Experimentally determined values of ΔΔ$G^0_{3\cdot x\text{-}3\cdot 4}$ (kJ mol^{-1}) for the association of ligands **4-8** to **3** in CDCl$_3$:MeOH-d_4 (1:1).

substituent	H	Me	Ph	Bn	Cy
(ligand **x**)	**(4)**	**(5)**	**(6)**	**(7)**	**(8)**
ΔΔ$G^0_{3\cdot x\text{-}3\cdot 6}$	3.33	1.67	0	4.70	5.96
ΔΔ$G^0_{3\cdot x\text{-}3\cdot 4}$	0 (3)[a]	-1.67 (2)	-3.34 (1)	1.35 (4)	2.60 (5)

[a] Ranking of the ligands with respect to the binding to the receptor.

Conformational analysis of the free ligand and the complex

NMR data of bound and free ligands. The free ligands, the receptor and their complexes, were analyzed using NMR spectroscopy (for ^{1}H NMR and ^{13}C NMR assignments see the supporting information). NOESY NMR spectroscopy of the free ligands suggested that certain conformations were adopted preferentially on a time average and these conformations were compared with the results of the conformational analysis using theoretical calculations.

Visualization of data. The structure of complexes **3·(4-8)** can be visualized by a combination of the experimental information obtained from NMR titrations, NOESY and ROSEY NMR spectra of solutions of the complexes and energy-minimized structures of the complexes obtained via calculations (molecular modelling). Images of the lowest energy conformation using an OPLS3 force field were used to compare the calculated conformation with the experimental one. The choice of the OPLS3 force field is based on the fact that the ΔΔG^0 values obtained from calculations using the OPLS3 force field were deviating the least from the experimentally estimated values of ΔΔG^0. Structural analysis of the complexes based on NMR spectroscopy requires a correct assignment of the NMR spectrum of the free receptor **3** and of the free bisammonium salts **4-8** prior to any comparison. The result of such an analysis is shown in the Supporting Information.

Investigation of free receptor 3 by ^{1}H NMR spectroscopy. For the numbering of the atoms of **3**, see Scheme 1. Two aromatic resonances can be observed in the ^{1}H NMR spectrum of **3**. The resonance at δ = 6.44 ppm is broadened compared to δ = 6.66 ppm and the former is hence assigned to H-1 (H-7) and the latter to H-4 (H-10) based on the literature about NMR assignments of Tröger's base analogues.[38] This assignment is supported by the observation of large cross peaks between N-CH$_2$ protons (H-6 and H-12) and the aromatic resonance at δ = 6.44 in the ^{1}H,^{1}H COSY spectrum of **3**, while only a small one was observed with the aromatic resonance at δ = 6.66. For Tröger's base derivatives, one expects the two AB doublet proton resonances to appear around the chemical shift 4-4.5 ppm.[38] The upfield doublet (δ = 4.06) is assigned to H-6$_{endo}$ and H-12$_{endo}$ due to the *endo* proton resonances being shielded by the aromatic protons of Tröger's base core.[38] The downfield doublet (δ = 4.56 ppm) is accordingly assigned to H-6$_{exo}$ and H-12$_{exo}$. In addition, H-4 and H-10 show cross peaks with H-6$_{endo}$ and H-12$_{endo}$, respectively, indicating that receptor **3** has a pronounced cavity. The crown ether moieties of **3** could be only partially assigned: in the ^{1}H NMR spectrum the crown-ether proton resonances appear as two groups, one downfield (3.81-4.12 ppm), integrating for 16 protons and one upfield (3.63-3.73 ppm), integrating for 24 protons. In The NOESY spectrum there are cross peaks between the proton resonance at 6.44 (H-1, H-

FULL PAPER

7) ppm and the resonance at 4.01-4.05 ppm. Hence, the latter resonance is assigned to the crown-ether methylene protons H-2'. In the ^{1}H,^{1}H COSY spectrum, a cross-peak is observed between proton resonances at 4.02-4.10 ppm and at 3.82-3.88 ppm, the latter resonance is thus assigned to H-3'. Correspondingly, using the same protocol as for the assignment of H-2' and H-3', the proton resonance at 4.10-4.12 ppm is assigned to H-15' and the resonance at 3.86-3.88 ppm is assigned to H-14'. Due to severe overlap of peaks in the NMR spectrum, none of the upfield proton resonances of the crown-ether moieties could be individually assigned.

Investigation of the conformation of free ligand 4 by ^{1}H NMR spectroscopy and molecular modelling. See Figure 5a and 5b. The NOESY spectrum shows cross peaks between protons H-1 and H-3/H-4, between H-2 and H-3/H-4 and between H-1 and H-2. If an all-*anti* conformation is adopted between C-2 and C-3, one would expect a NOE interaction between H-3 and H-1 and between H-2 and H-1 of roughly the same intensity and we observe this in the spectra. Although the chemical shifts of H-3 and H-4 are superimposed, precluding a perfect assignment, it is most likely that the molecule adopts an all-*anti* conformation on a time average, as supported by the NOESY spectrum. The lowest energy conformation obtained from molecular modelling using the OPLS3 force field with a solvent potential for water suggests an all-*anti* conformation with a N-N distance of 10.18 Å (Figure 5a). Using a solvent potential for chloroform instead of water, the same all-*anti* conformation is also observed with a N-N distance of 10.20 Å (Figure 5b). MD simulations conducted with an OPLS05[28] force field and using a methanol solvent model, (we used a methanol solvent model since it was found to be the one that matched our experimental data most closely when compared with other solvent models tested (water, chloroform and gas phase)), suggests that the ligand would diverge towards an all-*anti* conformation over a period of 12 ns, consistent with an all-*anti* conformation on a time average.
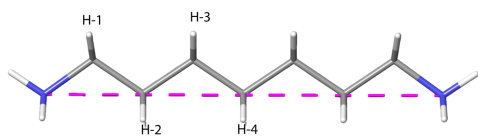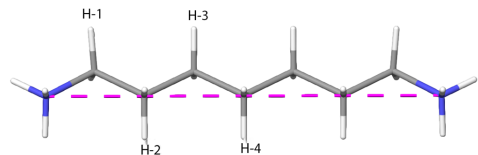
Hence, molecular modelling using a water or chloroform potential is in agreement with the experimental observation of an *all*-anti heptane chain of **4**.

Investigation of the conformation of complex 3•4 by ^{1}H NMR spectroscopy and molecular modelling. Se Figures 6a and 6b. Upon titration of **4** with **3**, the chemical shift of the resonance of H-4 of **4** is displaced dramatically upfield by 0.90 ppm on going from 0% to 95% bound **4**. In addition, the proton resonances of H-1, H-2 and H-3, exhibit upfield shifts of 0.22, 0.59 and 0.46 ppm, respectively. This suggests that **4** is situated in the aromatic cavity of **3**. The size of the upfield shifts of H-1, H-2, H-3, and H-4 correspond to their anti, syn, anti, syn orientation with respect to the aromatic cavity of **3**, this shows that **4** adopts an all-*anti* conformation of the heptane chain on a time-average as for free **4**. In the 2D ROESY spectra, crosspeaks can be seen between H-1 and H-2, between H-1 and H-3, Between H-2 and H-3 and H-4, further supporting the observation of all-*anti* conformation being adopted by **4** in its complex with **3**. The energy-minimized conformation of complex **3•4** obtained from molecular modelling using an OPLS3 force field using a water solvent model shows a conformation that is eclipsed between the C-1 and C-2 carbons, indicating that the carbon chain is not adopting an all-*anti* conformation, resulting in an N-N distance of 9.11 Å (Figure 5a), somewhat shorter than the calculated N-N distance of free **4** of 10.18 Å (vide supra), the latter displaying a perfect all-*anti* conformation. In contrast, using the solvent potential for chloroform instead of water, a perfect all-*anti* conformation is adopted by the bisammonium heptane chain with an N-N distance of 10.11 Å, the same as for free ligand **4** (Figure 5b).

Hence, molecular modelling using a water or chloroform potential is in agreement with the experimental observation of an *all*-anti heptane chain of complex **3•4**.

Figure 5a. The lowest energy conformation of ligand **4** as suggested by molecular modelling using an OPLS3 force field with a solvent potential for water. (N-N distance = 10.18 Å).

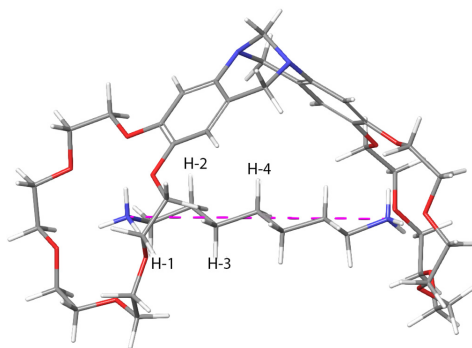**Figure 5b.** The lowest energy conformation of ligand **4** as suggested by molecular modelling using an OPLS3 force field with a solvent potential for chloroform. (N-N distance = 10.20Å).

Figure 6a. The lowest energy conformation of ligand **4** bound to receptor **3** as suggested by molecular modelling using an OPLS3 force field with a solvent potential for water. (N-N distance = 9.11 Å).

Figure 6b. The lowest energy conformation of ligand **4** bound to receptor **3** as suggested by molecular modelling using an OPLS3 force field with a solvent potential for chloroform. (N-N distance = 10.11 Å).

Investigation of the conformation of free ligand 5 by ^{1}H NMR spectroscopy and molecular modelling. See Figures 7a and 7b. The NOESY data (See SI for table and spectra) show that the ligand adopts an all-*anti* conformation on a time average. This view is supported by the absence of a NOE interaction between H-4 and H-3', indicating that the two protons are situated in positions opposite each other and that the distance between the two atoms are in fact too large to give a NOE interaction (>3 Å).[39] In addition, there is a NOE interaction between H-5 and H-3' indicating that the distance between H-5 and H-3' is less than 3 Å that would imply that H-3' is located syn to one of the H-5 protons and being consistent with an all-*anti* conformation. The lowest energy conformation obtained from molecular modelling using an OPLS3 force field with a potential for water suggests an all-*anti* conformation of the heptane chain with a N-N distance of 10.18 Å (Figure 7a). The heptane chain of **5** shows an all-*anti* conformation, when using an OPLS3 force field with the chloroform solvent potential resulting in a N-N distance of 10.20 Å (Figure 7b). Moreover, molecular mechanics calculations conducted using an OPLS05 force field and a methanol solvent model suggest that the ligand would diverge towards an all-*anti* conformation on a time average consistent with the results.

Figure 7a. The lowest energy conformation of ligand **5** as suggested by molecular modelling using an OPLS3 force field with a solvent potential for water. (N-N distance = 10.18 Å).
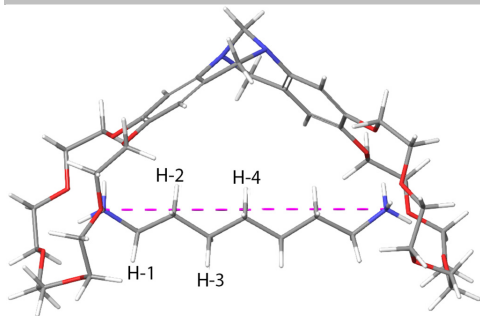
Hence, molecular modelling using a water or chloroform potential is in agreement with the experimental observation of an *all*-anti heptane chain of ligand **5**. The same result is also obtained using molecular dynamics simulations and a methanol solvent model.
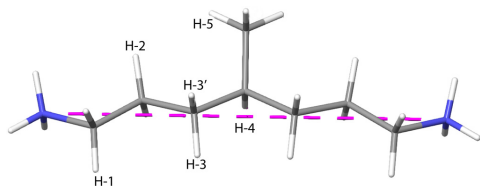

Figure 7b. The lowest energy conformation of ligand **5** as suggested by molecular modelling using an OPLS3 force field with a solvent potential for chloroform. (N-N distance = 10.20 Å).

Investigation of the conformation of complex 3•5 by ^{1}H NMR spectroscopy and molecular modelling. See Figures 8a and 8b. The most striking observations are the upfield displacement of the proton resonance of the hydrogen atoms of the methyl group and H-4 of **5** upon addition of **3**; from 0 to 92% bound **5**, an upfield displacement by 1.07 and 0.92 ppm, respectively. The magnitude of the displacement indicates that the aromatic rings of the cavity shield both the methyl group and the H-4 proton magnetically. This implies that both the methyl group and the H-4 proton are residing in the aromatic cavity on a time-average. In the ROSEY NMR spectra of **3•5** the shifts corresponding to the heptane chain exhibit an intense crosspeak between H-1 and H-2, and a somewhat weaker crosspeak between H-1 and H-3 are observed, this is consistent with an all-*anti* conformation.

The energy-minimized conformation of complex **3•5** obtained from molecular modelling using an OPLS3 force field with a water potential suggests that the heptane chain of **5** is **no**t adopting an all-*anti* conformation; one can observe a *gauche* conformation between C-3 and C-4 in the heptane chain and the N-N distance is reduced to 8.84 Å (Figure 8a). In addition, methyl group seems to be oriented outside the cavity of the receptor. When the molecular modelling is conducted using a solvent potential for chloroform instead of water, a different conformation compared to the one seen with the water potential is suggested. The N-N distance is 10.11 Å, similar as for perfectly all-*anti* staggered **5** and strongly suggesting that the heptane chain of **3·5** is per all-*anti*. Moreover, the calculations suggest that methyl group is somewhat oriented towards the inside of the hydrophobic cavity (Figure 8b).

Figure 8a. The lowest energy conformation of ligand **5** bound to receptor **3** as suggested by molecular modelling using an OPLS3 force field with a solvent potential for water. (N-N distance = 8.84 Å).

Figure 8b. The lowest energy conformation of ligand **5** bound to receptor **3** as suggested by molecular modelling using an OPLS3 force field with a solvent potential for chloroform. (N-N distance = 10.11 Å).
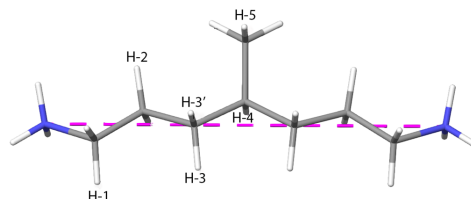
Hence, molecular modelling using a chloroform solvent model but **not** a water model is in agreement with the experimental observation of an all-*anti* heptane chain of complex **3·5** with the methyl side group and the central hydrogen atom of the backbone of the heptane chain of the ligand residing inside the aromatic cavity of the receptor.

Investigation of the conformation of free ligand 6 by ¹H NMR spectroscopy and molecular modelling. See Figures 9a and 9b. The NOESY spectra indicate that the bisammonium salt **6** is adopting an *all*-anti conformation in solution on a time average. The weak NOE between protons H-4 and H-3 indicates that the two protons are pointing away from each other on a time-average in relation to H-4 and H-3' that have a crosspeak between them indicating that H-4 and H-3' are within 3 Å, a distance setting the upper boundary for observing NOEs,[39] of each other most of the time this observation is consistent with an *all*-anti conformation. The presence of strong NOEs between

protons H-6 and H-4 and between protons H-6 and H-2, further supports the *all*-anti conformation. Further support for **6** adopting an *all*-anti conformation is the lack of a NOE between protons H-3/H-3' and H-6, where one would expect a NOE if an eclipsed conformation was adopted on a time average. The lowest energy conformation obtained from molecular modelling using the OPLS3 force field with the water solvent potential suggests a completely all-*anti* staggered conformation with a N-N distance of 10.22 Å (Figure 9a). In contrast, molecular modelling using a solvent potential for chloroform, shows a deviation from a completely all-*anti* staggered conformation also demonstrated by the modelled short N-N distance of 8.43 Å (Figure 9b).
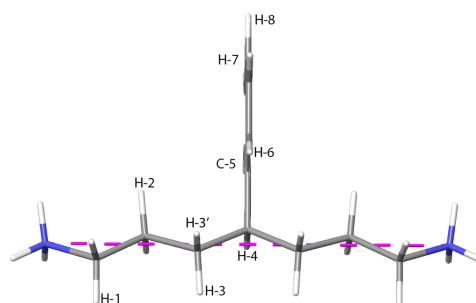
Figure 9a. The lowest energy conformation of ligand **6** as suggested by molecular modelling using an OPLS3 force field with a solvent potential for water. (N-N distance = 10.22 Å).
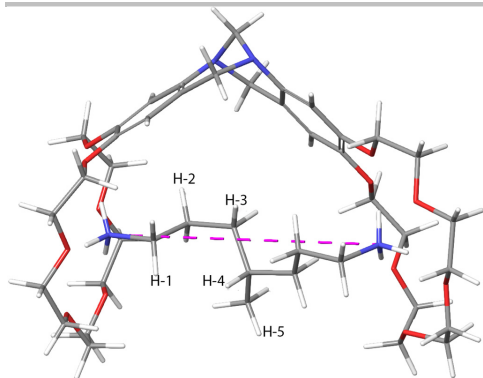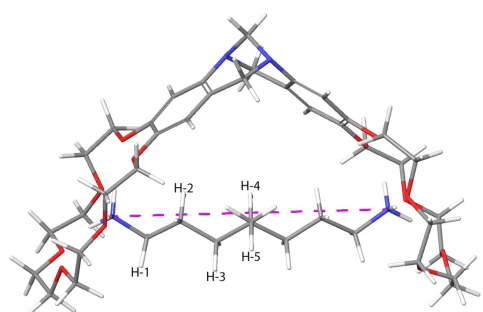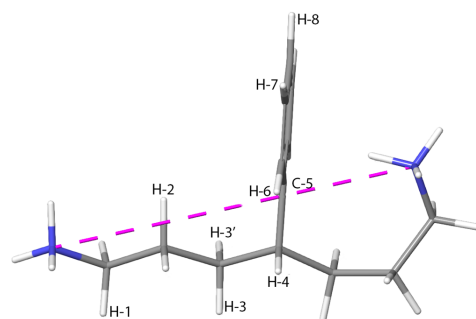

Figure 9b. The lowest energy conformation of ligand **6** as suggested by molecular modelling using an OPLS3 force field with a solvent potential for chloroform. (N-N distance = 8.43 Å). The numbering is too small.

Hence, molecular modelling using a water model but *not* a chloroform model is in agreement with the experimental observation of an *all*-anti heptane chain of ligand **6**. This is in agreement with the ability of ammonium groups to form strong complexes with benzene rings, in vacuo in non-polar solvent, giving rise to a collapsed conformation.[40] However, in a hydrogen bond accepting solvent like water, the interaction of

the ammonium group with the solvent is preferred, allowing formation of the all-*anti* conformation.

Investigation of the conformation of complex 3•6 by ¹H NMR spectroscopy and molecular modelling. See Figures 10a and 10b. The NMR data suggest that the phenyl substituent is residing inside the aromatic cavity of the receptor. The support for this is the upfield displacement of the resonance of the *ortho*-protons (H-6) of the phenyl substituent of the heptane chain and of the resonance of proton H-4 of **6** upon the addition of **3**. The displacements are 0.74 and 1.40 ppm, respectively, on going from 0 to 99% bound **6**. The ROESY spectrum of **3•6** provides further support for a conformation where the phenyl substituent of **6** on a time average is in close contact with the aromatic moieties of **3** due to the observation of a cross peak between the proton resonances of the *meta*-protons (H-7) of the phenyl group of **6** and H-6*endo* (H-12*endo*) of **3**. In the ROESY spectrum, a very clear crosspeak can be seen between the singlets at 6.65 /6.40 of the receptor (corresponding to its H-4/H-10 and H-1/H-7 aromatic protons respectively) and the multiplet at 7.33 ppm corresponding to H-7 of **6**. Indicating that H-7 on a time average is within 3 Å of the aromatic protons of the receptor. In the ROESY NMR spectra we see an intense crosspeak between H-1 and H-2, and a weaker crosspeak between H-1 and H-3 consistent with an all-*anti* conformation for the heptane chain. The energy-minimized conformation of complex **3•6** obtained from molecular modelling, using an OPLS3 force field, and a water solvent potential shows a perfectly all-*anti* staggered conformation of the heptane chain of **6** with a N-N distance of 10.14 Å. The phenyl group is oriented on a plane that is almost 60% situated inside the aromatic cavity (Figure 10a). The energy-minimized conformation of complex **3•6** using an OPLS3 force field and the chloroform solvent potential exhibits a gauche conformation being adopted by the heptane chain between C-2 and C-3 with a N-N distance of 9.77 Å (Figure 10b). Moreover, using either a water or a chloroform solvent potential, molecular modelling indicates that the phenyl group is oriented partly inside the cavity of the receptor.
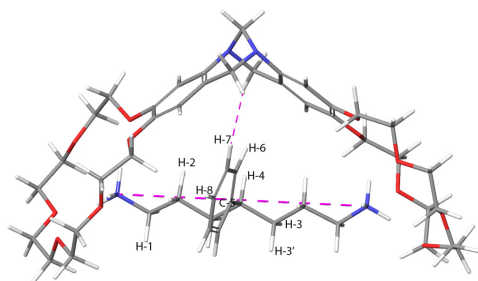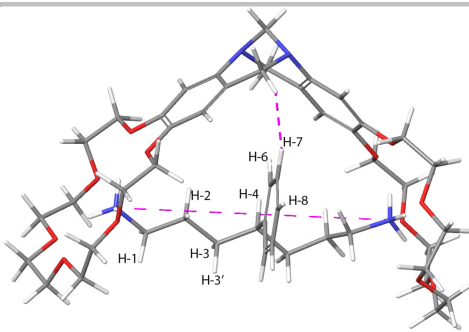
Figure 10b. The lowest energy conformation of ligand **6** bound to receptor **3** in chloroform as suggested by molecular modelling using an OPLS3 force field with a solvent potential for chloroform. (N-N distance = 9.79 Å, H-6 *Endo* – H-7 distance = 3.23 Å).

Hence, molecular modelling using a water or chloroform or methanol model is in agreement with the experimental observation of an *all-anti* heptane chain of complex **3·6**.

Investigation of the conformation of free ligand 7 by ¹H NMR spectroscopy and molecular modelling See Figures 11a and 11b. The magnitude of the NOEs between H-1 and H-2 or H-4 (the shifts of H-2 and H-4 are superimposed) and between H-1 and H-3 suggests that the H-1, H-2 and H-3 are adopting a conformation that is anti towards each other (assuming that the NOE between H-1 and H-2 and H-4 is mainly the result of an interaction between H-1 and H-2). A NOE between H-3 and H-2/4 also suggests that an all-*anti* staggered conformation is adopted. The NOE interaction between H-2 and H-4 and H-5 implies that one of the H-5 hydrogen atoms is situated anti to the H-4 hydrogen (assuming that the NOE between H-2 and H-4 and H-5 is solely due to the interaction between H-4 and H-5). There is a NOE interaction between H-7 and H-3 and between H-7 and H-2 and H-4. This implies that the benzyl group is orienting itself anti to one of the alkyl chains of C-4 on a time average. The above analysis of the NMR data would therefore conclude that the heptane chain is adopting an all anti conformation with the benzyl group oriented anti to one of the alkyl chains of C-4. The molecular model obtained using OPLS3 force field and a solvent potential for water predicts an all-*anti* conformation with a N-N distance of 10.16 Å being somewhat inconsistent with the NMR data, since in contrast to the NMR data, the obtained model predicts the benzyl group to be oriented anti to H-4 (Figure 11a). In contrast, the conformation obtained (OPLS3) using a solvent potential for chloroform results in a conformation where the heptane chain deviates strongly from an all-*anti* conformation. Moreover, this modelling suggests that the benzyl group orients itself such as that the plane of the aromatic ring can interact with one of the ammonium moieties, via a cation-π-interaction. Neither the orthogonal orientation of the aromatic ring with the ammonium

Figure 10a. The lowest energy conformation of ligand **6** bound to receptor **3** in water as suggested by molecular modelling using an OPLS3 force field with a solvent potential for water. (N-N distance = 10.14 Å, H-6 *Endo* – H-7 distance = 2.64 Å).
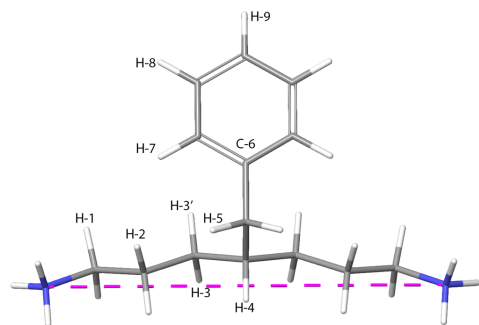
ion nor the N-N distance of 8.73 Å observed from modelling is consistent with an all-*anti* conformation as derived from the NOESY spectra (Figure 11b, See SI).

Figure 11a. The lowest energy conformation of **7** obtained using molecular modelling using an OPLS3 force field with a solvent potential for water. (N-N distance = 10.16 Å).

Figure 11b. The lowest energy conformation of **7** obtained using molecular modelling using an OPLS3 force field with a solvent potential for chloroform. (N-N distance = 8.73 Å).

Hence, molecular modelling using a water model but *not* a chloroform model is in agreement with the experimental observation of a more or less *all*-anti heptane chain of ligand **7**. However, molecular modelling could not reproduce the experimentally found position of the benzyl group anti to one of the alkyl chains of C-4.
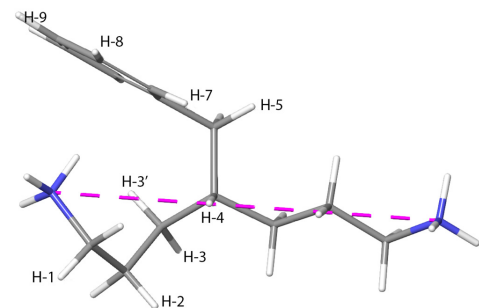
Investigation of the conformation of complex 3•7 by ¹H NMR spectroscopy and molecular modelling. See Figures 12a and 12b. The chemical shift of the proton resonances of H-4 in the heptane chain of **7**, the proton resonances of the methylene protons of the benzyl substituent (H-5), and the proton resonances of the *ortho*-hydrogen of the benzyl group (H-7), are

shifted upfield by 0.81, 0,31 and 0.10 ppm, respectively, upon titration with **3**; when 96% of **3** is bound to **7**. The other aromatic protons of the benzyl group are not displaced at all (see Supporting Information). Based on the above information, one can conclude that the H-4 proton of **7** is situated in the aromatic cleft of **3** on a time average. However, due to the smaller upfield displacement of the proton resonance H-4 of **3•7** compared to **3•5** and **3•6**, it can be assumed that the H-4 of ligand **7** is not that deeply situated inside the cleft of **3**. In addition, the above displacement of the resonance of the methylene protons of the benzyl substituent, demonstrates that they are situated in the vicinity of the aromatic cleft of **3**, although not as close to the aromatic surfaces as for instance the methyl group of **3•5** or the phenyl group of **3•6**. The minor displacement of the chemical shifts of the aromatic part of the benzyl group of **7** upon coordination with **3** on a time average suggests that the benzyl group is pointing away from the aromatic cavity of **3**; the *ortho*-hydrogen atoms being closest to the cavity (as seen in Figure 12b). This is supported by a crosspeak in the ROESY spectrum of **3•7** between the resonance of the *ortho*-protons of the benzylic substituent of **7** and the proton resonance H-1(7) of **3**. Also in the ROSEY spectra we observe an intense crosspeak between H-1 and H-2 and a weaker crosspeak between H-1 and H-3 consistent with an all-*anti* staggered chain conformation. When examining the model of the lowest energy conformation of **3•7** obtained using an OPLS3 force field and a water solvent model, the heptane chain adopts a conformation deviating from an *all*-anti conformation with the benzylic methylene hydrogen atoms directed away from the hydrophobic cavity. The aromatic ring of the benzylic group is pointing towards the hydrophobic cavity and the N-N distance is calculated to 8.81 Å (Figure 12a). The lowest energy conformation of **3•7** in chloroform differs from the conformation in water; the heptane chain adopts a nearly perfect all-*anti* staggered conformation with a calculated N-N distance of 9.98 Å and the benzyl group oriented inside the hydrophobic cavity (Figure 12b). Hence, molecular modelling using the OPLS3 force field and a chloroform model but *not* a water model is in agreement with the experimental observation of a more or less *all*-anti heptane chain of complex **3•7**. Hence, the conformation of **3•7** obtained from the OPLS3 force field with the chloroform potential is better supported by the NMR experiments than the one with the water potential.
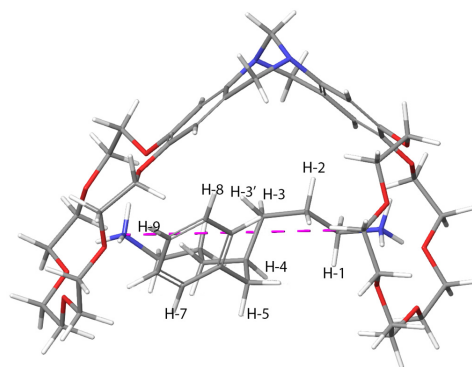
FULL PAPER

Figure 12a. The lowest energy conformation of ligand **7** bound to receptor **3** suggested by molecular modelling using an OPLS3 force field with a solvent potential for water. (N-N distance = 8.81 Å).

Figure 12b. The lowest energy conformation of ligand **7** bound to receptor **3** as suggested by molecular modelling using an OPLS3 force field with a solvent potential for chloroform. (N-N distance = 9.98 Å).

Hence, molecular modelling using a chloroform model but *not* a water model is in agreement with the experimental observation of a more or less *all*-anti heptane chain of ligand **7**. However, molecular modelling could not reproduce the experimentally found position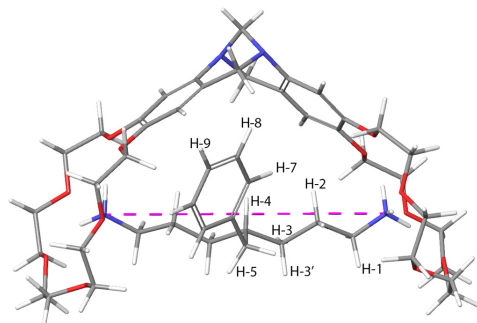 of the benzyl group anti to one of the alkyl chains of C-4. It seems that the model in water better represents the side chain while the model in chloroform better represents the heptane chain.

Investigation of the conformation of free ligand 8 by ¹H NMR spectroscopy and molecular modelling. See Figures 13a and 13b. Due to the severe overlap of chemical shifts in the ¹H NMR, the NOESY spectra of ligand **8,** the NMR spectra are difficult to interpret (For NMR assignments see supporting information). However, it can be concluded that, on a time average, the protons H-1, H-2, and H-3 adopt a conformation anti to each other, as NOEs can be observed between H-1 and H-2, and H-1 and both H-3 and H-3'. There is a NOE between both H-3 and H-3' and H-6 demonstrating that they are on a time average within 3 Å distance from each other.[39] One should note that there is a very weak NOE between H-4 and H-1, an NOE interaction even though weak, between these is not to be expected if the chain is adopting an *all*-anti conformation on a time average. This can be indicative of that a completely anti conformation in the heptane chain is *not* being adopted. A likely conformation is where a gauche interaction is adopted between C-3 and C-4, this could explain the weak NOE between H-4 and H-1. The lowest energy conformation obtained from molecular modelling using the OPLS3 force field and a water potential, suggests a conformation as depicted in Figure 13a with an N-N distance of 7.50 Å. In this model, the methylene groups of C-1 to C-7 are adopting an all-*anti* staggered conformation in relation to each other and this is consistent with the data obtained from NMR spectroscopy: the NMR data support the model provided using the water potential. The model obtained using the chloroform solvent potential suggests a N-N distance of 9.06 Å (Figure 11b). In this suggested model, the proximity between H-

2 and H-3 are not supported by the NOE data since the observed crosspeak for this interaction is relatively weak. This means that the conformation of **8** obtained from the OPLS3 force field with the water solvent potential is better supported by the NMR experiments than the one with the chloroform solvent potential.
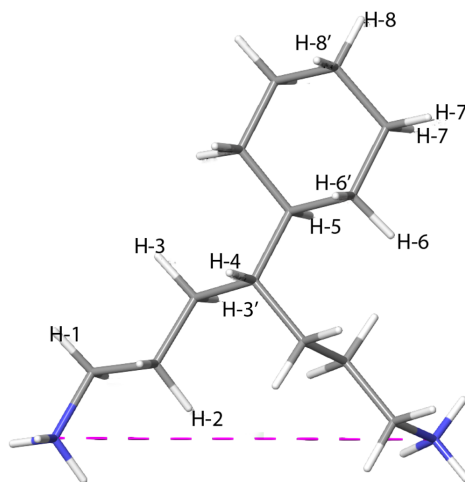
Figure 13a. The lowest energy conformation of ligand **8** as suggested by molecular modelling using an OPLS3 force field with a solvent potential for water. The dotted violet line represents the distance between the nitrogen atoms. (N-N distance = 7.5 Å).

Figure 13b. The lowest energy conformation of ligand **8** as suggested by molecular modelling using an OPLS3 force field with a solvent potential for chloroform. (N-N distance = 9.06 Å).
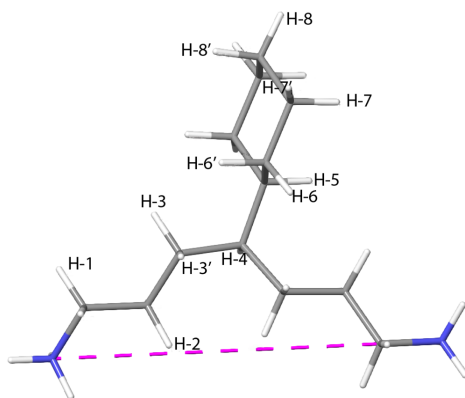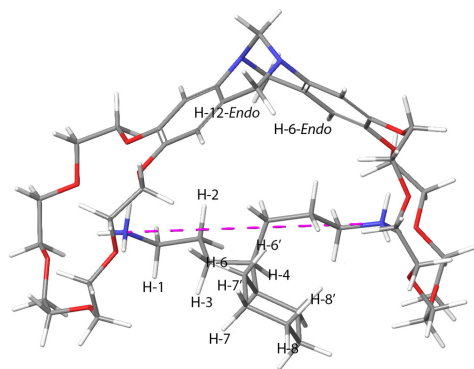
FULL PAPER

Hence, molecular modelling using a water model but *not* a chloroform model is in better agreement with the experimental observation of both halfs of the heptane chain of ligand **7** being staggered but with a central part being in a gauche conformation.
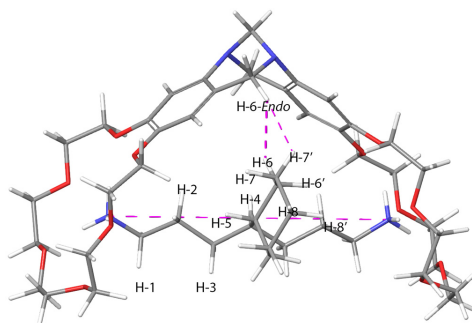
Investigation of the conformation of complex 3•8 by ^{1}H NMR spectroscopy and molecular modelling. Se Figures 14a and 14b Upon titration of **8** with **3**, the chemical shift of proton H-4 of **8** is displaced upfield by 0.75 ppm, going from 0 to 89% bound **8**, suggesting that proton H-4 is shielded by the receptor cavity and hence being situated inside or in the vicinity of the cavity. The ROESY spectra of complex **3•8** show crosspeaks between proton resonances H-6$_{endo}$(H-12$_{endo}$) of **3** and the downfield proton resonances, of H-7 and H-7' of the methylene protons, of the cyclohexyl substituent of **8**, respectively, this could only be possible if the cyclohexyl group is somewhat located inside the receptor cavity. There is also a weak crosspeak between the resonance of the downfield proton resonance of the H-8' of the cyclohexyl substituent and the H-1 the carbon chain of **3**. The ROESY exhibits an intense crosspeak between H-1 and H-2 and a somewhat weaker crosspeak between H-1 and H-3 this observation is consistent with an all-*anti* staggered conformation of the heptane chain. The lowest energy conformation obtained from molecular modelling using the OPLS3 force field and water potential, suggests a conformation where the heptane chain is adopting *gauche* conformations between C-2, C-3, and C-4 as depicted in Figure 14a with a N-N distance of 8.90 Å, with the cyclohexyl group oriented away from the hydrophobic cavity. The model obtained using the OPLS3 force field using the chloroform solvent potential suggests that the heptane chain adopts an *all*-anti staggered conformation with a N-N distance of 10.01 Å with the cyclohexyl group pointing inside of the hydrophobic cavity (Figure 14b).
Hence, the molecular modelling using a potential for chloroform could reproduce the experimental finding of the cyclohexyl side group residing inside the cavity of the receptor.

A summary of the results of the finding about the conformation of the heptane chain of ligands **4-8**, free and bound to receptor **3**, as well as the corresponding prediction using theoretical models, are given in Table 4.

Figure 14b. The lowest energy conformation of ligand **8** bound to receptor **3** in chloroform as suggested by molecular modelling using an OPLS3 force field with a solvent potential for chloroform. (N-N distance = 10.01 Å, H-6-*Endo* – H-6 = 2.20 Å, H-6-*Endo* – H-7 = 2.74 Å).

Table 4. Qualitative summary of the investigations of the prediction of the conformation of ligands and complexes as obtained from NMR studies and by molecular modelling.

Ligand/complex	NMR (CDCl$_3$:MeOH-d_4) (1:1)	OPLS3 (water)	OPLS3 (CHCl$_3$)
free **4** ligand chain	all-*anti* aaaaaa	all-*anti* aaaaaa	all-*anti* aaaaaa
3•4 ligand chain	all-*anti* aaaaaa	all-*anti* aaaaaa	all-*anti* aaaaaa
free **5** ligand chain	all-*anti* aaaaaa	all-*anti* aaaaaa	all-*anti* aaaaaa
5•3 ligand chain	all-*anti* aaaaaa	partly *gauche* aaggaa	all-*anti* aaaaaa
5•3 ligand substituent	inside cavity	outside cavity	Inside cavity
free **6** ligand chain	all-*anti* aaaaaa	all-*anti* aaaaaa	partly *gauche* agaaaa
6•3 ligand chain	all-*anti* aaaaaa	all-*anti* aaaaaa	partly *gauche* agaaaa
6•3 ligand substituent	(partly) inside cavity	partly inside cavity	partly inside cavity
free **7** ligand chain	all-*anti* aaaaaa	all-*anti* aaaaaa	partly *gauche* agaaaa
7•3 ligand chain	all-*anti* aaaaaa	mostly *gauche* agggga	all-*anti*

Figure 14a. The lowest energy conformation of ligand **8** bound to receptor **3** in water as suggested by molecular modelling using an OPLS3 force field with a solvent potential for water. (N-N distance = 8.90 Å).

7·3 ligand substituent	Partly inside cavity	outside cavity	*aaaaaa* partly inside cavity
free 8 ligand chain	partly *gauche* aagaaa	partly *gauche* aagaaa	partly- *gauche* aagaaa
8·3 ligand chain	all-*anti* aaaaaa	partly *gauche* aaggaa	all-*anti* aaaaaa
8·3 ligand substituent	Partly inside the cavity	outside the cavity	partly inside the cavity

An attempt to quantify the interaction between the ligand side group and the receptor. Having the experimental results from both the association constant estimation and the conformational analysis, it is possible to at least make a rough estimate of the interaction energy between the substituent itself and the receptor in some of the binding cases. Looking at Table 4 we found that in all complexes **3•(4-7)**, the same conformation of the ligand framework has been retained, all-*anti*, upon complexation. This means that the interaction between the substituent and the receptor cavity can be roughly estimated from the $\Delta\Delta G^0_{3\cdot x\text{-}3\cdot 4}$ values in Table 3 for x = **5-7**. The strongest binding to the receptor has the phenyl- (**6**), followed by the methyl group (**5**), $\Delta\Delta G° = $ -3.34 and -1.67 kJ mol^{-1}, respectively. The benzyl group has a repulsive interaction with the receptor (**7**) with $\Delta\Delta G° = $ 1.35 kJ mol^{-1}. The free energy of the interaction between the methyl group of **6** and the aromatic cavity of **3** agrees roughly with the value obtained for the same interaction by Wilcox's torsion balance also involving a TB analogue (the system containing an isopropyl group), Both in CDCl$_3$, (2.1 kJ mol^{-1}) and in D$_2$O (3.0 kJ mol^{-1}),[41] and provides a value of the C-H aromatic interaction involving the solvophobic effect from CDCl$_3$:MeOH-d_4 (1:1). The $\Delta\Delta G°$ value for the interaction between the phenyl group and the aromatic cavity is rather high suggesting π-π interactions between both aromatic moieties of the receptor.[42] The solvophobic contribution to the binding should also be larger for a phenyl group compared to a methyl-, because of the large size of the former.

Calculations of binding energies using computational chemistry. First a molecular mechanics (MM) conformational search using the OPLS05 force field was conducted due to that it was developed to model proteins, carbohydrates and nucleic acids, molecules our system wanted to mimic, using a chloroform and water potential, respectively. This resulted in two arrays of conformations, one in chloroform and one in water, with calculated energy values, E_0, for each of the ligands **4-8**, receptor **3**, and the complexes of **3·(4-8)** in each array. To compare the different flexible species in solution, we accounted for the conformational entropy of the ensembles by calculation a Boltzmann sum over all conformers, Eq. 15, using the default

cutoff of 21 kJ mol^{-1}. After the minimization a linear combination was made between each of the E_0 values of each conformation in water and chloroform. This combination was done using 85% of the E_0 value of the conformation obtained using a chloroform potential and 15% of the E_0 value of the conformation obtained using a water potential to more closely resemble the polarity of the solvent mixture. This ratio was found by altering the ratio of water and chloroform in the linear combination equation until the average deviation of the calculated value of $\Delta\Delta G°$ from the measured value was as low as possible. Rewardingly, this ratio turned out to be the best for all the binding reactions of **4-8** to **3**, and all the force fields.

$$E_{Boltzmann} = E_0 - RT\ln\sum e^{(E_0-E_i)/RT} \qquad (15)$$

The so-obtained $E_{Boltzmann}$ value was used to generate the ΔG^0_x (where x stands for ligand **4-8**) for each association reaction between **4-8**, receptor **3**, generating the complexes of **3·(4-8)** in the theoretical chloroform-water solvent mixture (Eq 16).

$$\Delta G^0_x = E_{Boltzmann\ \mathbf{3}\cdot x} - E_{Boltzmann\ \mathbf{3}} - E_{Boltzmann\ x} \qquad (16)$$

We were primarily interested in the relative free energies of binding, which were calculated according to Eq. 17, using **3·4** as the reference system. We note that this subtraction, in effect making the comparison isodesmic, is expected to cancel many systematic errors arising from previous assumptions (such as neglect of some entropy terms) as well as deficiencies in the force fields.

$$\Delta\Delta G^0_x = \Delta G^0_x - \Delta G^0_4 = E_{Boltzmann\ \mathbf{3}\cdot x} - E_{Boltzmann\ x}$$
$$- E_{Boltzmann\ \mathbf{3}\cdot\mathbf{4}} + E_{Boltzmann\ \mathbf{4}} \qquad (17)$$

Using ligand system **3·4** as the reference system that has no substituent no substituent on the ligand would roughly make the ΔG^0_x value to represent the individual energy contribution of each ligand substituent to the complexation reaction. The theoretical $\Delta\Delta G^0_x$ corresponds to the experimental $\Delta\Delta G^0_{3\cdot x\text{-}3\cdot 4}$ values.

In Table 5, the binding energies of each of the ligands **4-8** to receptor **3** are given as $\Delta\Delta G^0_x$ values estimated by MM using the MM3, MMFFs, OPLS05 and OPLS3 force fields together with the corresponding experimentally determined $\Delta\Delta G^0_{3\cdot x\text{-}3\cdot 4}$ values. From Table 6 it can be seen that the different force fields make different estimates of how strong each of the ligands will bind to the receptor. The MM3 force field estimates that the phenyl-substituted ligand will bind most favourably, followed by the benzyl, unsubstituted, methyl and cyclohexyl with $\Delta\Delta G^0_x$ values ranging between -4.52 to 7.45 kJ mol^{-1i} in the series. The MMFFs force field estimates that the benzyl-substituted ligand (**7**) binds most favourably followed by the unsubstituted (**4**), phenyl- (**6**), methyl- (**5**) and cyclohexyl- (**8**) substituted ligands, respectively, with $\Delta\Delta G^0_x$ values ranging between -1.21 and 9.16 kJ mol^{-1}. The OPLS05 force field estimates the benzyl-substituted ligand to bind most favourably, followed by the phenyl-, cyclohexyl-, methyl- and unsubstituted ligands respectively, with $\Delta\Delta G^0_x$ values ranging from -19.807 to 0 kJ mol^{-1}. The OPLS3 force field estimates that the phenyl-substituted ligand would bind most favourably followed by the benzyl-, unsubstituted-, methyl- and cyclohexyl-substituted ligands respectively, with $\Delta\Delta G^0_x$ values ranging from -6.75 to 0.96 kJ mol^{-}

FULL PAPER

[1]. As comparison, the observed experimental order was phenyl > methyl > unsub > benzyl > cyclohexyl with values of $\Delta\Delta G_x^0$

Table 5. Calculated $\Delta\Delta G_x^0$ values corresponding to experimental $\Delta\Delta G_{3\text{-}x\text{-}3\text{-}4}^0$ values in kJ mol^{-1} using molecular modelling with different force fields. The E_0 values are determined from calculations involving conformations obtained using calculations in a chloroform potential to 85% and a water potential to 15% to best resemble the experimental conditions of chloroform:methanol (1:1) (see above). Values including[a] and not including[b] Boltzmann corrections are reported.

Ligand	4	5	6	7	8	MUE
Experimental	0 (3)[e]	-1.67 (2)	-3.34 (1)	1.35 (4)	2.60 (5)	
MM3[a]	0 (2)	2.79 (3)	-1.54 (1)	3.42 (4)	11.02 (5)	4.2
MM3[b,c]	0 (3)	1.81(4)	-4.52 (1)	-0.67 (2)	7.45 (5)	2.9
MMFFs[a]	0 (2)	8.39 (4)	-1.28 (1)	9.84 (5)	2.97 (3)	5.2
MMFFs[b]	0 (3)	6.64 (5)	-5.68 (1)	4.13 (4)	-1.78 (2)	4.5
OPLS05[a]	0 (5)	-5.88 (4)	-17.14 (2)	-19.57 (1)	-13.74 (3)	13.8
OPLS05[b]	0 (5)	-6.94 (4)	-17.45 (2)	-24.98 (1)	-14.82 (3)	15.8
OPLS3 [a,d]	0 (2)	3.75(4)	-5.52 (1)	2.81 (3)	5.09 (5)	2.9
OPLS3 [b]	(2)	3.77 (5)	-9.31 (1)	0.52 (3)	2.01 (4)	3.2

[a] Values obtained using only the lowest energy conformation. [b] Values obtained using the lowest energy conformation corrected with a Boltzmann term. [c] The MM3 force field is closest in estimating the $\Delta\Delta G^0$ values after to Boltzmann correction. [d] The OPLS3 force field is closest in estimating the $\Delta\Delta G^0$ values prior to Boltzmann correction. [e] Ranking of the ligands with respect to the binding to the receptor.

between -3.34 and 2.64 kJ mol^{-1}. One could argue that the OPLS3 force field is the most accurate representation since it qualitatively predicts that the phenyl bearing ligand **6** has the strongest binding and the cyclohexyl bearing ligand **8** has the weakest binding in agreement with the experiments. In addition, using this force field it also generates the lowest absolute mean error value of $E°$ before the Boltzmann correction of 2.9 kJ mol^{-1}. Quantitatively, the values of $\Delta\Delta G_x^0$ obtained using the OPLS3 force field are closer to the experimentally determined $\Delta\Delta G_{3\text{-}x\text{-}3\text{-}4}^0$ values and roughly in the same order of magnitude. Notably, the Boltzmann correction according to Equation 15 does not alter this order. One could argue that MM3 is the most accurate of the investigated computational methods because it actually qualitatively estimates better which ligand binds more favourably to the receptor than the OPLS3 force field, predicting phenyl > unsubstituted > methyl > benzyl > cyclohexyl before

Boltzmann correction. However this order is altered to phenyl > benzyl > unsubstituted > methyl > cyclohexyl upon Boltzmann correction. Even after the Boltzmann correction the MM3 force field exhibits the lowest mean absolute error (2.9 kJ mol^{-1}). The OPLS05 force field estimates binding energies, $\Delta\Delta G_x^0$, that are numerically an order of magnitude larger than the experimental values: Importantly, it fails to predict which of ligands **4-8** that binds strongest to **3**. Finally, regarding the MMFFs force field, one could argue that is more accurate than it the OPLS05 force field since it manages to predict $\Delta\Delta G_x^0$ values in the correct order of magnitude to the $\Delta\Delta G_{3\text{-}x\text{-}3\text{-}4}^0$ values and manages to predict that the cyclohexyl substituted ligand has the lowest free energy of binding to the receptor.

Density functional theory (DFT) calculations were done using B3LYP-3D[43] functional in gas phase, and also using the same functional but with a SM8[44] solvent model for both methanol and chloroform, on the free ligands, receptor and each of the complexes resulting in E_0 values. The lowest energy conformation of ligand **4-8** and complex 3·(**4-8**) used in the calculation was obtained from MM using the OPLS3 force field. For gas phase DFT calculations and the DFT calculations using a methanol potential, the water potential was used for the OPLS3 force field. For the DFT calculations using a chloroform potential, the chloroform potential was used for the OPLS3 force field. The $\Delta\Delta G_x^0$ value for each of the ligands binding to the receptor was determined using the obtained E_0 values using equation 18 below, where the E_0^3 term is cancelled out and it is assumed that the two complexes, respectively, and the two free ligands, respectively, have the same value of the entropic terms and the entropic contribution to the binding will thus be zero.

$$\Delta\Delta G_x^0 = E_0^{3\text{-}x} - E_0^x - E_0^{3\text{-}4} + E_0^4 \qquad (18)$$

For each the ligands, this resulted in the following values on $\Delta\Delta G_x^0$ (see Table 6).

Table 6 Calculated $\Delta\Delta G_x^0$ values corresponding to experimental $\Delta\Delta G_{3\text{-}x\text{-}3\text{-}4}^0$ values in kJ mol^{-1} for the binding of ligands **5-8** to receptor **3**, obtained using DFT calculations (B3LYP-3D) and different solvent models.

Ligand	4	5	6	7	8	MUE[a]
Experimental	0 (3)[b]	-1.67 (2)	-3.34 (1)	1.35 (4)	2.60 (5)	
gas phase	0 (2)	8.41 (4)	3.76 (3)	17.80 (5)	-12.20 (1)	12.1
methanol	0 (3)	10.60 (4)	11.50 (5)	-46.70 (1)	-9.95 (2)	21.9
chloroform	0 (4)	18.86 (5)	-6.78 (3)	-46.16 (1)	-13.39 (2)	21.9

[a] Mean absolute error. [b] [e] Ranking of the ligands with respect the binding to the receptor.

In general, the DFT calculations show deviations in $\Delta\Delta G_x^0$ values compared to the experimental values in the order of 10 kJ mol^{-1}, corresponding to a deviation of an order of magnitude as a mean. The calculations conducted in the gas phase predict that

14

FULL PAPER

3 forms the most stable complex with the cyclohexyl-substituted ligand **8**, followed by unsubstituted (**4**), phenyl- (**6**), methyl- (**5**), and benzyl- substituted ligand (**7**). The calculations using the methanol solvent potential predict that **3** forms the most stable complex with the benzyl substituted ligand, followed by cyclohexyl-, unsubstituted, methyl- and phenyl-substituted ligand. The calculations conducted using the chloroform potential predict that **3** forms the most stable complex with the benzyl-substituted ligand, followed by cyclohexyl-, phenyl-, unsubstituted, and methyl-substituted ligand. The by DFT predicted order does not match the order from the experimental results and the estimated values of $\Delta\Delta G_x^0$ are an order of magnitude larger than the experimental ones with a mean unsigned error in the ranges of 12.1-21.9 kJ mol^{-1}.

Summary and Conclusions

We have used an 18-crown-6 Tröger's base receptor **3** and 4-substituted hepta-1,7-diyl bisammonium salts **4-8** as a model for the interaction between the side chain of a small peptide and a protein receptor containing an aromatic receptor cavity in a biological context. We have justified this in several instances above. We have studied the binding association experimentally by NMR techniques. We have compared different computational methods used to study binding, against each other, using the experimentally obtained results to see which is more accurate in predicting the experiments.

The bidentate binding of the ligands to the receptor was demonstrated in a job plot and then for by the good fitting of a 1:1 binding model to the chemical shifts in the NMR titrations.

We have also attempted to *qualitatively* describe the contribution of the substituent and the conformation of each ligand backbone to the binding. These results are summarized in Table 4. The experimental result is that the phenyl group of ligand **6** and the methyl group of ligand **5** are residing in the aromatic pocket of receptor **3** because of most probably C-H-π interaction in the first case and C-H-π interaction/π-π interactions in second case. Since ROESY/NOESY interactions are observed between relevant protons, this means that the distance between each of the side-group and the aromatic surface of the cavity are within 3.5 Å, supporting the presence of such interactions. The benzyl group of ligand **7** and the cyclohexyl group of ligand **8** are positioned partly inside the aromatic cavity of **3**. Probably also contributing to the binding are solvophobic interactions.

From Table 6, it is evident that force field methods (OPLS3) are rather effective at predicting the experimental found conformations of the carbon framework if the environment is lipophilic (7 of 10 predictions correct using CHCl$_3$ potential) compared to if the environment is hydrophilic (3 of 10 predictions correct using H$_2$O potential). When it comes to predicting the position of the ligand in relation to the receptor cavity, the force field method could correctly predict the position if the environment is lipophilic (4 of 4 predictions correct using CHCl$_3$ potential) compared to if the environment is hydrophilic (0 of 4 predictions correct using H$_2$O potential).

We have *quantitatively* estimated the binding of the ligands **4-8** to receptor **3** in terms of absolute- $K_{3\cdot x}^{bis}$ and relative association constants $K_{3\cdot x}^{bis}/K_{3\cdot 4}^{bis}$, determined by direct and competitive NMR titrations, respectively. The relative association constants are determined using the association reaction of ligand **4**, the one without side substituent in the 4-position, to receptor **3**, as a reference system. The results from each of the estimation of absolute and relative binding constants (Table 1 and 2) show that the phenyl-containing ligand **6** binds strongest to receptor **3**, followed by the methyl- (**5**), unsubstituted (**4**), benzyl (**7**) and cyclohexyl-substituted ligand (**8**). The relative association constants have also been expressed as relative binding values $\Delta\Delta G_{3\cdot x\cdot 3\cdot 4}^0$ and the corresponding values for the binding of respective ligand **5** and **6** to **3**, -1.67 and -3.34 kJ mol^{-1}, respectively, are of very similar magnitude as would be expected for the attractive binding of a methyl group and a phenyl group to an aromatic cavity, respectively. In contrast, the corresponding values for the bonding of respective **7** and **8** to **3** are of positive values, 1.35 and 2.60 kJ mol^{-1}, meaning that the benzyl and the cyclohexyl groups attached in the 4-position of each ligand exert a repulsive contribution to the binding compared to the substituent-free ligand **4**.

We have then used the experimentally estimated values of $\Delta\Delta G_{3\cdot x\cdot 3\cdot 4}^0$ to compare different computational methods against each other to see which is more accurate in predicting the experimental values. The *quantitative* results are summarized in Tables 5-6. The investigation made it evident that the calculated $\Delta\Delta G^0$ values deviated from the experimental value and this was corrected for by using a combination of energies obtained from conformations of two different solvent potentials and in addition adding a Boltzmann term that took into account the dynamic nature of molecules in solution. The predictions of the *strength of the binding* between the receptor and each of the ligands in the form relative free binding energies, $\Delta\Delta G_x^0 = \Delta G_x^0 - \Delta G_4^0$, where ΔG_4^0 is the free energy of binding of ligand **4**, (having no side group,) to receptor **3**, was reported in Table 5. The Results from DFT is given in Table 6. These results are based on DFT calculations using the lowest energy conformation obtained using the OPLS3 force field and a water potential. It can be concluded that molecular mechanics have superior results to DFT (B3LYP-3D functional) calculations for the systems investigated here. This is based on the fact that molecular mechanics managed to predict which of the ligands that will form the most stable and least stable complexes correctly and predicts the values of $\Delta\Delta G_x^0$ closer to the experimentally determined values, $\Delta\Delta G_{3\cdot x\cdot 3\cdot 4}^0$. This is seen clearly when the MM3 force field is used to predict the $\Delta\Delta G_6^0$ value of **3•6**, the predicted value is -4.52 kJ mol^{-1} (Table 5), this value is only -1.18 kJ mol^{-1} from the experimentally determined value of $\Delta\Delta G_{3\cdot 6\cdot 3\cdot 4}^0 = -3.34$ kJ mol^{-1} (Table 3). This result is remarkable since the MM3 method has not been optimized for aqueous solutions.[26] The DFT method used predicted a value of $\Delta\Delta G_6^0 = -6.78$ kJ mol^{-1} for **3•6** (Table 6), a value that is differing by -3.44 kJ mol^{-1} from the experimental value (table 3). We should note that the DFT method is disadvantaged by the exclusion of conformational entropy, since a full conformational search at this level was beyond our computational resources. The recent OPLS3 force field shows results similar to that of MM3 in predicting the $\Delta\Delta G_{3\cdot x\cdot 3\cdot 4}^0$ values. Both these force fields demonstrate an absolute mean error of roughly 3 kJ mol^{-1}. We note that this is similar to the results for the best force fields when calculating conformational energies of small molecules, ca. 2 kJ mol^{-1}.[45] The MM3 force field shows to be superior to OPLS3 and other force fields tested after correcting with a Boltzmann

FULL PAPER

term that takes into account all low energy conformations, where the MM3 shows an absolute error of 2.9 kJ/mol. Finally, we can see that the pinnacle in accuracy reached almost 30 years ago with the development of the MM3 force field still has not been surpassed by the more modern force fields.

Considering that many of the computational methods that were tested against our experimental results had been developed for the modelling of peptides, it is convenient to have a benchmark to evaluate new computational methods against, something our model would work well for. This holds also for new computational methods in this context, where they can be bench marked against our experimental binding and conformational data.

Experimental Section

General Methods: All air-sensitive reactions were performed under nitrogen or argon atmosphere drying all glassware in oven overnight (220°C) or with flame prior to use. TLC-analyses (Merck 60 $_{F254}$ sheets) were visualized using UV light (254 nm) or treated with a solution of KMnO$_4$. Column chromatography was performed using silica gel (Matrex 0.063-0.200 mm). Melting points (mp) were determined in capillary tubes and were verified or corrected using standard substances. NMR spectra were recorded on a Bruker DRX400 NMR spectrometer. Chemical shifts are given in ppm relative to TMS using residual CHCl$_3$ peaks 7.26 (^{1}H NMR) and 77.16 (^{13}C NMR) in CDCl$_3$ and the residual MeOH peaks 3.31 (^{1}H NMR) and 49.00 (^{13}C NMR) in MeOH-d_4 as internal standards. Assignments of peaks were done using ^{1}H-^{1}H COSY, ^{1}H-^{1}H ROESY, ^{1}H-^{1}H NOESY, ^{1}H-^{13}C HMQC and ^{1}H-^{13}C HMBC experiments. Elemental analysis was performed after CC or crystallization if required (according to NMR) by A. Kolbe, Mikroanalytisches Laboratorium, Germany.

Materials: All the chemicals were used as received from commercial sources without further purification with the exception of α-nitrotoluene and cyclohexylnitromethane that were prepared as previously described and methylammonium chloride (BDH chemicals Ltd) that was dried over KOH *in vacuo* until analytically pure as determined by elemental analysis. Only analytically pure receptor **3**, methylammonium chloride and bisammonium salts **4-8**, were used in the determinations of association constants. Benzene (p.a) was dried over 4Å MS. MeOH (p.a), Et$_2$O (p.a) and EtOH (p.a) dried over MS 4Å were used for the preparation of the bisammonium salts. THF (p.a) was dried with Na and distilled under nitrogen prior to use.

6H,   12H-**5,11-Methanobis(benzo-18-crown-6)[4,5-*b*,4,5-*f*]diazocine (3):** To a stirred solution of 4-aminobenzo-18-crown-6 (496 mg, 1.515 mmol) and formaldehyde (37% in H$_2$O; 739 μL, 9.09 mmol) in EtOH (1.36 mL) at 0 °C, HCl (37% in H$_2$O; 616 μL, 7.37 mmol) was added drop wise over 5 min. Subsequently it was left to reach ambient temperature and stirred for 30 h. (TLC samples were treated with a few drops of NH$_3$ (25% in H$_2$O) before elution). The volume of the reaction mixture was reduced to approximately half in vacuo at ambient temperature and H$_2$O (20 mL) and Me$_4$NOH (25% in H$_2$O; 5 mL) were added. After separation of the two layers, the aqueous layer was extracted with CH$_2$Cl$_2$ (4 × 50 mL) and the combined organic layers were evaporated to dryness in vacuo at ambient temperature. The resulting gray/green/black solid was dissolved in MeCN/toluene (1:1) (3 mL). The filtered solution was put on Bio-Beads SX-1 size-exclusion column (3 × 40 cm) and eluted with MeCN/toluene (1:1) yielding 408 mg (77%) of 2 as a white powder. R_f = 0.6 (MeOH/2M NH$_4$Cl/MeNO$_2$ 7:2:1). The product could be further purified by crystallization from acetone: mp 134.0-135.5 °C; ^{1}H NMR (400 MHz, CDCl$_3$): δ = 6.65 (s, 2H), 6.40 (s, 2H), 4.567 (d, *J* = 16.4 Hz, 2H), 4.25 (s, 2H), 4.15-4.10 (m, 4H), 4.08-

4.03 (m, 4H), 4.00 (d, *J* = 16.4 Hz, 2H), 3.94-3.89 (m, 4H), 3.89-3.84 (m, 4H), 3.68-3.78 (m, 16H), 3.57 (s, 8H) ppm. ^{13}C NMR (100 MHz, CDCl$_3$): δ = 148.92 (2C), 146.49 (2C), 141.70 (2C), 120.12 (2C), 112.81 (2C), 111.13 (2C), 71.31 (2C), 71.26 (2C), 71.23 (2C), 71.21 (4C), 71.19 (2C), 70.11 (2C), 70.06 (2C), 70.01 (2C), 69.61 2C), 67.435 (1C), 58.42 (2C) ppm. HRMS (EI$^+$) calcd for C$_{35}$H$_{50}$N$_2$O$_{12}$: 690.3365; found: 690.3363. Anal. Calcd. For C$_{35}$H$_{50}$N$_2$O$_{12}$: C, 60.86; H, 7.30; N, 4.06. Found: C, 60.86; H, 7.29; N, 3.96.

Heptane-1,7-diylbisammonium chloride (8): 1,7-Diaminoheptane (612 mg, 4.70 mmol) was dissolved in MeOH (2 mL) and treated with a 4M solution of HCl in 1,4-dioxane (3 mL). After concentration in vacuo the white crystals formed were dissolved in MeOH (5 mL) and precipitated with Et$_2$O (30 mL), which after filtration, washing with dry Et$_2$O and drying in vacuo gave 691 mg (72%) of **8** as colorless crystals. The precipitation procedure was repeated twice to obtain pure crystals of **8**. ^{1}H NMR(400 MHz, 0.27 M, MeOH-d_4): δ = 2.97 (t, *J* = 7.7 Hz, 4H, H-1 and H-7), 1.80-1.63 (m 4H, H-2 and H-6), 1.52-1.39 (m, 6H, H-3, H-4 and H-5), 0.99 (d, *J* = 6.5 Hz,) ppm. ^{13}C NMR (100 MHz, MeOH-d_4): δ = 40.70 (2C, C-1 and C-7), 29.53 (1C, C-4), 28.34 (2C, C-2 and C-6), 27.14 (2C, C-3 and C-5) ppm. Anal- calcd. for C$_7$H$_{20}$N$_2$Cl$_2$: C, 41.39; H, 9.92; N, 13.79. Found: C, 41.46; H, 10.04; N, 13.64.

4-Methyl-4-nitro-heptanedinitrile (5b): To a stirred solution of nitroethane (4a) (7.5 ml, 104 mmol), acrylonitrile (15 ml, 228 mmol) and KF (1.05 g, 18 mmol) in DCM (100 mL) was added slowly 18-crown 6-ether (558 mg, 2.11 mmol) and stirring was continued at ambient temperature for 24 h. The reaction mixture was concentrated in vacuo, re-dissolved in CHCl$_3$ (100 mL) and washed with 0.1 M HCl (4 x 50 mL). The organic layer was dried (MgSO$_4$), filtered, concentrated in vacuo and the residue purified by CC using EtOAc/heptane 5:5 as the eluent to give 15.6 g (83%) of 4b as a pale yellow oil; R_f = 0.40 (EtOAc/heptane 6:4). Bulb to bulb distillation gave 13.5 g (72%) of analytically pure **5b** as a colorless oil (bp: 140-145 °C, 0.1 torr). ^{1}H NMR (400 MHz, CDCl$_3$): δ = 2.51-2.38 (m, 6H), 2.26-2.20 (m, 2H), 1.68 (s, 3H, CH$_3$) ppm. ^{13}C NMR (100 MHz, CDCl$_3$): δ = 117.9 (2C, C-1 and C-7), 88.7 (1C, C-4), 34.6 (2C, C-2 and C-6), 21.6 (1C, *CH*$_3$), 12.7 (2C, C-3 and C-5) ppm. HRMS (EI$^+$) for C$_8$H$_{12}$N$_3$O$_2$ calcd 182.0930, found 182.0928. Anal. calcd. for C$_8$H$_{11}$N$_3$O$_2$: C, 53.03; H, 6.12; N, 23.19. Found: C, 53.01; H, 6.20; N, 23.11.

4-Nitro-4-phenyl-heptanedinitrile (6b): To a stirred solution of   -nitrotoluene (5a) (1.95 g, 14.2 mmol), acrylonitrile (10 mL, 152 mmol) and KF (436 mg, 7.52 mmol) in DCM (100 mL) was added slowly 18-crown 6-ether (558 mg, 2.11 mmol) and stirring was continued at ambient temperature for 72 h. The reaction mixture was concentrated in vacuo, re-dissolved in CHCl$_3$ (50 mL) and washed with 0.1 M HCl (3 x 25 mL). The organic layer was dried (MgSO$_4$), filtered, concentrated in vacuo and the residue was crystallized twice from MeOH (15 and 10 mL, respectively) to give 2.58 g (75%) of analytically pure **6b** as pale yellow crystals; mp 98.5-100 ^{0}C (MeOH). ^{1}H NMR (400 MHz, CDCl$_3$): δ = 7.50-7.46 (m, 3H), 7.18-7.15 (m, 2H), 2.85-2.67 (m, 4H), 2.53-2.42 (m, 2H), 2.29-2.18 (m, 2H) ppm. ^{13}C NMR (75 MHz, CDCl$_3$): δ = 134.8 (1C), 130.2 (1C), 130.0 (1C), 125.3 (2C), 117.9 (2C, C-1 and C-7), 94.8 (1C, C-4), 33.6 (2C, C-2 and C-6), 13.2 (2C, C-3 and C-5) ppm. HRMS (CI+) for C$_{13}$H$_{14}$N$_3$O$_2$ calcd 244.1086, found 244.1085. Anal. calcd. for C$_{13}$H$_{13}$N$_3$O$_2$: C, 64.19; H, 5.39; N, 17.27. Found: C, 64.04; H, 5.31; N, 17.16.

4-Benzyl-4-nitro-heptanedinitrile (7b): To a stirred solution of   -nitroethylbenzene (1.38 g, 9.13 mmol), acrylonitrile (5 mL, 76 mmol) and KF (187 mg, 3.2 mmol) in DCM (10 mL) was added slowly 18-crown 6-ether (533 mg, 2.02 mmol) and stirring was continued at ambient temperature for 16 h. The reaction mixture was concentrated in vacuo, re-dissolved in CHCl$_3$ (20 mL) and washed with 0.1 M HCl (3 x 35 mL). The organic layer was dried (MgSO$_4$), filtered, concentrated in vacuo. The residue was crystallized twice from MeOH to give 1.90 g (81%) of **7b** as pale yellow crystals; mp 139.0-140.5 °C (MeOH). ^{1}H NMR (300 MHz,

FULL PAPER

CDCl₃): 7.38-7.33 (m, 3H), 7.08-7.04 (m, 2H), 3.28 (s, 2H, CH_2Ph), 2.53-2.27 (m, 8H) ppm. ^{13}C NMR (100 MHz, CDCl₃): δ = 132.4 (1C), 129.7 (2C), 129.4 (2C), 128.7 (1C), 117.9 (2C, C-1 and C-7), 91.9 (1C, C-4), 42.1 (1C, CH_2-Ph), 30.8 (2C, C-2 and C-6), 12.8 (2C, C-3 and C-5) ppm. HRMS (CI+) for C₁₄H₁₆N₃O₂ calcd 258.1243, found 258.1250. Anal. calcd. for C₁₄H₁₅N₃O₂: C, 65.35; H, 5.88; N, 16.33. Found: C, 65.25; H, 5.79; N, 16.22.

4-Cyclohexyl-4-nitro-heptanedinitrile (8b): To a stirred solution of nitroethylcyclohexane (1.02 g, 7.1 mmol), acrylonitrile (3.5 mL, 53 mmol) and KF (150 mg, 58 mmol) in DCM (12 mL) was added slowly 18-crown 6-ether (500 mg, 1.9 mmol) and stirring was continued at ambient temperature for 48 h. The reaction mixture was concentrated in vacuum, redissolved in CHCl₃ (20 mL) and washed with 0.1 M HCl (3 x 15 mL). The organic layer was dried (MgSO₄), filtered and concentrated in vacuum. The residue was purified by CC (EtAc/hexanes 2:8) to give 1.2 g (69 %) of analytically pure **8b** as white crystals; R_f 0.24 (EtAc/heptane 3:7). mp 94.5-96.0 °C. ^{1}H NMR (400 MHz, CDCl₃) δ 2.60-2.56 (m, 4H), 2.48-2.40 (m, 2H), 2.24-2.16 (m, 2H), 1.97 (tt, 1H, J = 2.8 Hz, J = 11.9 Hz), 1.88 (m, 2H), 1.75 (m, 1H), 1.59 (m, 2H), 1.35-1.05 (m, 5H); ^{13}C NMR (100 MHz, CDCl₃) δ 118.3, 94.0, 44.0, 29.3, 27.6, 26.3, 25.9, 12.8; HRMS (CI+) for C₁₃H₁₉N₃O₂ calcd 249.1477, found 249.1527 Anal. Calcd. for C₁₃H₁₉N₃O₂: C, 62.63; H, 7.68; N, 16.85. Found C, 62.71; H, 7.74; N, 16.88.

4-Methylheptanedinitrile (5c): A solution of **5b**(8.39 g, 46.3 mmol), tributyltin hydride (25.0 mL, 92.6 mmol) and AIBN (2.53 g, 15.4 mmol) in anhydrous benzene (100 mL) was refluxed for 14 h. The reaction mixture was concentrated in vacuo and the residue purified by CC using hexane and subsequently EtOAc (10-30%) in heptane as the eluent. The crude product was re-dissolved in Et₂O (100 mL) and stirred with a 10% aqueous solution of KF (100 mL) for 24h. The white solid was filtered off and after separation of the two layers, the aqueous layer was extracted with Et₂O (2 x 25 mL). The combined organic layers were dried (MgSO₄), filtered, concentrated in vacuo to give 5.32 g (84%) of analytically pure **5c** as a colorless oil; R_f = 0.20 (EtOAc (40%) in heptane). ^{1}H NMR (300 MHz, CDCl₃): δ = 2.43-2.27 (m, 4H), 1.78-1.66 (m, 3H), 1.54-1.47 (m, 2H), 0.95 (d, J = 6.1 Hz, 3H, CH_3) ppm. ^{13}C NMR (100 MHz, CDCl₃): δ = 119.9 (2C, C-1 and C-7), 32.1 (2C, C-2 and C-6), 31.8 (1C, C-4), 18.3 (1C, CH_3), 15.2 (2C, C-3 and C-5) ppm. HRMS (CI+) for C₈H₁₃N₂ calcd 137.1079, found 137.1065. Anal. Calcd. for C₈H₁₂N₂: C, 70.55; H, 8.88; N, 20.57. Found: C, 70.38; H, 8.95; N, 20.44.

4-Phenylheptanedinitrile (6c): A solution of **6b** (4.22 g, 17.3 mmol), tributyltin hydride (9.3 mL, 34.6 mmol) and AIBN (952 mg, 5.8 mmol) in anhydrous benzene (38 mL) was refluxed for 22 h. The reaction mixture was concentrated in vacuo and the residue purified by CC using EtOAc (20%) in heptane as the eluent. The crude product was re-dissolved in Et₂O (25 mL) and stirred with a 10% aqueous solution of KF (25 mL) for 14h. The white solid was filtered off and after separation of the two layers, the aqueous layer was extracted with Et₂O (2 x 25 mL). The combined organic layers were dried (MgSO₄), filtered, concentrated in vacuo to give 2.88 g (84%) of analytically pure **6c** as a pale yellow oil; R_f = 0.25 (EtOAc (40%) in heptane). ^{1}H NMR (400 MHz, CDCl₃): δ = 7.40-7.27 (m, 3H), 7.19-7.7.17 (m, 2H), 2.84-2.79 (m, 1H, H-4), 2.23-1.91 (m, 8H) ppm. ^{13}C NMR (100 MHz, CDCl₃): δ = 140.0 (1C) 129.6 (2C), 128.1 (1C), 127.7 (2C), 119.2 (2C, C-1 and C-7), 44.2 (1C, C-4), 32.2 (2C, C-2 and C-6), 15.5 (2C, C-3 and C-5) ppm. HRMS (EI+) for C₁₃H₁₄N₂ 198.1157, found 198.1157. Anal. calcd. for C₁₃H₁₄N₂: C, 78.75; H, 7.12; N, 14.13. Found C, 78.78; H, 7.18; N, 14.04.

4-Benzylheptanedinitrile (7c): A solution of **7b** (1.37 g, 5.3 mmol), tributyltin hydride (2.88 mL, 10.7 mmol) and AIBN (294 mg, 1.8 mmol) in anhydrous benzene (20 mL) was refluxed for 4 h. The reaction mixture was concentrated in vacuo and the residue purified by CC using EtOAc (20%) in heptane as the eluent. The crude product was re-dissolved in Et₂O (10 mL) and stirred with a 10% aqueous solution of KF (10 mL) for 1h. The white solid was filtered off and after separation of the two layers,

the aqueous layer was extracted with Et₂O (2 x 10 mL). The combined organic layers were dried (MgSO₄), filtered, concentrated in vacuo to give 999 mg (89%) of analytically pure **7c** as a pale yellow oil; R_f = 0.20 (EtOAc (40%) in heptane). ^{1}H NMR (300 MHz, CDCl₃): δ= 7.36-7.22 (m, 3H), 7.17-7.14 (m, 2H), 2.61 (d, J = 7.2 Hz, 2H, CH_2Ph), 2.34 (J = 7.5 Hz, 4H, H-2 and H-6), 2.00-1.91 (m, 1H, H-4), 1.72-1.63 (m, 4H, H-3 and H-5) ppm. ^{13}C NMR (100 MHz, CDCl₃): δ= 138.6 (1C), 129.0 (2C), 128.9 (2C), 126.8 (1C), 119.3 (2C, C-1 and C-7), 39.4 (1C), 38.2 (1C, C-2 and C-6), 14.9 (2C, C-3 and C-5) ppm. HRMS (EI+) for C₁₄H₁₆N₂ calcd 212.1313, found 212.1315. Anal. calcd. for C₁₄H₁₆N₂: C, 79.21; H, 7.60; N, 13.20. Found C, 79.08; H, 7.55; N, 13.29.

4-Cyclohexyl-heptanedinitryle (8c): A solution of **8b** (620 mg, 2.5 mmol), tributyltin hydride (1.5 mL, 5.0 mmol) and AIBN (150 mg, 0.9 mmol) in anhydrous benzene (8 mL) was refluxed for 24 h. The reaction mixture was concentrated in vacuum and the residue purified by CC (gradient, 0-20 % EtAc/hexans). The crude product was redissolved in Et₂O (5 mL) and stirred with 10 % aqueous solution of KF (5 mL) for 16 h. The white solid was filtered off and after separation of the two layers, the aqueous layer was extracted with Et₂O (2 x 5 mL). The combined organic phases were dried (MgSO₄), filtered and concentrated in vacuum to give 423 mg (83 %) of analytical pure **8c** as a colorless oil; R_f 0.31 (EtAc/heptane 3:7). ^{1}H NMR (400 MHz, CDCl₃): δ = 2.36 (t, 4H, J = 7.3 Hz), 1.80-1.66 (m, 5H), 1.59-1.50 (m, 4H), 1.43-0.99 (m, 7H); ^{13}C NMR (100 MHz, CDCl₃): δ= 119.5, 42.0, 39.1, 29.3, 26.6, 26.5, 26.1, 15.6; HRMS (CI+) for C₁₃H₂₀N₂ 204.1626, found 204.1680. Anal. Calcd. for C₁₃H₂₀N₂: C, 76.42; H, 9.87; N, 13.71. Found C, 76.58; H, 9.82; N, 13.64.

4-Methylheptane-1,7-diyl-bisammonium chloride (5): To a stirred 1 M solution of BH₃ in THF (53 mL, 53 mmol) was added slowly **5c** (905 mg, 6.65 mmol) in THF (5 mL) at rt. The reaction mixture was refluxed for 3 h. after which it was cooled to rt. with an ice-bath and slowly treated with a 6 M solution of HCl (15 mL). The THF was evaporated in vacuo and the resulting solution was made alkaline (pH ≈ 14), while cooling on an ice-bath. The aqueous layer was extracted with CHCl₃ (8 x 50 mL) and the combined organic layers were dried (MgSO₄), filtered and concentrated in vacuo. The residue was re-dissolved in MeOH (4 mL) and treated with a 4 M solution of HCl in 1,4-dioxane (3 mL). After concentration in vacuo the white crystals formed were dissolved in MeOH (2 mL) and precipitated with Et₂O (20 mL), which after filtration, washing with dry Et₂O and drying in vacuo gave 613 mg (42%) of analytically pure **c** as colorless crystals. ^{1}H NMR (400 MHz, 0.26 M, MeOH-d_4): δ = 0.99 (d, J = 6.5 Hz, 3H, CH_3), 1.18-1.34 (m, 2H, H-3 and H-5), 1.40-1.52 (m, 3H, H-3', H-5' and H-4), 1.62-1.83 (m, 4H, H-2 and H-6), 2.96 (t, J = 7.6 Hz, 4H, H-1 and H-7); ^{13}C NMR (100 MHz, MeOH-d_4): δ = 19.51 (1C, CH₃), 26.00 (2C, C-2 and C-6), 33.26 (1C, C-4), 34.32 (2C, C-3 and C-5), 41.00 (2C, C-1 and C-7); HRMS (CI+) for C₈H₂₁N₂ 145.1705, found, 145.1704. Anal. calcd. for C₈H₂₂N₂Cl₂: C, 44.24; H, 10.21; N, 12.90. Found C, 44.05; H, 10.28; N, 12.82.

4-Phenylheptane-1,7-diyl-bisammonium chloride (6): To a stirred 1 M solution of BH₃ in THF (80 mL, 80 mmol) at rt. was added slowly **6c** (2.1 g, 10.6 mmol) in THF (10 mL). The reaction mixture was refluxed for 3 h. after which it was cooled to rt. with an ice-bath and slowly treated with a 6 M solution of HCl (20 mL). The THF was evaporated in vacuo and the resulting solution was made alkaline (pH ≈ 14) with solid KOH, while cooling on an ice-bath. The aqueous layer was extracted with CHCl₃ (5 x 50 mL) and the combined organic layers were dried (MgSO₄), filtered and concentrated in vacuo. The residue was re-dissolved in MeOH (7 mL) and treated with a 4 M solution of HCl in 1,4-dioxane (5 mL). After concentration in vacuo the white crystals formed were dissolved in MeOH (10 mL) and precipitated with Et₂O (70 mL), which after filtration, washing with dry Et₂O and drying in vacuo gave 1.99 g (67%) of analytically pure **6** as colorless crystals. ^{1}H NMR (400 MHz, 0.16 M, MeOH-d_4): δ = 7.38-7.33 (m, 2H, m-H), 7.29-7.21 (m, 3H, o-H and p-H), 2.96-2.82 (m, 4H, H-1 and H-7), 2.66 (apparent septet, J = 4.9 Hz, 1H, H-4), 1.88-1.78 (m, 2H, H-3' and H-5'), 1.77-1.68 (m, 2H, H-3 and H-5), 1.66-1.55 (m, 2H, H-2' and H-6'), 1.55-1.42 (m, 2H, H-2 and H-6) ppm. ^{13}C NMR (100 MHz, MeOH-d_4): δ = 145.17 (1C, i-C), 129.79 (2C, m-C), 128.83 (2C, o-C),

FULL PAPER

127.69 (1C, *p*-C), 46.43 (1C, C-4), 40.71 (2C, C-1 and C-7), 34.53 (2C, C-3 and C-5), 26.75 (2C, C-2 and C-6)) ppm. HRMS (EI+) for $C_{13}H_{22}N_2$ calcd 206.1783, found, 206.1778. Anal. calcd. for $C_{13}H_{24}N_2Cl_2$: C, 55.91; H, 8.66; N, 10.03. Found C, 56.08; H, 8.76; N, 9.85.

4-Benzylheptane-1,7-diyl-bisammonium chloride (7): To a stirred 1 M solution of BH_3 in THF (26 mL, 26 mmol) at rt. was added slowly **7c** (693 mg, 3.26 mmol) in THF (3 mL). The reaction mixture was refluxed for 3 h. after which it was cooled to rt. with an ice-bath and slowly treated with a 6 M solution of HCl (8 mL). The THF was evaporated in vacuo and the resulting solution was made alkaline (pH ≈ 14), while cooling on an ice-bath. The aqueous layer was extracted with $CHCl_3$ (5 x 25 mL) and the combined organic layers were dried ($MgSO_4$), filtered and concentrated in vacuo. The residue was re-dissolved in MeOH (9 mL) and treated with a 4 M solution of HCl in 1,4-dioxane (3 mL). After concentration in vacuo the white crystals formed were dissolved in MeOH (4 mL) and precipitated with Et_2O (50 mL), which after filtration, washing with dry Et_2O and drying in vacuo gave 505 mg (53%) of analytically pure **7** as colorless crystals. ^1H NMR (400 MHz, 0.24 M, MeOH-d_4): δ = 7.32-7.28 (m, 2H, *m*-H), 7.24-7.18 (m, 3H, *o*-H and *p*-H), 2.91 (t, *J* = 7.7 Hz, 4H, H-1 an H-7), 2.64 (d, *J* = 7.1 Hz, 2H, PhC*H*₂), 1.85-1.65 (m, 5H, H-2, H-4 and H-6), 1.44-1.38 (m, 4H, H-3 and H-5) ppm. ^{13}C NMR (100 MHz, MeOH-d_4): δ = 141.88 (1C, *i*-C), 130.19 (2C, *o*-C), 129.38 (2C, *m*-C), 127.01 (1C, *p*-C), 41.04 (2C, C-1 and C-7), 40.95 (1C, CH_2Ph), 40.28 (1C, C-4), 30.71 (2C, C-3 and C-5), 25.54 (2C, C-2 and C-6) ppm. HRMS (FAB+) for $C_{14}H_{25}N_2$ calcd 221.2018, found 221.1999. Anal. calcd. for $C_{14}H_{26}N_2Cl_2$: C, 57.34; H, 8.94; N, 9.55. Found C, 57.26; H, 9.05; N, 9.38.

4-Cyclohexyl-heptane-1,7-diyl-bisammonium chloride (8): Adam's catalyst was suspended in EtOH (25 mL) and a solution of **8b** (0.275 gr, 1.3 mmol) in EtOH (5 mL) was added to the solution, followed by bench $CHCl_3$ (1.2 mL). The mixture was stirred under H_2 (50 psi) at room temperature for 24 hr. The catalyst was filtered off, and the filtrate was evaporated to get clear oil that becomes solid after addition of Et_2O. The solid was dissolved in MeOH (1.5 mL) and precipitate by addition of Et_2O (15 mL). The white solid was filtered off and dried under vacuum to get 360 mg of **8** as a white solid. ^1H NMR (400 MHz, MeOH-d_4): δ = 2.93 (t, 4H, *J* = 3.8 Hz), 1.75-1.61 (m, 9H), 1.45-1.15 (m, 11H) ppm. ^{13}C NMR (100 MHz, MeOH-d_4): δ = 44.2, 41.2, 41.1, 30.7, 28.5, 27.9, 27.8, 26.8 ppm. HRMS (EI+) for $C_{13}H_{29}N_2^+$ calcd 213.2326, found 213.2334. Anal. Calcd. for $C_{13}H_{30}Cl_2N_2$: C, 54.73; H, 10.60; N, 9.82. Found C, 54.64; H, 10.75; N, 9.73.

NMR titrations: Direct and competitive methods are described below.

Direct method: Stock solutions of each the bisammonium salts (**4-8**) (c_{3-7} = 0.0267-0.0268 M), MenH₃Cl (**9**, c_8 = 0.275 M) and receptor **3** with **9** present (c_2 = 0.08693 M, c_8 = 0.080 M) were prepared in $CDCl_3$:MeOH-d_4 (1:1). For each bisammonium salt (**4-8**), four separate solutions were made in 1 ml volumetric flasks using 100 and 250, 220 and 230, 440 and 185, and 880 and 98 μL of parent bisammonium salt solution and **9** solution respectively and filling up the mark with $CDCl_3$:MeOH-d_4 1:1. In 4 different NMR tubes, 500 μL of each of the bisammonium/**9** solutions was added, and the spectra recorded. Following the measurements 15 μL of the parent receptor solution was added to each of the tubes and the spectra were recorded. The procedure was repeated adding 18, 40 and 80 μL to each of the NMR Tubes.

Competitive method: Stock solutions of each the bisammonium salts (**4-8**, c_{3-7} = 0.034 M), **9** (c_8 = 0.085 M) and receptor **3** with **9** present (c_2 = 0.100 M, c_8 = 0.074 M) were prepared in $CDCl_3$:MeOH-d_4 (1:1). 150 μL of bisammonium **5** and 200 μL of **9** solutions were added to 4 separate NMR tubes. To one of each of these NMR tubes was added 150 μL of one of the other bisammonium solutions **4**, **6**, **7** or **8**. The NMR spectra were then recorded. Following the measurement 10 μL of the receptor solution was added to each of the tubes and the NMR was recorded again. The procedure was repeated adding additional receptor solution (10 μL) to each sample and then repeating the measurement. This

iterative process was continued with 10 μL going to 15 μL and finally to 30 μL until a total of 390 μL of receptor solution had been added to each sample.

[1]   a) V. du Vigeneaud, C. Ressler, J. M. Swan, C. W. Roberts, P. G. Katsoyannis, S. Gordon, *J. Am. Chem. Soc.* **1953**, *75*, 4879-80; b) V. du Vigeneaud, H. C. Lawler, E. A. Popenoe, *J. Am. Chem. Soc.* **1953**, *75*, 4880-1.

[2]   S. L. Schreiber, *Science* **1991**, *251*, 283-7.

[3]   a) R. L. Stanfield, I. A. Wilson, A. *Curr. Opin. Struct. Biol.* **1995**, *5*, 103-13.

[4]   a) M. J. Zvelebil, J. M Thornton, *Q. Rev. Biophys.* **1993**, *26*, 333-63; b) G. R. Marshall, *Curr. Opin. Struct. Biol.* **1992**, *2*, 904-19.

[a]   R. H. Abeles, P. A. Frey, W. P. Jencks, *Biochemistry*, Jones and Bartlett Publishers, Boston, 1992.

[5]   V. Neduva, R. B. Russel, *Curr. Opin. Biotech.* **2006**, *17*, 465-71.

[6]   T. Cserhati, M. Szoegyi, *Peptides.* **1995**, *16*, 165-73.

[7]   a) S. Tsuda, S. Aimoto, K. Hikichi, *J. Biochem.* **1992**, *112*, 665-70; b) M. Ikura, G. M. Clore, A. M. Gronenborn, G. Zhu, C.B Klee, A. Bax, *Science.* **1992**, *256*, 632-8; c) P. W. Jeffs, L. Muller, C. DeBrosse, S. L. Heald, R. Fisher, *J. Am. Chem. Soc.* **1986**, *108*, 3063-75; d) J. P. Waltho, D. H. Williams, *J. Am. Chem. Soc.* **1989**, *111*, 2475-80; e) L. M. Gordon, C. C. Curtain, Y. C. Zhong, A. Kirkpatrick, P. W. Mobley, A. J. Waring, *BBA-Mol. Basis. Dis.* **1992**, *1139*, 257-74.

[8]   M. L. Moore in *Synthetic Peptides: A User's Guide*, (Ed.: G. A. Grant), W.H Freeman and Company, New York, **1992**, pp 11.

[9]   a) E. A. Meyer, R. K. Castellano, F. Diederich, *Angew. Chem. Int. Ed.* **2003**, *42*, 1210-50; b) C. A. Hunter, K. R. Lawson, J. Perkin, C. J. Urch, *J. Chem. Soc., Perkin. Trans. 2* **2001**, 651-69.

[10] M. L. Waters, *Biopolymers* **2004**, *76*, 435-445.

[11] S. K. Burley, G. A. Petsko, *Science* **1985**, *229*, 23-8.

[12] G. B. McGaughey, M. Gagne, A. Rappe, *J. Biol. Chem.* **1998**, *273*, 15458-15463.

[13] a) Y. Umezawa, S. Tsuboyama, H. Takahashi, J. Uzawa, M. Nishio, *Bioorgan. Med. Chem.* **1999**, *7*, 2021-2026; b) M. Brandl, M. S. Weiss, A. Jabs, J. Suhnel, R. Hilgenfeld, *J. Mol. Biol.* **2001**, *307*, 357-377.

[14] a) S. Paliwal, S. Geib, C. S. Wilcox, *J. Am. Chem. Soc.* **1994**, *116*, 4497-8; b) U.Obst, P. Betschmann, C. Lerner, P. Seiler, F. Diederich, V. Gramlich, L. Weber, D. W. Banner, P. Schonholzer, *Helv. Chim. Acta.* **2000**, *83*, 855-909; c) J. A. Turk, D. B. Smithrud, *J. Org. Chem.* **2001**, *66*, 8328-8335.

[15] D. J. Sandman in *Modern Physical Organic Chemistry*, (Eds.: E. V. Anslyn, D. A. Dougherty), Wiley-VCH, Weinheim, **2006**, pp. 461.

[16] a) T. Haino, D. M. Rudkevich, A. Shivanyuk, K. Rissanen, J. Rebek Jr., *Chem. Eur. J.* **2000**, *6*, 3797-3805; b) F. Hof, L. Trembleau, E. C. Ullrich, J. Rebek Jr., *Angew. Chem. Int. Ed.* **2003**, 42, 3150-3; c) S. M. Biros, E. C. Ullrich, F. Hof, L. Trembleau, J. Rebek Jr., *J. Am. Chem. Soc.* **2004**, *126*, 2870-2876; d) S. M. Butterfield, J. Rebek Jr., *J. Am. Chem. Soc.* **2006**, *128*, 2870-2874.

[17] J. H. Arevalo, E. A. Stura, J. M. Taussig, I. A. Wilson, *J. Mol. Biol.* **1993**, *231*, 103-18.

[18] S. S. Hoog, J. E. Pawlowski, P. M. Alzari, T. M. Penning, M. Lewis, *Proceedings of the National Academy of Sciences of the United States of America* **1994**, *91*, 2517-21.

[19] S. Spinelli, R. Ramoni, S. Grolli, J. Bonicel, C. Cambillau, M. Tegoni, *Biochemistry* **1998**, *37*, 7913-7918.

FULL PAPER

[20] R. Schwarzenbacher, F. Stenner-Liewen, H. Liewen, J. C. Reed, J. R. Liddington, *Proteins* **2004**, *56*, 401-3.

[21] M. Rizzi, J. B. Wittenberg, A. Coda, M. Fasano, P. Ascenzi, M. Bolognesi, *J. Mol. Biol.* **1994**, *244*, 86-99.

[22] a) S. A. Adcock, J. A. McCammon, *Chem. Rev.* **2006**, *106*, 1589-1615; b) A. M. Wasserman, D. Dimova, P. Iyer, J. Bajorath, *Drug. Dev. Res.* **2012**, *73*, 518-527; c) G. Vettoretti, E. Moroni, S. Sattin, J. Tao, D. A. Agard, A. Bernardi, G. Colombo, *Sci. Rep-UK.* **2016**, *6*, 23830.

[23] a) S. Ehrlich, J. Moellmann, S. Grimme, *Acc. Chem. Res.* **2013**, *46*, 916– 926; b) C. Corminboeuf, *Acc. Chem. Res.* **2014**, *47*, 3217– 3224; c) P. Hobza, *Acc. Chem. Res.* **2012**, *45*, 663– 672.

[24] Chapters 2 and 6 in *Introduction to Computational Chemistry 2nd Edition* (Ed.: F. Jensen), Wiley-VCH, Weinheim, **2007**, pp. 22-77, 232-264.

[25] S. A. Adcock, J. A. McCammon, *Chem. Rev.* **2006**, *1589-1615*.

[26] N. L. Allinger, Y. H. Yuh, J-H. Lii, *J. Am. Chem. Soc.* **1989**, *111*, 8551-8565.

[27] T. A. Hallgren, *J. Comp. Chem.* **1996**, *17*, 490-519.

[28] a) G. A. Kaminski, R. A. Friesner, J. Tirado-Rives, W. Jorgensen, *J. Phys. Chem B* **2001**, *105*, 6474-6487; b) J. L. Banks, H. S. Beard, Y. Cao, A. E. Cho, W. Damm, R. Farid, A. K. Felts, T. A. Halgren, D. T. Mainz, J. R. Maple, R. Murphy, D. M. Philipp, M. P.Repasky, L. Y. Zhang, B. J. Berne, R. A. Friesner, E. Gallicchio, R. M. Levy. Integrated Modelling Program, *J. Comp. Chem.* **2005**, *26*, 1752.

[29] E. Harder, W. Damm, J. Maple, C. Wu, M. Reboul, J. Y. Xiang, L. Wang, D. Lupyan, M. K. Dahlgren, J. L. Knight, J. W. Kaus, D. S. Cerutti, G. Krilov, W. L. Jorgensen, R. Abel, R. A. Friesner, *J. Chem. Theory. Comput.* **2016**, *12*, 281-296.

[30] A. P. Hansson, P.-O. Norrby, K. Wärnmark, *Tetrahedron Lett.* **1998**, *39*, 4565-4568.

[31] I. Belsky, *J. Chem. Soc. Chem. Comm.* **1977**, 237.

[32] N. Ono, H. Miyake, R. Tamura, A. Kaji, *Tetrahedron Lett.* **1981**, *22*, 1705-1708.

[33] S. Nagarajan, B. Ganem, *J. Org. Chem* **1986**, *51*, 4856-4861.

[34] V. Voorhees, R. Adams, *J. Am. Chem. Soc.* **1922**, *44*, 1397-1405.

[35] a) C. S. Wilcox, *Front.Supramol. Org. Chem. Photochem.* **1991**, 123-143; b) L. Fielding, *Tetrahedron* **2000**, *56*, 6151-6170.

[36] P. Job, *Ann. Chim.* **1928**, *9*, 109-123.

[37] B. J. Whitlock, H.W. Whitlock, *J. Am. Chem. Soc.* **1990**, *112*, 3910-3915.

[38] F. Salort, C. Pardo, J. Elguero, *Magn. Reson. Chem.* **2002**, *40*, 743-746.

[39] D. Neuhaus, M. P. Willaimson in *The Nuclear Overhauser Effect in Structural and Conformational Analysis*, Wiley-VCH, New York, Chichester, Weinheim, Brisbane, Singapore, Toronto, **2000**, pp. 49-51.

[40] C. A. Deakyne, M. Meot-Ner, *J. Am. Chem. Soc.* **1985**, *107*, 474-479.

[41] B. Bhayana, C. S. Wilcox *Ang. Chem. Int. Ed.* **2007**, *46*, 6833-6836.

[42] L. Yang, C. Adam, G. S. Nichols, S. L. Cockroft *Nature Chem.* **2013**, *5*, 1006-1010.

[43] S. Grimme, J. Antony, S. Ehrlich, H. Krieg, *J. Chem. Phys,* **2010**, *132,* 154104.

[44] C. J. Cramer, D. G. Truhlar, *Acc. Chem. Res.* **2008**, *41*, 760-768.

[45] a) K. Gundertofte, T. Liljefors, P-O. Norrby, I. Pettersson, *J. Comput. Chem.* **1996,** *17,* 429-449; b) T. Liljefors, K. Gundertofte, P-O. Norrby, I. Pettersson in *Computational Medicinal Chemistry for Drug Discovery,* (Eds: P. Bultinck, J. P. Tollenaere, H. De Winter, and W. Langenaeker), Marcel Dekker, New York, **2004**, 1-28.

Centre for Analysis and Synthesis
Department of Chemistry
Faculty of Science
Lund University

LUND
UNIVERSITY